

PREPARED FOR SUBMISSION TO JHEP

# Correlation of the hidden-charm molecular tetraquarks and the charmonium-like structures existing in the $B \rightarrow XYZ + K$

---

Fu-Lai Wang,<sup>a,b</sup> Xin-Dian Yang,<sup>a,b</sup> Rui Chen,<sup>c</sup> Xiang Liu<sup>a,b,d</sup>

<sup>a</sup>*School of Physical Science and Technology, Lanzhou University, Lanzhou 730000, China*

<sup>b</sup>*Research Center for Hadron and CSR Physics, Lanzhou University and Institute of Modern Physics of CAS, Lanzhou 730000, China*

<sup>c</sup>*Center of High Energy Physics, Peking University, Beijing 100871, China*

<sup>d</sup>*Lanzhou Center for Theoretical Physics, Key Laboratory of Theoretical Physics of Gansu Province, and Frontiers Science Center for Rare Isotopes, Lanzhou University, Lanzhou 730000, China*

*E-mail:* [wangfl2016@lzu.edu.cn](mailto:wangfl2016@lzu.edu.cn), [yangxd20@lzu.edu.cn](mailto:yangxd20@lzu.edu.cn),  
[chen\\_rui@pku.edu.cn](mailto:chen_rui@pku.edu.cn), [xiangliu@lzu.edu.cn](mailto:xiangliu@lzu.edu.cn)

ABSTRACT: The molecular assignments to the three  $P_c$  states and the similar production mechanism between the  $\Lambda_b \rightarrow P_c + K$  and  $B \rightarrow XYZ + K$  convince us the  $B$  decaying to a charmonium state plus light mesons could be the appropriate production process to search for the charmonium-like molecular tetraquarks. In this work, we systematically study the interactions between a charmed (charmed-strange) meson and an anti-charmed (anti-charm-strange) meson, which include the  $D^{(*)}\bar{D}^{(*)}$ ,  $\bar{D}^{(*)}\bar{D}_1$ ,  $D^{(*)}\bar{D}_2^*$ ,  $D_s^{(*)}\bar{D}_s^{(*)}$ ,  $D_s^{(*)}\bar{D}_{s0}^*$ ,  $D_s^{(*)}\bar{D}_{s1}'$ ,  $D_s^{(*)}\bar{D}_{s1}$ ,  $D_s^{(*)}\bar{D}_{s2}^*$  systems. After adopting the one-boson-exchange effective potentials, our numerical results indicate that, on one hand, there can exist a serial of isoscalar charmonium-like  $\mathcal{D}\bar{\mathcal{D}}$  and  $\mathcal{D}_s\bar{\mathcal{D}}_s$  molecular states, on the other hand, we can fully exclude the charged charmonium-like states as the isovector charmonium-like molecules. Meanwhile, we discuss the two-body hidden-charm decay behaviors for these possible charmonium-like molecular tetraquarks. By analyzing the experimental data collected from the  $B \rightarrow XYZ + K$  and the mass spectrum and strong decay behaviors for the obtained  $\mathcal{D}\bar{\mathcal{D}}$  and  $\mathcal{D}_s\bar{\mathcal{D}}_s$  molecules, we find possible hints of the existence of the charmonium-like molecular tetraquarks, i.e., a peculiar characteristic mass spectrum of the isoscalar  $D^*\bar{D}^*$  molecular systems can be applied to identify the charmonium-like molecule. By checking the reported  $XYZ$  data of the  $B \rightarrow XYZ + K$  decays, there exists the evidence of double peaks and single peak structures below the  $D^*\bar{D}^*$  threshold in the  $J/\psi\omega$  invariant mass distribution of the  $B \rightarrow J/\psi\omega K$  process and in the  $J/\psi\eta$  invariant mass distribution of the  $B \rightarrow J/\psi\eta K$  process, respectively. Here, the double peaks structure is due to the isoscalar  $D^*\bar{D}^*$  molecular states with  $J^{PC} = 0^{++}$  and  $2^{++}$  while the single peak structure may correspond to isoscalar  $D^*\bar{D}^*$  molecule with  $J^{PC} = 1^{+-}$ . The very broad structure around 4.3 GeV in the  $J/\psi\omega$  invariant mass distribution of the  $B \rightarrow J/\psi\omega K$  process and the structures in the  $J/\psi\phi$  invariant mass distribution of the  $B \rightarrow J/\psi\phi K$  process could be complicated as many possible charmonium-like  $\mathcal{D}\bar{\mathcal{D}}$  and  $\mathcal{D}_s\bar{\mathcal{D}}_s$  molecular states mainly decay into the  $J/\psi\omega$  and  $J/\psi\phi$ , respectively. We look forward to the future experiments like the LHCb, Belle II, and BESIII Collaborations can test our results with more precise experimental data.

---

## Contents

<b>1</b>	<b>Introduction</b>	<b>1</b>
<b>2</b>	<b>A comparison of the experimental data and the corresponding thresholds</b>	<b>3</b>
2.1	Isoscalar $XYZ$ data without hidden-strange quantum number	5
2.2	Isoscalar $XYZ$ data with hidden-strange quantum number	7
2.3	Isovector $XYZ$ data without hidden-strange quantum number	10
<b>3</b>	<b>Mass spectrum and decays of the charmoniulike molecular tetraquark systems</b>	<b>13</b>
3.1	Theoretical framework	14
3.1.1	OBE effective potentials	14
3.1.2	Quark-interchange model	19
3.2	Numerical results and discussions	23
3.2.1	Isoscalar charmonium-like molecular systems without hidden-strange quantum number	24
3.2.2	Charmonium-like molecular tetraquark systems with hidden-strange quantum number	36
3.2.3	Isovector charmonium-like molecular tetraquark systems	43
<b>4</b>	<b>Summary</b>	<b>44</b>
<b>A</b>	<b>Relevant subpotentials</b>	<b>46</b>
A.1	Hidden-charm molecular tetraquark systems without hidden-strange quantum number	47
A.2	Hidden-charm tetraquark systems with hidden-strange quantum number	50
<b>B</b>	<b><math>D\bar{D}</math> and <math>D\bar{D}^*</math> systems</b>	<b>52</b>

---

## 1 Introduction

In 2015, the LHCb Collaboration analyzed the  $\Lambda_b \rightarrow J/\psi p K$  decay and reported two  $P_c$  structures ( $P_c(4380)$  and  $P_c(4450)$ ) existing in the  $J/\psi p$  invariant mass spectrum [1]. After four years, the LHCb revised  $\Lambda_b \rightarrow J/\psi p K$  process with higher precision data and found that former  $P_c(4450)$  contains two substructures  $P_c(4440)$  and  $P_c(4457)$  [2]. Besides, a new enhancement structure  $P_c(4312)$  was announced [2]. In fact, this updated result of  $P_c$  states provides a direct evidence to support the existence of the hidden-charm molecular pentaquark states [3–9].

In Figure 1, we present the quark level description of the  $\Lambda_b \rightarrow P_c K$ , which is a typical hadronic weak decay. If replacing  $ud$  quarks of the  $\Lambda_b$  by an anti-quark  $\bar{q}$ , we may get the

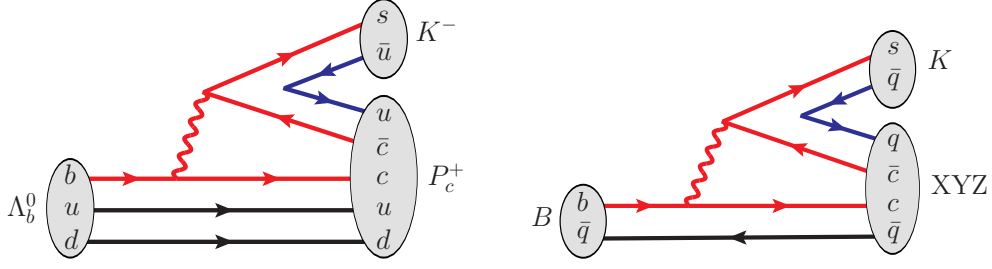


**Figure 1.** The production mechanisms of the  $P_c$  states from the  $\Lambda_b$  baryon decays and the  $XYZ$  states from the  $B$  meson decays.

$B \rightarrow XYZ + K$  process, where  $XYZ$  denote the charmonium-like structures. Obviously, due to the similar production mechanism between the  $\Lambda_b \rightarrow P_c K$  and  $B \rightarrow XYZ + K$  (see Figure 1), we naturally conjecture that the  $B \rightarrow XYZ + K$  should be the ideal processes to produce the hidden-charm molecular tetraquark states, especially with establishing the hidden-charm molecular tetraquark states.

In fact, the road of identifying the hidden-charm molecular tetraquark states is getting confusing [10–16]. In 2004, the Belle Collaboration reported the observation of the charmonium-like state  $Y(3940)$  in the  $J/\psi\omega$  invariant mass spectrum of the  $B \rightarrow J/\psi\omega K$  [17]. In 2009, the CDF Collaboration observed another charmonium-like state  $Y(4140)$  in the  $J/\psi\phi$  invariant mass spectrum of the  $B \rightarrow J/\psi\phi K$  [18]. In Ref. [19], Liu and Zhu noticed the similarity between the  $Y(3940)$  and  $Y(4140)$ , and proposed  $S$ -wave  $D^*\bar{D}^*$  and  $D_s^*\bar{D}_s^*$  molecular states assignment to the  $Y(3940)$  and  $Y(4140)$ , respectively, where the  $J^{PC}$  quantum numbers for the  $Y(3940)$  and  $Y(4140)$  should be either  $0^{++}$  or  $2^{++}$  due to a simple selection rules from the parity and angular momentum conservation [19]. In the subsequent experiments, the LHCb analyzed the  $B \rightarrow J/\psi\phi K$  process, where the  $Y(4140)$  was confirmed and other three new structures  $X(4274)$ ,  $X(4500)$  and  $X(4700)$  were discovered in the  $J/\psi\phi$  invariant mass spectrum [20]. However, the LHCb announced that the preferred  $J^{PC}$  quantum number of the  $Y(4140)$  is  $1^{++}$  [21], which obviously cannot support the molecular assignment to the  $Y(4140)$  suggested in Ref. [19]. If checking the experimental and theoretical research status of the  $Z(4430)$ , which was reported by the Belle in the  $B \rightarrow \psi(3686)\pi K$  [22], the same situation again happens. Since the  $Z(4430)$  is near the threshold of  $D^*\bar{D}_1^{(\prime)}$  channel, the authors of Refs. [23, 24] suggested that the  $Z(4430)$  can be the good candidate of the  $S$ -wave  $D_1\bar{D}^*$  molecular state<sup>1</sup> with  $J^P = 0^-, 1^-, 2^-$  by the one-boson-exchange (OBE) model calculation. However, the Belle [25] and LHCb [26] reanalyzed the  $B \rightarrow \psi(3686)\pi K$  and indicated that the  $Z(4430)$  has quantum number  $J^P = 1^+$ , which is contradict with the  $S$ -wave  $D_1\bar{D}^*$  molecular state assignment [23, 24].

Although there were a dozen of charmonium-like structures reported by experiments in the  $B$  meson decays [14], unfortunately we have not definitely identify one hidden-charm molecular tetraquark state until now [10–16]. It is big challenge to assign the molecular state explanations to the charmonium-like structures from the  $B \rightarrow XYZ + K$  processes.

<sup>1</sup>To be convenient, we use the shorthand notation  $\mathcal{A}\bar{\mathcal{B}}$  to denote the  $\mathcal{A}\bar{\mathcal{B}} + c.c.$  system in the following parts, where the notations  $\mathcal{A}$  and  $\mathcal{B}$  represent two different charmed (charmed-strange) mesons, respectively.

If we still believe the similar production mechanism between the  $\Lambda_b \rightarrow P_c K$  and  $B \rightarrow XYZ + K$  (see Figure 1), we have reason to believe the existence of the hidden-charm molecular tetraquark state in the  $B \rightarrow XYZ + K$  processes. Facing this situation mentioned above, we should try to find possible solutions existing in the reported experimental data of the  $B \rightarrow XYZ + K$ . In fact, the lesson of observation of the  $P_c$  states in 2015 [1] and 2019 [2] may inspire us. In 2015, the LHCb measured the  $J^P$  quantum numbers of the  $P_c(4380)$  and  $P_c(4450)$ , gave that their preferred  $J^P$  quantum numbers are of opposite parity [1], which is a challenge to the hadronic molecular assignment [9]. This situation was dramatically changed with further LHCb experiment in 2019, where the  $P_c(4450)$  is composed of two substructures  $P_c(4440)$  and  $P_c(4457)$  [2], which means that the measurement of spin-parity quantum number of the observed  $P_c(4450)$  can be ignored [1]. To some extent, this fact reflects the importance of higher precision to the study of hadron spectroscopy.

With the running of the Belle II [27] and the accumulation of Run II and Run III data at the LHCb [28], obviously investigation of the charmonium-like  $XYZ$  states must enter a new era. Thus, we should systematically reexamine the correlation of the hidden-charm molecular states and the charmonium-like structures existing in the  $B \rightarrow XYZ + K$  processes [10–16], where the constraint from  $J^{PC}$  quantum numbers and so-called resonance parameters of depicting these observed charmonium-like  $XYZ$  structures should be more cautious in the interpretation of these resonances as the molecular states.

Along this line, we systematically restudy the  $S$ -wave interactions between a charmed (charmed-strange) meson and an anti-charmed (anti-charmed-strange) meson in the framework of the one-boson-exchange (OBE) model in this work [10, 13]. In concrete calculations, both the  $S$ - $D$  wave mixing effect and the coupled channel effect are taken into account. Additionally, we focus on two-body hidden-charm decay behaviors of these possible molecular tetraquark candidates with the quark-interchange model [29–32], which may play important role to search and identify these discussed molecular tetraquark candidates. Based on above discussion, we find a series of possible hints of the hidden-charm molecular tetraquarks existing in the released experimental data of the  $B$  meson decays, which will be a main task of the present work.

The remainder of this paper is organized as follows. In Sec. 2, a comparison of the relevant experimental data and the corresponding thresholds will be given. In Sec. 3, the mass spectrum and the two-body hidden-charm decay behaviors of these discussed hidden-charm molecular tetraquark systems will be given, and a series of possible hints of the hidden-charm molecular tetraquarks existing in the reported experimental data of the  $B$  meson decays will be presented. Finally, a brief summary will be given in Sec. 4.

## 2 A comparison of the experimental data and the corresponding thresholds

In this work, the main task is to find possible hints of the hidden-charm molecular tetraquarks existing in the reported experimental data of the  $B \rightarrow XYZ + K$  [14], and the hidden-charm molecular tetraquarks are composed of a charmed (charmed-strange) meson and an anti-charmed (anti-charmed-strange) meson. Thus, we need to make comparison of the

involved experimental data and the corresponding thresholds of charmed meson pairs or charmed-strange meson pairs.

**Table 1.** The thresholds of charmed (charmed-strange) meson pairs (in unit of MeV).

Without hidden-strange quantum number						
$DD$	$DD^*$	$D^*D^*$	$DD_0^*$	$DD_1$	$DD_1'$	$DD_2^*$
3734.48	3875.80	4017.12	4191.74	4289.24	4294.24	4330.29
$D^*D_0^*$	$D^*D_1$	$D^*D_1'$	$D^*D_2^*$	$D_0^*D_0^*$	$D_0^*D_1$	$D_0^*D_1'$
4333.06	4430.56	4435.56	4471.61	4649.00	4746.50	4751.50
$D_0^*D_2^*$	$D_1D_1$	$D_1'D_1$	$D_1'D_1'$	$D_1D_2^*$	$D_1'D_2^*$	$D_2^*D_2^*$
4787.55	4844.00	4849.00	4854.00	4885.05	4890.05	4926.10
With hidden-strange quantum number						
$D_sD_s$	$D_sD_s^*$	$D_s^*D_s^*$	$D_sD_{s0}^*$	$D_sD_{s1}'$	$D_s^*D_{s0}^*$	$D_sD_{s1}$
3936.68	4080.54	4224.40	4286.14	4427.84	4430	4503.45
$D_sD_{s2}^*$	$D_s^*D_{s1}'$	$D_{s0}^*D_{s0}^*$	$D_s^*D_{s1}$	$D_s^*D_{s2}^*$	$D_{s0}^*D_{s1}'$	$D_{s0}^*D_{s1}$
4537.44	4571.70	4635.60	4647.31	4681.30	4777.30	4852.91
$D_{s0}^*D_{s2}^*$	$D_{s1}'D_{s1}'$	$D_{s1}'D_{s1}$	$D_{s1}D_{s1}$	$D_{s1}'D_{s2}^*$	$D_{s1}D_{s2}^*$	$D_{s2}^*D_{s2}^*$
4886.90	4919.00	4994.61	5028.60	5070.22	5104.20	5138.20

Usually, the  $S$ -wave and  $P$ -wave charmed mesons can be grouped into three doublets  $H = [D(0^-), D^*(1^-)]$ ,  $S = [D_0^*(0^+), D_1'(1^+)]$ , and  $T = [D_1(1^+), D_2^*(2^+)]$  according to the heavy quark spin symmetry [33]. Similarly, there also exist three doublets for the  $S$ -wave and  $P$ -wave charmed-strange mesons, i.e.,  $H = [D_s, D_s^*]$ ,  $S = [D_{s0}^*, D_{s1}']$ , and  $T = [D_{s1}, D_{s2}^*]$  [33]. In Table 1, we list these thresholds of charmed meson pairs or charmed-strange meson pairs [34], which are distributed over a very wide energy range  $3.7 \sim 5.2$  GeV. However, if only considering the kinetics of the  $B \rightarrow XYZ + K$  decays, the maximum mass of the involved  $XYZ$  structures should be  $M(XYZ)_{max} = M(B) - M(K) = 4783$  MeV, which makes us select these thresholds with mass lower than 4783 MeV when making further analysis. Additionally, the charmed mesons in  $S$ -doublet have broad widths around several hundred MeV [34], which may be a obstacle for the formation of the hadronic molecular states [35, 36]. Different from the charmed mesons in  $S$ -doublet, these charmed mesons in the  $H$ -doublet and  $T$ -doublet have narrow widths [34], which can be regarded as the suitable components to form the hadronic molecular states [24, 35, 36]. Just considering

the above fact, we consider the cases of  $H\bar{H}$  and  $H\bar{T}$  for charmed meson pairs and the cases of  $H\bar{H}$ ,  $H\bar{S}$ , and  $H\bar{T}$  for charmed-strange meson pairs when performing a comparison of these thresholds with the released experimental data.

At present, the experimental information of the  $B \rightarrow XYZ + K$  are very abundant [10–16]. Here, the  $XYZ$  data are from the  $J/\psi\pi\pi$  invariant mass spectrum<sup>2</sup> of the  $B \rightarrow J/\psi\pi\pi K$  [37], the  $J/\psi\omega$  invariant mass spectrum of the  $B \rightarrow J/\psi\omega K$  [17, 51, 52], the  $J/\psi\eta$  invariant mass spectrum of the  $B \rightarrow J/\psi\eta K$  [53], the  $J/\psi\phi$  invariant mass spectrum of the  $B \rightarrow J/\psi\phi K$  [18, 20, 21, 54–58], the  $\eta_c\pi$  invariant mass spectrum of the  $B \rightarrow \eta_c\pi K$  [60], the  $J/\psi\pi$  invariant mass spectrum of the  $B \rightarrow J/\psi\pi K$  [61–63], the  $\psi(3686)\pi$  invariant mass spectrum of the  $B \rightarrow \psi(3686)\pi K$  [22, 25, 26, 64], the  $\chi_{c1}\pi$  invariant mass spectrum of the  $B \rightarrow \chi_{c1}\pi K$  [65–68], and the  $\chi_{c2}\pi$  invariant mass spectrum of the  $B \rightarrow \chi_{c2}\pi K$  [67]. For clearly discussing the present issue, we categorized these  $XYZ$  data into three groups:

- Isoscalar  $XYZ$  data without hidden-strange quantum number are involved in the  $B \rightarrow J/\psi\omega K$  and  $B \rightarrow J/\psi\eta K$ ;
- Isoscalar  $XYZ$  data with hidden-strange quantum number are relevant to the  $B \rightarrow J/\psi\phi K$ ;
- Isovector  $XYZ$  data without hidden-strange quantum number have relation to five decay processes, i.e., the  $B \rightarrow \eta_c\pi K$ ,  $B \rightarrow J/\psi\pi K$ ,  $B \rightarrow \psi(3686)\pi K$ ,  $B \rightarrow \chi_{c1}\pi K$ , and  $B \rightarrow \chi_{c2}\pi K$ .

In the following, we adopt this line to make comparison of the released experimental data and the corresponding thresholds.

## 2.1 Isoscalar $XYZ$ data without hidden-strange quantum number

In 2005, the Belle Collaboration analyzed the  $J/\psi\omega$  invariant mass spectrum of the  $B \rightarrow J/\psi\omega K$  decay, where the charmonium-like structure  $Y(3940)$  was reported, which can be depicted by resonance parameters  $M = (3943 \pm 11 \pm 13)$  MeV and  $\Gamma = (87 \pm 22 \pm 26)$  MeV [17]. In 2008, the BaBar Collaboration confirmed this observation in the same process with a lower mass, named as the  $Y(3915)$ , and its mass and width were measured to be  $(M, \Gamma) = (3914.6^{+3.8}_{-3.4} \pm 2.0$  MeV,  $34^{+12}_{-8} \pm 5$  MeV) [51]. In the subsequent BaBar experiment in 2010 [52], the mass and width of the  $Y(3915)$  were measured to be  $M = (3919.1^{+3.8}_{-3.5} \pm 2.0)$  MeV and  $\Gamma = (31^{+10}_{-8} \pm 5)$  MeV, respectively.

If checking these data of the  $J/\psi\omega$  invariant mass spectrum of the  $B \rightarrow J/\psi\omega K$  from the Belle and BaBar [17, 51, 52], we may find the impact of experimental precision on reflecting the details. In the Belle data [17], there are only four experimental points sandwiched by the  $D\bar{D}^*$  and  $D^*\bar{D}^*$  thresholds. After several years, the number of experimental points in this energy range reach up to 12 and 14, which correspond to the BaBar data measured in 2008 [51] and 2010 [52], respectively. In Figure 2, we collect all reported data

<sup>2</sup>In the measured  $J/\psi\pi\pi$  invariant mass spectrum, the charmonium-like state  $X(3872)$  was observed [37], which can be considered as the isoscalar  $D\bar{D}^*$  molecular state with  $J^{PC} = 1^{++}$ . There were extensive discussions of the dynamics of the isoscalar  $D\bar{D}^*$  molecular states [38–50]. Thus, we will not discuss the  $B \rightarrow J/\psi\pi\pi K$  and the relevant  $X(3872)$  in this work.

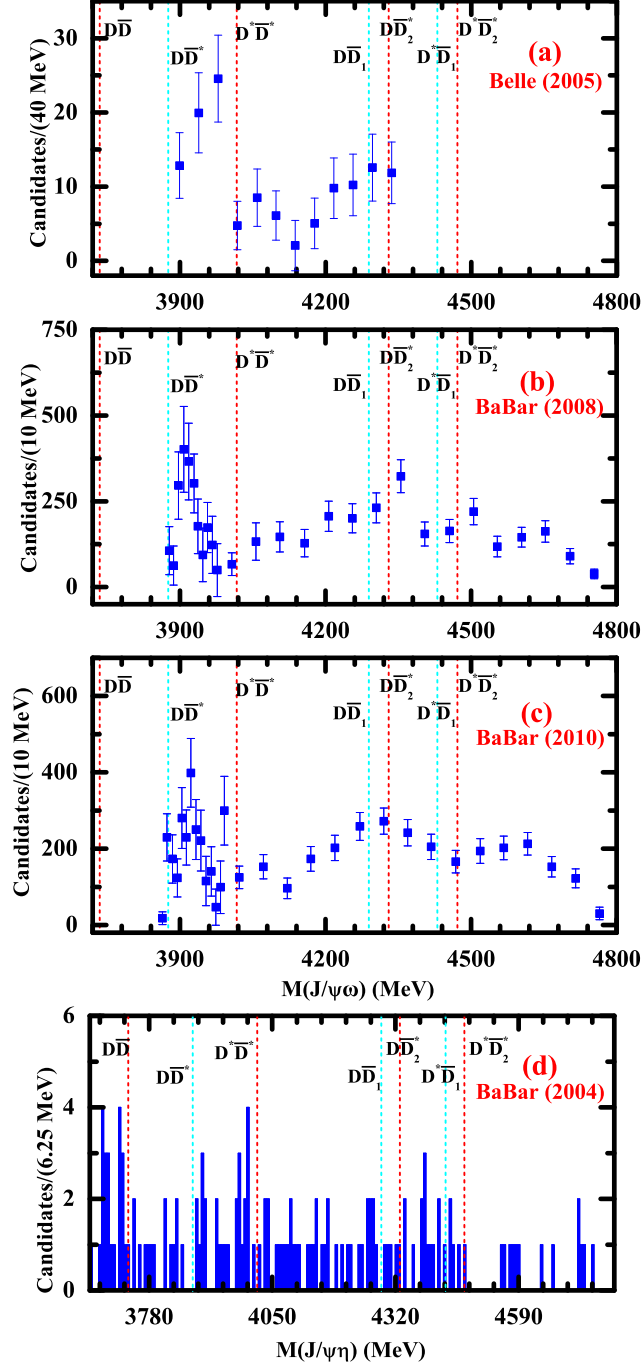


**Figure 2.** (color online) The  $J/\psi\omega$  and  $J/\psi\eta$  invariant mass distributions in the  $B \rightarrow J/\psi\omega K$  and  $B \rightarrow J/\psi\eta K$ , respectively, and the comparison with the thresholds of charmed meson pairs. Here, the experimental data of the  $J/\psi\omega$  invariant mass spectrum are taken from the Belle [17], BaBar [51], and BaBar [52], which correspond to diagrams (a)-(c), and the experimental data of the  $J/\psi\eta$  invariant mass spectrum is from the BaBar measurement [53] (see diagram (d)).



of the  $J/\psi\omega$  invariant mass spectrum from the  $B \rightarrow J/\psi\omega K$  [17, 51, 52]. In fact, the BaBar data released in 2008 [51] show the possibility of existing two structures around 3.9 GeV below the  $D^*\bar{D}^*$  threshold in the  $J/\psi\omega$  invariant mass spectrum. Especially, the BaBar measurement in 2010 further enforce this possibility [52].

If  $D^*$  and  $\bar{D}^*$  can be bound together to form the hidden-charm molecular tetraquarks, the  $J^{PC}$  quantum numbers of the  $S$ -wave isoscalar  $D^*\bar{D}^*$  molecular system must be  $0^{++}$ ,  $1^{+-}$ , and  $2^{++}$  [19]. Under this assumption, the behavior of mass spectrum of the  $S$ -wave isoscalar  $D^*\bar{D}^*$  molecular states can explain why two substructures around 3.9 GeV exist in the  $J/\psi\omega$  invariant mass spectrum of the  $B \rightarrow J/\psi\omega K$  [17, 51, 52]. Thus, we strongly encourage our experimental colleagues to focus on the detail of the structures around 3.9 GeV with more precise data. If these substructures can be confirmed in future experiments discussed above, it will provide strong evidence of existing the hidden-charm molecular tetraquark. Later, we will revisit a dynamics study of the  $S$ -wave isoscalar  $D^*\bar{D}^*$  system, and come back to address this point.

Besides the enhancement structures around 3.9 GeV exist in the  $J/\psi\omega$  invariant mass spectrum, we may find a very broad structure around 4.3 GeV exists in the  $J/\psi\omega$  invariant mass spectrum of the  $B \rightarrow J/\psi\omega K$  [17, 51, 52], where there exist four thresholds ( $D\bar{D}_1$ ,  $D\bar{D}_2^*$ ,  $D^*\bar{D}_1$ , and  $D^*\bar{D}_2^*$ ) in this energy range, which inspire our interest in exploring whether the isoscalar  $D\bar{D}_1$ ,  $D\bar{D}_2^*$ ,  $D^*\bar{D}_1$ , and  $D^*\bar{D}_2^*$  molecular tetraquarks exist in nature, which will be one of tasks in this work. Obviously, the details of such broad structure around 4.3 GeV should be given in future experiments with more precise data accumulation.

For the isoscalar  $XYZ$  data without hidden-strange quantum number, we should mention the measurement of the  $J/\psi\eta$  invariant mass spectrum in the  $B \rightarrow J/\psi\eta K$  decay. In 2004, the BaBar released the result of the  $J/\psi\eta$  invariant mass spectrum in the  $B \rightarrow J/\psi\eta K$  [53]. In Figure 2, we compare the BaBar data with the several thresholds of charmed meson pairs, and may find the evidence of one structure below  $D^*\bar{D}^*$  threshold and possible enhancement structure around 4.3 GeV which overlaps with the  $D\bar{D}_1$ ,  $D\bar{D}_2^*$ ,  $D^*\bar{D}_1$ , and  $D^*\bar{D}_2^*$  thresholds. In fact, this phenomenon again shows studying the isoscalar  $D^*\bar{D}^*$ ,  $D\bar{D}_1$ ,  $D\bar{D}_2^*$ ,  $D^*\bar{D}_1$ , and  $D^*\bar{D}_2^*$  hadronic molecular states is an urgent research issue, which may provide crucial information to find the evidence of the existence of the hidden-charm molecular tetraquark.

## 2.2 Isoscalar $XYZ$ data with hidden-strange quantum number

Up to now, the  $B \rightarrow J/\psi\phi K$  decay have been analyzed by the different experiment collaborations [18, 20, 21, 54–59], where we are mainly interested in the experimental data of the  $J/\psi\phi$  invariant mass spectrum from the CDF [18], CMS [54], and LHCb [20] in the following discussion. Since the quark components of the  $\phi$  and  $J/\psi$  are the  $s\bar{s}$  and  $c\bar{c}$ , respectively, we present the thresholds of charmed-strange meson pairs in Figure 3 when making comparison with these released experimental data.

First, we should brief introduce the experimental status of the obtained  $J/\psi\phi$  invariant mass spectrum in the  $B \rightarrow J/\psi\phi K$  decay [18, 20, 54]. As shown in Figure 3 (a), the CDF Collaboration reported the charmonium-like structure  $Y(4140)$  in the  $J/\psi\phi$  mass

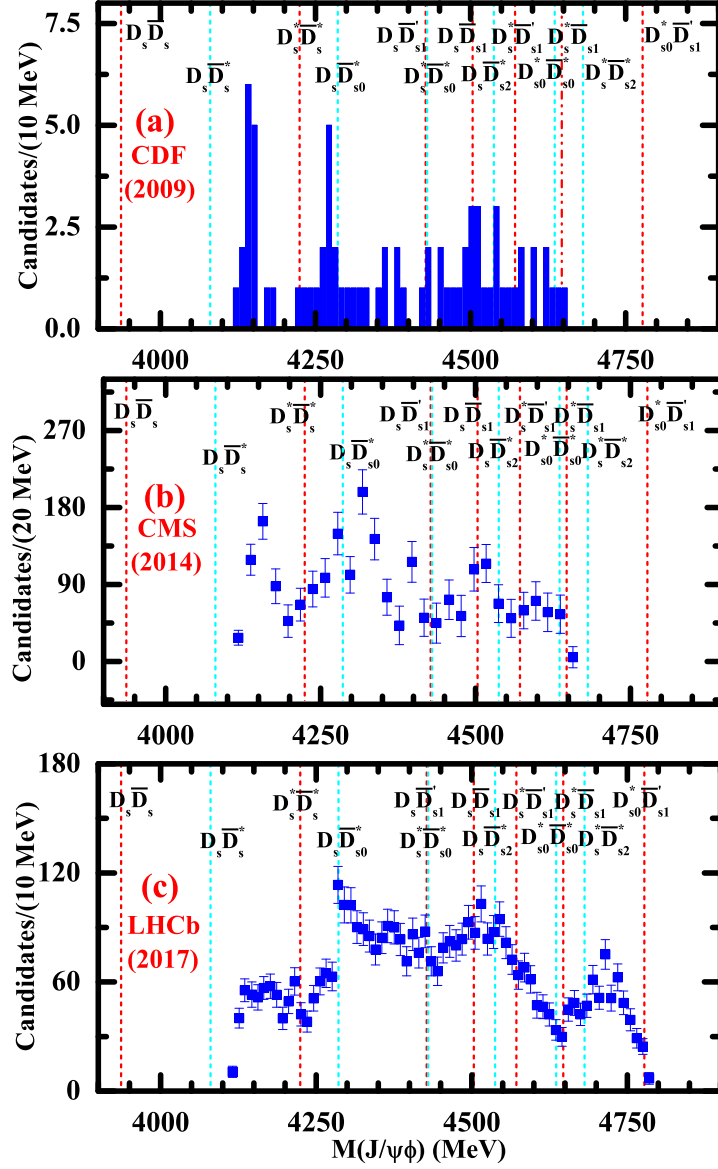


**Figure 3.** (color online) The measured  $J/\psi\phi$  invariant mass distribution of the  $B \rightarrow J/\psi\phi K$  and the thresholds of charmed-strange meson pairs. Here, the experimental data are taken from the CDF [18], CMS [54], and LHCb [20], which correspond to diagrams (a)-(c).

spectrum of the  $B \rightarrow J/\psi\phi K$  decay in 2009 [18]. When depicting this enhancement structure, the resonance parameters can be obtained, i.e., the mass and width of the  $Y(4140)$  were measured to be  $M = (4143.0 \pm 2.9 \pm 1.2) \text{ MeV}$  and  $\Gamma = (11.7^{+8.3}_{-5.0} \pm 3.7) \text{ MeV}$  [18], respectively. Besides the  $Y(4140)$  structure, the CDF also reported another enhancement structure, named as the  $Y(4274)$ , in the  $J/\psi\phi$  invariant mass spectrum, where its mass and width are  $(M, \Gamma) = (4274.4^{+8.4}_{-6.7} \pm 1.9 \text{ MeV}, 32.3^{+21.9}_{-15.3} \pm 7.6 \text{ MeV})$  [18], respectively. Later, the CMS confirmed these two structures  $Y(4140)$  and  $Y(4274)$  in the same decay process in 2014, where the resonance parameters of the  $Y(4140)$  and  $Y(4274)$

were measured to be  $(M, \Gamma)_{Y(4140)} = (4148.0 \pm 2.4 \pm 6.3 \text{ MeV}, 28_{-11}^{+15} \pm 19 \text{ MeV})$  and  $(M, \Gamma)_{Y(4274)} = (4313.8 \pm 5.3 \pm 7.3 \text{ MeV}, 38_{-15}^{+30} \pm 16 \text{ MeV})$  [54], respectively. Surprisingly, the LHCb Collaboration announced four charmonium-like resonances in the  $J/\psi\phi$  mass spectrum of the  $B \rightarrow J/\psi\phi K$  decay in 2017 [20]. Here, we collect their resonance parameters, i.e.,  $(M, \Gamma)_{Y(4140)} = (4146.5 \pm 4.5_{-2.8}^{+4.6} \text{ MeV}, 83 \pm 21_{-14}^{+21} \text{ MeV})$ ,  $(M, \Gamma)_{Y(4274)} = (4273.3 \pm 8.3_{-3.6}^{+17.2} \text{ MeV}, 56.2 \pm 10.9_{-11.1}^{+8.4} \text{ MeV})$ ,  $(M, \Gamma)_{X(4500)} = (4506 \pm 11_{-15}^{+12} \text{ MeV}, 92 \pm 21_{-20}^{+21} \text{ MeV})$ , and  $(M, \Gamma)_{X(4700)} = (4704 \pm 10_{-24}^{+14} \text{ MeV}, 120 \pm 31_{-33}^{+42} \text{ MeV})$  [20].

If comparing three experimental data listed in Figure 3, we find that the precision of the LHCb data [20] is higher than the CDF and CMS data [18, 54], where there are 12 experimental points in the energy range sandwiched by the  $D_s\bar{D}_s^*$  and  $D_s^*\bar{D}_s^*$  thresholds for the LHCb data [20], which reflect some abundant details difference from former CDF and CMS [18, 54]. When only adopting a Breit-Wigner formula to describe this resonance structure around 4140 MeV, the width given by the LHCb [20] becomes wider than that from the CDF and CMS [18, 54]. This phenomenon is puzzling for us since the LHCb released this result [20], especially the recent LHCb result of the  $Y(4140)$  [59].

We notice an interesting fact that this structure around 4140 MeV reported by the CDF is below the  $D_s^*\bar{D}_s^*$  threshold [18], and Liu and Zhu proposed that the  $Y(4140)$  observed by the CDF can be regarded as partner of the  $Y(3940)$  due to the similarity between the  $Y(3940)$  and  $Y(4140)$  in 2009 [19]. Thus, the  $D_s^*\bar{D}_s^*$  hadronic molecular state explanation to the  $Y(4140)$  was given [19]. Along this line, there may exist  $S$ -wave  $D_s^*\bar{D}_s^*$  molecular states, which is similar to the situation of the  $S$ -wave isoscalar  $D^*\bar{D}^*$  molecular system discussed in Sec. 2.1. Facing such abundant details given by the LHCb in 2017 [20], we may conjecture that the  $Y(4140)$  structure may be contain at least two substructures, which can be tested by future experiments based on more precise data. If introducing this proposal, the conclusion of the spin-parity quantum number  $J^{PC} = 1^{++}$  for the  $Y(4140)$  given by the LHCb seems unreliable<sup>3</sup> [20]. Here, we need to mention that the recent LHCb Collaboration updated the amplitude analysis of the  $B^+ \rightarrow J/\psi\phi K^+$  decay with higher precision data and reported the  $X(4140)$  with  $J^{PC} = 1^{++}$  and  $X(4150)$  with  $J^{PC} = 2^{-+}$  [59], which imply the very complicated structures around the  $D_s^*\bar{D}_s^*$  threshold. In the following, the investigation of the  $S$ -wave  $D_s^*\bar{D}_s^*$  hadronic molecular system will become a main point of this work, which will be further discussed in the next section.

Besides the structure around 4140 MeV existing in the  $J/\psi\phi$  invariant mass spectrum, we should focus on the  $Y(4274)$  [18, 20, 54], which is just near the  $D_s\bar{D}_{s0}^*$  threshold. Thus, the study of the  $D_s\bar{D}_{s0}^*$  molecular system will be paid attention in this work. Although the LHCb reported  $X(4500)$  and  $X(4700)$  in 2017 [20], we can find more abundant structures above 4250 MeV existing in the  $J/\psi\phi$  invariant mass spectrum if carefully checking the LHCb data [20]. Indeed, the recent LHCb Collaboration announced the observation of other new resonance structures existing in this energy range with more precise data, i.e., the  $X(4630)$  with  $J^{PC} = 1^{-+}$  and  $X(4685)$  with  $J^{PC} = 1^{++}$  [59]. We also notice that there are

---

<sup>3</sup>For the  $S$ -wave  $D_s^*\bar{D}_s^*$  molecular system, its  $J^{PC}$  quantum numbers are either  $0^{++}$  or  $2^{++}$ , which is due to a selection rule for the quantum numbers [19]. However, the LHCb measurement suggested  $J^{PC} = 1^{++}$  for the  $Y(4140)$  [20], which results in the difficulty to understand the  $Y(4140)$  under the hadronic molecular state assignment.

abundant thresholds of charmed-strange meson pairs in this interesting energy range. Thus, we will investigate the hidden-charm and hidden-strange molecular tetraquarks involved these thresholds in this work.

### 2.3 Isovector $XYZ$ data without hidden-strange quantum number

In the past 18 years, the isovector  $XYZ$  data from the  $B \rightarrow XYZ + K$  were accumulated [10–16]. In Figs. 4–5, we collected all relevant experimental data and make a comparison with several typical thresholds of charmed meson pairs. For different decay processes listed in Figs. 4–5, we briefly review the experimental information:

1. The  $B \rightarrow \psi(2S)\pi K$  decay: As a super star among these reported charged charmonium-like structures, the  $Z^+(4430)$  structure was first observed by the Belle Collaboration in the  $\psi(2S)\pi$  invariant mass distribution of the  $B \rightarrow \psi(2S)\pi K$  decay in 2008 [22]. Here, its mass and width were measured to be  $M = (4433 \pm 4 \pm 2)$  MeV and  $\Gamma = (45_{-13}^{+18+30})$  MeV, respectively [22]. In the following years, the Belle Collaboration continued their studies on the  $Z^+(4430)$ , and the measured mass of the  $Z^+(4430)$  structure are  $M = (4443_{-12}^{+15+19})$  MeV [64] and  $M = (4485_{-22}^{+22+28})$  MeV [25], respectively. After ten years, the LHCb Collaboration confirmed the existence of the  $Z^+(4430)$  structure [26], and the resonance parameters are  $M = (4475 \pm 7_{-25}^{+15})$  MeV and  $\Gamma = (172 \pm 13_{-34}^{+37})$  MeV, respectively. But, the width from the LHCb [26] is more broad than that from the Belle [22, 25, 64]. Additionally, the LHCb found a new structure  $Z^+(4240)$  in the  $\psi(2S)\pi$  invariant mass distribution of the  $B \rightarrow \psi(2S)\pi K$ , which can be depicted by resonance parameters  $M = (4239 \pm 18_{-10}^{+45})$  MeV and  $\Gamma = (220 \pm 47_{-74}^{+108})$  MeV, respectively [26]. Comparing with the Belle data [22, 25, 64], the LHCb data have smaller error bars [26]. Since the  $Z^+(4430)$  structure is near several thresholds of charmed meson pair, there were extensive discussion of the hidden-charm molecular tetraquark explanation to the  $Z^+(4430)$  [23, 24, 69]. In this work, we will still dedicate this topic, which is the study of the isovector hidden-charm molecular tetraquark involved in this energy range.
2. The  $B \rightarrow \eta_c \pi K$  decay: In 2018, the LHCb found the evidence of a broad charmonium-like structure in the  $\eta_c \pi$  invariant mass spectrum of the  $B \rightarrow \eta_c \pi K$  decay, which was named as the  $X(4100)$  with the mass  $M = (4096 \pm 20_{-22}^{+18})$  MeV and the width  $\Gamma = (152 \pm 58_{-35}^{+60})$  MeV [60]. In fact, there exists event accumulation around 4.5 GeV, where several thresholds of charmed meson pairs can be found (see Figure 4 (e)).
3. The  $B \rightarrow \chi_{c1} \pi K$  decay: For the  $\chi_{c1} \pi$  invariant mass distribution in the  $B \rightarrow \chi_{c1} \pi K$  decay, two charged charmonium-like structures  $Z^+(4051)$  and  $Z^+(4248)$  were announced by the Belle Collaboration in the exclusive  $B \rightarrow \chi_{c1} \pi K$  decay [65], where their resonance parameters were measured to be  $(M, \Gamma)_{Z^+(4051)} = (4051 \pm 14_{-41}^{+20}, 82_{-17}^{+21+47})$  MeV and  $(M, \Gamma)_{Z^+(4248)} = (4248_{-29}^{+44+180}, 177_{-39}^{+54+316})$  MeV [65], respectively. However, these two charged charmonium-like structures were not seen in the following BaBar experiment [66]. In 2016, the Belle Collaboration carried

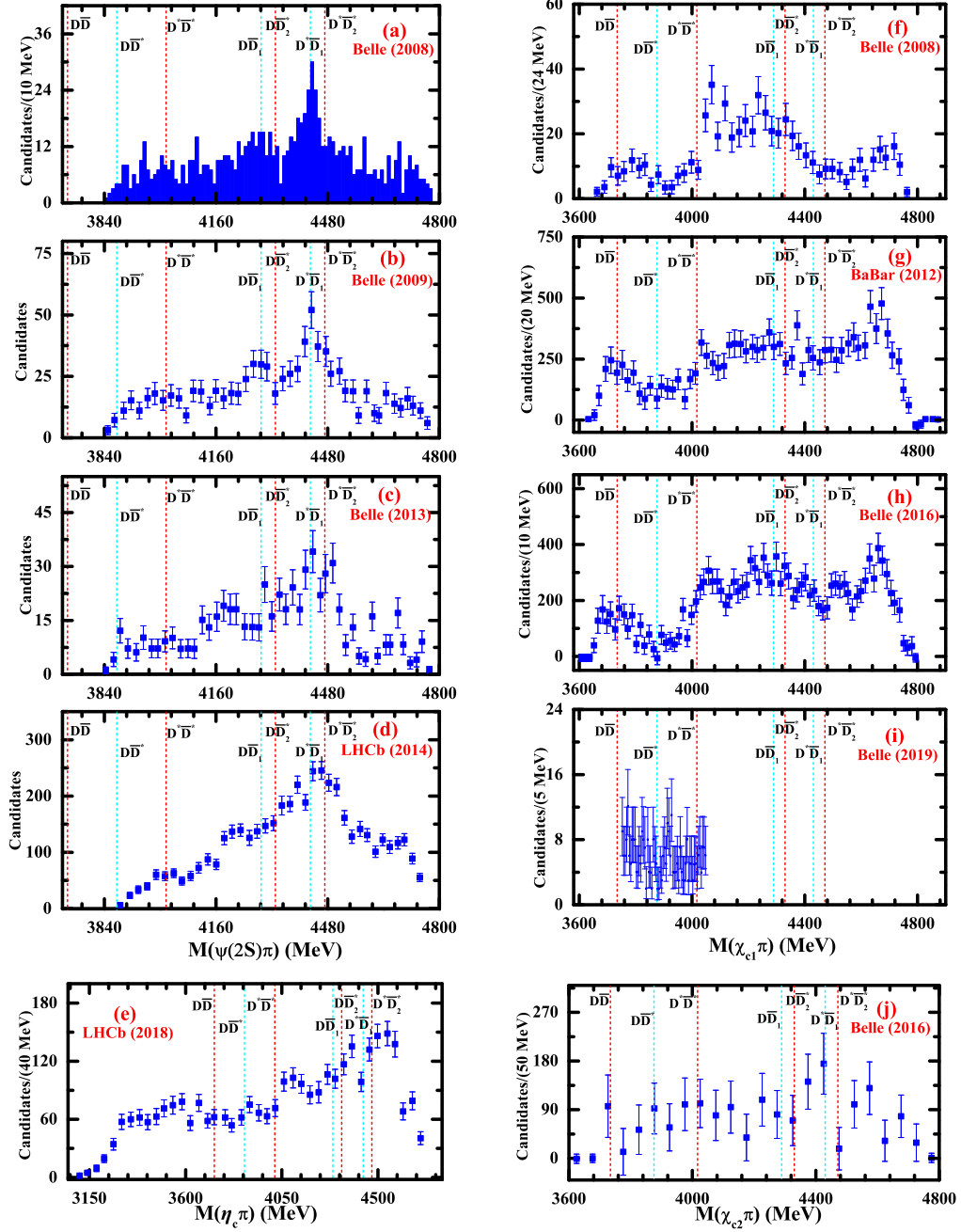


**Figure 4.** (color online) The measured  $\psi(2S)\pi$ ,  $\eta_c\pi$ ,  $\chi_{c1}\pi$  and  $\chi_{c2}\pi$  invariant mass distributions in the  $B \rightarrow XYZ + K$  decays, and the comparison with the thresholds of charmed meson pairs. Here, the experimental data of the  $\psi(2S)\pi$  are taken from (a) the Belle [22], (b) the Belle [64], (c) the Belle [25], and (d) the LHCb [26], while the experimental data of  $\eta_c\pi$  is taken from the LHCb [60] (see diagram (e)). In addition, the experimental data of  $\chi_{c1}\pi$  are taken from (f) the Belle [65], (g) the BaBar [66], (h) the Belle [67], and (i) the Belle [68], while the experimental result of the  $\chi_{c2}\pi$  invariant mass spectrum is given by the Belle [67] (see diagram (j)).

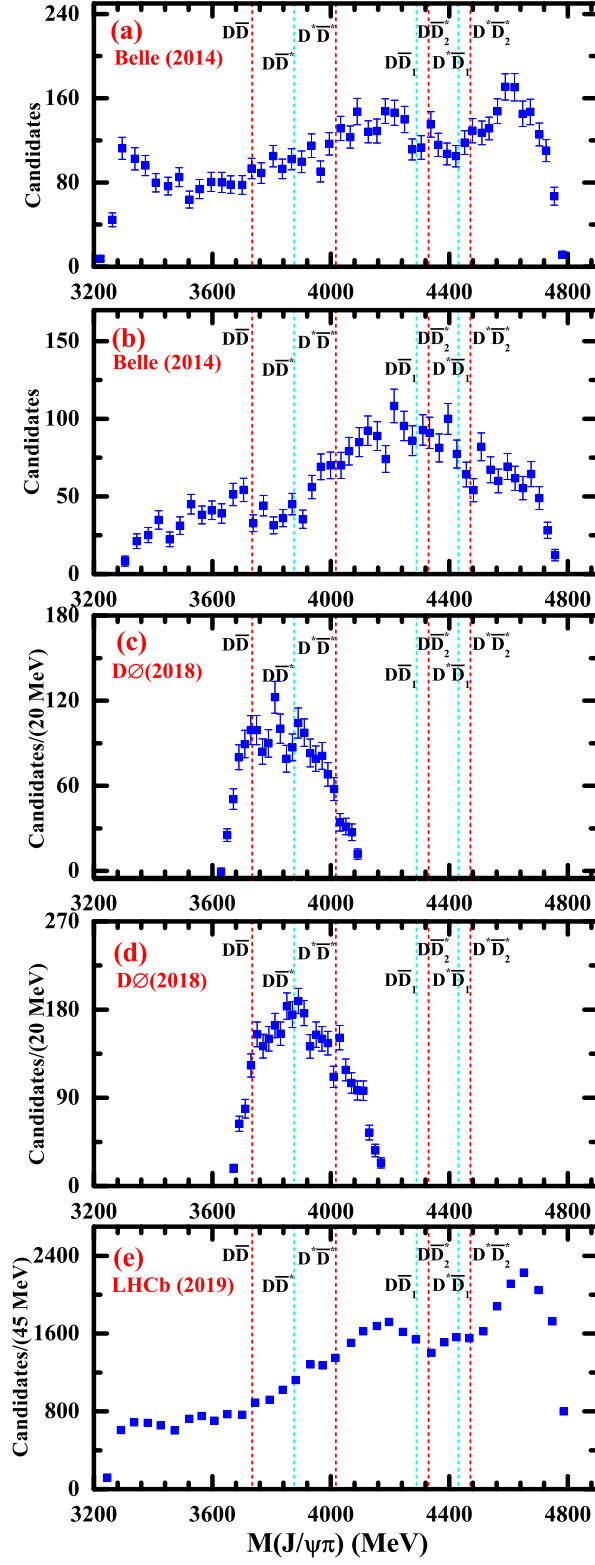


**Figure 5.** (color online) The  $J/\psi\pi$  invariant mass distribution in the  $B \rightarrow J/\psi\pi K$  and the relevant thresholds of charmed meson pairs. Here, the experimental data are taken from the Belle [61] ((a) for  $1.20 \text{ GeV}^2 < m^2(K\pi) < 2.05 \text{ GeV}^2$  and (b) for  $2.05 \text{ GeV}^2 < m^2(K\pi) < 3.20 \text{ GeV}^2$ ), the DØ [62] ((c) for  $4.25 \text{ GeV} < m(J/\psi\pi^+\pi^-) < 4.30 \text{ GeV}$  and (d) for  $4.30 \text{ GeV} < m(J/\psi\pi^+\pi^-) < 4.40 \text{ GeV}$ ), and (e) the LHCb [63], respectively.

out a new measurement of the  $B \rightarrow \chi_{c1}\pi K$ , where the distribution of the  $\chi_{c1}\pi$  invariant mass spectrum was given [67]. In fact, the line shape of the  $\chi_{c1}\pi$  invariant mass spectrum is complicated. Additionally, for searching for the  $X(3872)$  and  $X(3915)$  decaying to the final state  $\chi_{c1}\pi$  in the  $B$  meson decay, the Belle measured the  $\chi_{c1}\pi$  invariant mass spectrum from the  $B$  meson decay, by which they did not find the significant signals of the  $X(3872)$  and  $X(3915)$  [68].

4. The  $B \rightarrow \chi_{c2}\pi K$  decay: In 2016, the Belle Collaboration provided the measured  $\chi_{c2}\pi$  invariant mass spectrum with low precision [67]. Here, the comparison of data and thresholds is shown.
5. The  $B \rightarrow J/\psi\pi K$  decay: As shown in Figure 5 (a)-(b), the Belle<sup>4</sup> Collaboration presented the results of an amplitude analysis of the  $B \rightarrow J/\psi\pi K$  decay in 2014, and reported a very broad charged charmonium-like structure  $Z_c(4200)^+$ , where its mass and width were measured to be  $(M, \Gamma) = (4196_{-29}^{+31+17} \text{ MeV}, 370_{-70}^{+70+70} \text{ MeV})$  [61], respectively. We may find such broad structure overlaps with many thresholds (see Figure 5 (a)-(b) for more details). The correlation of this broad structure with the corresponding isovector hidden-charm molecular tetraquarks should be investigated, which will become an important issue in this work. In 2018, the DØ Collaboration analyzed the data of the  $J/\psi\pi$  invariant mass spectrum from the  $B \rightarrow J/\psi\pi K$  [62], where they only focused on  $3600 < m_{J/\psi\pi} < 4200 \text{ MeV}$  range inspired by the observed  $Z_c(3900)^\pm$  from the BESIII [70] and Belle [71]. And the DØ data show the evidence of charged charmonium-like structure similar to the  $Z_c(3900)^\pm$ , where the measured mass of the  $Z_c(3900)^\pm$  is  $3895.0 \pm 5.2_{-2.7}^{+4.0} \text{ MeV}$ . Since the width information of such structure is still absent in the DØ measurement, it is hard to conclude that the DØ evidence truly corresponds to the  $Z_c(3900)^\pm$  [70, 71]. Additionally, the  $J/\psi\pi$  invariant mass spectrum of the  $B \rightarrow J/\psi\pi K$  decay has been studied by the LHCb Collaboration in 2019 [63], and two enhancement structures are visible at 4200 MeV and 4600 MeV.

As introduced above, the isovector  $XYZ$  data of the  $B \rightarrow XYZ + K$  decays stimulate our interest in exploring the isovector hidden-charm molecular systems, which will be illustrated in Sec. 3. By this study, we want to answer whether these isovector  $XYZ$  structures have close relation to the isovector hidden-charm molecular tetraquarks.

### 3 Mass spectrum and decays of the charmoniulike molecular tetraquark systems

In this section, we restudy the mass spectrum behaviors from a pair of charmed (charm-strange) meson and anti-charmed (anti-charm-strange) meson interactions, these charmed or anti-charmed mesons are in the  $H$ ,  $S$ , and  $T$  doublets. Here, we still adopt the OBE model and consider the  $S - D$  wave mixing effect and the coupled channel effect. As is well

---

<sup>4</sup>Besides announcing the  $Z_c(4200)^+$  structure, the Belle also gave the evidence for the  $Z(4430)^+$  structure [61].



known, since Yukawa firstly proposed the nucleon-nucleon interaction is mediated through the pion-exchange in 1935 [72], the OBE model obtains great promotion. On one hand, theorists consider the scalar meson ( $\sigma$ ) and vector meson ( $\rho/\omega$ ) exchanges interactions to depict the intermediate and short range interactions, respectively. On the other hand, several various corrections are introduced to discuss the fine properties of the hadron-hadron interactions, like the isospin breaking effects, the coupled-channel effects, the spin-orbit force, and the recoil corrections. Up to now, the OBE model have been frequently adopted to study the hadron-hadron interactions in the heavy flavor sector [10, 13].

Besides the investigations of the mass spectrum behaviors of the possible charmonium-like molecular states [10, 13], we would like to further discuss their two-body hidden-charm strong decay behaviors. The decay properties can be very sensitive to the inner structures for the investigated systems. Experimentally, there are a large number of charmonium-like states have been observed in the charmonium state plus light-flavor meson invariant mass spectrum from the  $B$  meson decays [14]. In this work, we adopt the quark-interchange model to estimate the transition amplitudes for the two-body scattering processes [29–32]. It is often adopted to depict the very short range interactions, like the hidden-charm decay processes for the  $Z_c$  states [73, 74], the  $X(3872)$  [75], the  $P_c$  states [76], the open-charm strange tetraquarks [77], the  $P_{c\bar{s}s}$  states [78], and the  $X(4630)$  [79] in the hadronic molecular or resonant scenario.

### 3.1 Theoretical framework

Here, we firstly derive the OBE effective potentials in the coordinate space for these discussed tetraquark systems by performing several typical steps [78, 80–84], and then adopt the quark-interchange model [29–32] to study two-body hidden-charm decay behaviors of these possible molecular tetraquark candidates.

#### 3.1.1 OBE effective potentials

For deducing the OBE effective potentials for the hadron-hadron interactions at the hadronic level quantitatively, we usually adopt the effective Lagrangian approach. The general procedures include three typical steps [78, 80–84]. Firstly, we can write out the scattering amplitude  $\mathcal{M}(h_1 h_2 \rightarrow h_3 h_4)$  for the relevant scattering process  $h_1 h_2 \rightarrow h_3 h_4$  according to the effective Lagrangians. And then, the effective potentials in the momentum space  $\mathcal{V}_E^{h_1 h_2 \rightarrow h_3 h_4}(\mathbf{q})$  can be related to the corresponding scattering amplitudes  $\mathcal{M}(h_1 h_2 \rightarrow h_3 h_4)$  by using the Breit approximation [85, 86], i.e.,

$$\mathcal{V}_E^{h_1 h_2 \rightarrow h_3 h_4}(\mathbf{q}) = -\frac{\mathcal{M}(h_1 h_2 \rightarrow h_3 h_4)}{\sqrt{\prod_i 2m_i \prod_f 2m_f}}, \quad (3.1)$$

where  $m_i$  ( $i = h_1, h_2$ ) and  $m_f$  ( $f = h_3, h_4$ ) denote the masses of the initial and final states, respectively. Finally, the effective potentials in the coordinate space  $\mathcal{V}_E^{h_1 h_2 \rightarrow h_3 h_4}(\mathbf{r})$  can be obtained by performing the Fourier transformation, i.e.,

$$\mathcal{V}_E^{h_1 h_2 \rightarrow h_3 h_4}(\mathbf{r}) = \int \frac{d^3 \mathbf{q}}{(2\pi)^3} e^{i\mathbf{q} \cdot \mathbf{r}} \mathcal{V}_E^{h_1 h_2 \rightarrow h_3 h_4}(\mathbf{q}) \mathcal{F}^2(q^2, m_E^2), \quad (3.2)$$



which will be applied to search for the bound state solutions by solving the coupled channel Schrödinger equation, and we can further extract the bound state properties from the obtained bound state solutions. Because the discussed hadrons are not point-like particles, we introduce the monopole type form factor in each interaction vertex [87, 88], i.e.,

$$\mathcal{F}(q^2, m_E^2) = \frac{\Lambda^2 - m_E^2}{\Lambda^2 - q^2}, \quad (3.3)$$

which reflects the finite size effect of the discussed hadrons and compensate the off-shell effect of the exchanged light mesons [82]. Here,  $\Lambda$ ,  $m_E$ , and  $q$  are the cutoff parameter, the mass, and the four momentum of the exchanged light mesons, respectively.

Subsequently, let us construct the relevant effective Lagrangians. According to the heavy quark limit [33], the relevant super-fields  $H_a^{(Q)}$ ,  $H_a^{(\bar{Q})}$ ,  $S_a^{(Q)}$ ,  $S_a^{(\bar{Q})}$ ,  $T_a^{(Q)\mu}$ , and  $T_a^{(\bar{Q})\mu}$  can be defined as as [89]

$$\begin{aligned} H_a^{(Q)} &= \mathcal{P}_+ \left( D_a^{*(Q)\mu} \gamma_\mu - D_a^{(Q)} \gamma_5 \right), \\ H_a^{(\bar{Q})} &= \left( \bar{D}_a^{*(\bar{Q})\mu} \gamma_\mu - \bar{D}_a^{(\bar{Q})} \gamma_5 \right) \mathcal{P}_-, \\ S_a^{(Q)} &= \mathcal{P}_+ \left( D_{1a}^{(Q)\mu} \gamma_\mu \gamma_5 - D_{0a}^{*(Q)} \right), \\ S_a^{(\bar{Q})} &= \left( D_{1a}^{(\bar{Q})\mu} \gamma_\mu \gamma_5 - D_{0a}^{*(\bar{Q})} \right) \mathcal{P}_-, \\ T_a^{(Q)\mu} &= \mathcal{P}_+ \left[ D_{2a}^{*(Q)\mu\nu} \gamma_\nu - \sqrt{\frac{3}{2}} D_{1a\nu}^{(Q)} \gamma_5 \left( g^{\mu\nu} - \frac{1}{3} \gamma^\nu (\gamma^\mu - v^\mu) \right) \right], \\ T_a^{(\bar{Q})\mu} &= \left[ \bar{D}_{2a}^{*(\bar{Q})\mu\nu} \gamma_\nu - \sqrt{\frac{3}{2}} \bar{D}_{1a\nu}^{(\bar{Q})} \gamma_5 \left( g^{\mu\nu} - \frac{1}{3} \gamma^\nu (\gamma^\mu - v^\mu) \right) \right] \mathcal{P}_-, \end{aligned} \quad (3.4)$$

respectively. Here,  $\mathcal{P}_\pm = (1 \pm \not{v})/2$  are the projection operators, and  $v^\mu = (1, \mathbf{0})$  denotes the four velocity in the non-relativistic approximation. Their conjugate fields read as  $\bar{X} = \gamma_0 X^\dagger \gamma_0$  with  $X = H_a^{(Q)}$ ,  $H_a^{(\bar{Q})}$ ,  $S_a^{(Q)}$ ,  $S_a^{(\bar{Q})}$ ,  $T_a^{(Q)\mu}$ , and  $T_a^{(\bar{Q})\mu}$ .

According to the heavy quark symmetry, the chiral symmetry, and the hidden local symmetry [90–94], one can construct the effective Lagrangians describing the interactions between the (anti-)charmed mesons in the  $H/S/T$ -doublet and the light scalar, pseudoscalar, and vector mesons [89],

$$\begin{aligned} \mathcal{L} &= g_\sigma \langle H_a^{(Q)} \sigma \bar{H}_a^{(Q)} \rangle + g_\sigma \langle \bar{H}_a^{(\bar{Q})} \sigma H_a^{(\bar{Q})} \rangle + g'_\sigma \langle S_a^{(Q)} \sigma \bar{S}_a^{(Q)} \rangle + g'_\sigma \langle \bar{S}_a^{(\bar{Q})} \sigma S_a^{(\bar{Q})} \rangle \\ &+ g''_\sigma \langle T_a^{(Q)\mu} \sigma \bar{T}_{a\mu}^{(Q)} \rangle + g''_\sigma \langle \bar{T}_a^{(\bar{Q})\mu} \sigma T_{a\mu}^{(\bar{Q})} \rangle + \frac{h_\sigma}{f_\pi} \left[ \langle S_a^{(Q)} \gamma^\mu \partial_\mu \sigma \bar{H}_a^{(Q)} \rangle \right. \\ &- \left. \langle \bar{H}_a^{(\bar{Q})} \gamma^\mu \partial_\mu \sigma S_a^{(\bar{Q})} \rangle + h.c. \right] + \frac{h'_\sigma}{f_\pi} \left[ \langle T_a^{(Q)\mu} \partial_\mu \sigma \bar{H}_b^{(Q)} \rangle + \langle \bar{H}_a^{(\bar{Q})} \partial_\mu \sigma T_b^{(\bar{Q})\mu} \rangle + h.c. \right] \\ &+ ig \langle H_b^{(Q)} \mathcal{A}_{ba} \gamma_5 \bar{H}_a^{(Q)} \rangle + ig \langle \bar{H}_a^{(\bar{Q})} \mathcal{A}_{ab} \gamma_5 H_b^{(\bar{Q})} \rangle + i\tilde{k} \langle S_b^{(Q)} \mathcal{A}_{ba} \gamma_5 \bar{S}_a^{(Q)} \rangle \\ &+ i\tilde{k} \langle \bar{S}_a^{(\bar{Q})} \mathcal{A}_{ab} \gamma_5 S_b^{(\bar{Q})} \rangle + ik \langle T_b^{(Q)\mu} \mathcal{A}_{ba} \gamma_5 \bar{T}_{a\mu}^{(Q)} \rangle + ik \langle \bar{T}_a^{(\bar{Q})\mu} \mathcal{A}_{ab} \gamma_5 T_{b\mu}^{(\bar{Q})} \rangle \end{aligned}$$

$$\begin{aligned}
& + \left[ i h \left\langle S_b^{(Q)} \mathcal{A}_{ba} \gamma_5 \bar{H}_a^{(Q)} \right\rangle + i h \left\langle \bar{H}_a^{(\bar{Q})} \mathcal{A}_{ab} \gamma_5 S_b^{(\bar{Q})} \right\rangle + h.c. \right] \\
& + \left[ i \left\langle T_b^{(Q)\mu} \left( \frac{h_1}{\Lambda_\chi} D_\mu \mathcal{A} + \frac{h_2}{\Lambda_\chi} \not{D} \mathcal{A}_\mu \right)_{ba} \gamma_5 \bar{H}_a^{(Q)} \right\rangle + h.c. \right] \\
& + \left[ i \left\langle \bar{H}_a^{(\bar{Q})} \left( \frac{h_1}{\Lambda_\chi} \mathcal{A} \overleftarrow{D}_\mu + \frac{h_2}{\Lambda_\chi} \mathcal{A}_\mu \overleftarrow{\not{D}} \right)_{ab} \gamma_5 T_b^{(\bar{Q})\mu} \right\rangle + h.c. \right] \\
& + \left\langle i H_b^{(Q)} (\beta v^\mu (\mathcal{V}_\mu - \rho_\mu) + \lambda \sigma^{\mu\nu} F_{\mu\nu}(\rho))_{ba} \bar{S}_a^{(Q)} \right\rangle \\
& - \left\langle i \bar{H}_a^{(\bar{Q})} (\beta v^\mu (\mathcal{V}_\mu - \rho_\mu) - \lambda \sigma^{\mu\nu} F_{\mu\nu}(\rho))_{ab} H_b^{(\bar{Q})} \right\rangle \\
& + \left\langle i S_b^{(Q)} (\beta' v^\mu (\mathcal{V}_\mu - \rho_\mu) + \lambda' \sigma^{\mu\nu} F_{\mu\nu}(\rho))_{ba} \bar{H}_a^{(Q)} \right\rangle \\
& - \left\langle i \bar{S}_a^{(\bar{Q})} (\beta' v^\mu (\mathcal{V}_\mu - \rho_\mu) - \lambda' \sigma^{\mu\nu} F_{\mu\nu}(\rho))_{ab} S_b^{(\bar{Q})} \right\rangle \\
& + \left\langle i T_{b\lambda}^{(Q)} (\beta'' v^\mu (\mathcal{V}_\mu - \rho_\mu) + \lambda'' \sigma^{\mu\nu} F_{\mu\nu}(\rho))_{ba} \bar{T}_a^{(Q)\lambda} \right\rangle \\
& - \left\langle i \bar{T}_{a\lambda}^{(\bar{Q})} (\beta'' v^\mu (\mathcal{V}_\mu - \rho_\mu) - \lambda'' \sigma^{\mu\nu} F_{\mu\nu}(\rho))_{ab} T_b^{(\bar{Q})\lambda} \right\rangle \\
& + \left[ \left\langle H_b^{(Q)} (i \zeta \gamma^\mu (\mathcal{V}_\mu - \rho_\mu) + i \mu \sigma^{\lambda\nu} F_{\lambda\nu}(\rho))_{ba} \bar{S}_a^{(Q)} \right\rangle + h.c. \right] \\
& + \left[ \left\langle \bar{S}_a^{(\bar{Q})} (i \zeta \gamma^\mu (\mathcal{V}_\mu - \rho_\mu) + i \mu \sigma^{\lambda\nu} F_{\lambda\nu}(\rho))_{ab} H_b^{(\bar{Q})} \right\rangle + h.c. \right] \\
& + \left[ \left\langle T_b^{(Q)\mu} (i \zeta_1 (\mathcal{V}_\mu - \rho_\mu) + \mu_1 \gamma^\nu F_{\mu\nu}(\rho))_{ba} \bar{H}_a^{(Q)} \right\rangle + h.c. \right] \\
& - \left[ \left\langle \bar{H}_a^{(\bar{Q})} (i \zeta_1 (\mathcal{V}_\mu - \rho_\mu) - \mu_1 \gamma^\nu F_{\mu\nu}(\rho))_{ab} T_b^{(\bar{Q})\mu} \right\rangle + h.c. \right]. \tag{3.5}
\end{aligned}$$

Here, the covariant derivatives are written as  $D_\mu = \partial_\mu + \mathcal{V}_\mu$  and  $D'_\mu = \partial_\mu - \mathcal{V}_\mu$ . And the axial current  $\mathcal{A}_\mu$ , the vector current  $\mathcal{V}_\mu$ , the vector meson field  $\rho_\mu$ , and the vector meson strength tensor  $F_{\mu\nu}(\rho)$  are defined as

$$\begin{aligned}
\mathcal{A}_\mu &= \frac{1}{2} (\xi^\dagger \partial_\mu \xi - \xi \partial_\mu \xi^\dagger)_\mu, & \mathcal{V}_\mu &= \frac{1}{2} (\xi^\dagger \partial_\mu \xi + \xi \partial_\mu \xi^\dagger)_\mu, & \xi &= \exp(i\mathbb{P}/f_\pi), \\
\rho_\mu &= \frac{ig_V}{\sqrt{2}} \mathbb{V}_\mu, & F_{\mu\nu}(\rho) &= \partial_\mu \rho_\nu - \partial_\nu \rho_\mu + [\rho_\mu, \rho_\nu].
\end{aligned} \tag{3.6}$$

respectively. The light pseudoscalar meson matrix  $\mathbb{P}$  and the light vector meson matrix  $\mathbb{V}_\mu$  have the conventional form [78, 83, 84], which can be expressed as

$$\mathbb{P} = \begin{pmatrix} \frac{\pi^0}{\sqrt{2}} + \frac{\eta}{\sqrt{6}} & \pi^+ & K^+ \\ \pi^- & -\frac{\pi^0}{\sqrt{2}} + \frac{\eta}{\sqrt{6}} & K^0 \\ K^- & \bar{K}^0 & -\sqrt{\frac{2}{3}}\eta \end{pmatrix}, \quad \mathbb{V}_\mu = \begin{pmatrix} \frac{\rho^0}{\sqrt{2}} + \frac{\omega}{\sqrt{2}} & \rho^+ & K^{*+} \\ \rho^- & -\frac{\rho^0}{\sqrt{2}} + \frac{\omega}{\sqrt{2}} & K^{*0} \\ K^{*-} & \bar{K}^{*0} & \phi \end{pmatrix}_\mu, \tag{3.7}$$

respectively. After expanding the compact effective Lagrangians in Eq. (3.5) to the leading order of the pseudo-Goldstone field  $\xi$ , we can further obtain the concrete effective Lagrangians (see Refs. [80–82, 95, 96] for more information). The normalized relations for

these discussed charmed mesons are written as

$$\begin{aligned}
\langle 0|D|c\bar{q}(0^-)\rangle &= \sqrt{m_D}, & \langle 0|D^{*\mu}|c\bar{q}(1^-)\rangle &= \epsilon^\mu \sqrt{m_{D^*}}, \\
\langle 0|D_0^*|c\bar{q}(0^+)\rangle &= \sqrt{m_{D_0^*}}, & \langle 0|D_1^{\prime\mu}|c\bar{q}(1^+)\rangle &= \epsilon^\mu \sqrt{m_{D_1'}}, \\
\langle 0|D_1^\mu|c\bar{q}(1^+)\rangle &= \epsilon^\mu \sqrt{m_{D_1}}, & \langle 0|D_2^{*\mu\nu}|c\bar{q}(2^+)\rangle &= \zeta^{\mu\nu} \sqrt{m_{D_2^*}},
\end{aligned} \tag{3.8}$$

respectively. Here,  $\epsilon_m^\mu$  ( $m = 0, \pm 1$ ) and  $\zeta_m^{\mu\nu}$  ( $m = 0, \pm 1, \pm 2$ ) correspond to the polarization vector and tensor, respectively. In the static limit, they have the form of  $\epsilon_0^\mu = (0, 0, 0, -1)$ ,  $\epsilon_\pm^\mu = (0, \pm 1, i, 0)/\sqrt{2}$ , and  $\zeta_m^{\mu\nu} = \sum_{m_1, m_2} \langle 1, m_1; 1, m_2 | 2, m \rangle \epsilon_{m_1}^\mu \epsilon_{m_2}^\nu$  [97].

In order to obtain the concrete effective potentials, one need to further construct the wave functions for the investigated systems. They include the color part, the flavor part, the spin-orbit part, and the spatial wave functions. For the systems composed by colorless hadrons, the color wave functions are simply **1**. In Table 2, we summarize the flavor wave functions  $|I, I_3\rangle$  for the  $\mathcal{A}\bar{\mathcal{A}}$  and  $\mathcal{A}\bar{\mathcal{B}}$  systems, here, notations  $\mathcal{A}$  and  $\mathcal{B}$  stand for the different charmed mesons, and  $J$ ,  $J_1$ , and  $J_2$  correspond to the total angular momentum quantum numbers of the discussed charmonium-like systems  $\mathcal{A}\bar{\mathcal{B}}$ , the charmed (charmed-strange) mesons  $\mathcal{A}$ , and the charmed (charmed-strange) mesons  $\mathcal{B}$ , respectively. In particular, we need to emphasize the  $C$  parity for the discussed systems is determined by  $C = -c(-1)^{J_1+J_2-J}$  with  $c = \pm 1$  [41, 43, 82, 98].

**Table 2.** Flavor wave functions  $|I, I_3\rangle$  for these discussed  $\mathcal{A}\bar{\mathcal{A}}$  and  $\mathcal{A}\bar{\mathcal{B}}$  systems. Here, the notations  $\mathcal{A}$  and  $\mathcal{B}$  stand for different charmed mesons, and  $I$  and  $I_3$  represent their isospin and the third component of these discussed charmonium-like systems, respectively.

Systems	$ I, I_3\rangle$	Flavor wave functions
$\mathcal{A}\bar{\mathcal{A}}$	$ 1, 1\rangle$	$\mathcal{A}^+\bar{\mathcal{A}}^0$
	$ 1, 0\rangle$	$\frac{1}{\sqrt{2}} (\mathcal{A}^0\bar{\mathcal{A}}^0 - \mathcal{A}^+\mathcal{A}^-)$
	$ 1, -1\rangle$	$\mathcal{A}^0\mathcal{A}^-$
	$ 0, 0\rangle$	$\frac{1}{\sqrt{2}} (\mathcal{A}^0\bar{\mathcal{A}}^0 + \mathcal{A}^+\mathcal{A}^-)$
$\mathcal{A}\bar{\mathcal{B}}$	$ 1, 1\rangle$	$\frac{1}{\sqrt{2}} (\mathcal{A}^+\bar{\mathcal{B}}^0 + c\mathcal{B}^+\bar{\mathcal{A}}^0)$
	$ 1, 0\rangle$	$\frac{1}{2} [(\mathcal{A}^0\bar{\mathcal{B}}^0 - \mathcal{A}^+\mathcal{B}^-) + c(\mathcal{B}^0\bar{\mathcal{A}}^0 - \mathcal{B}^+\mathcal{A}^-)]$
	$ 1, -1\rangle$	$\frac{1}{\sqrt{2}} (\mathcal{A}^0\mathcal{B}^- + c\mathcal{B}^0\mathcal{A}^-)$
	$ 0, 0\rangle$	$\frac{1}{2} [(\mathcal{A}^0\bar{\mathcal{B}}^0 + \mathcal{A}^+\mathcal{B}^-) + c(\mathcal{B}^0\bar{\mathcal{A}}^0 + \mathcal{B}^+\mathcal{A}^-)]$

The spin-orbit wave functions  $|^{2S+1}L_J\rangle$  for the  $|\mathcal{D}_{J_1}\bar{\mathcal{D}}_{J_2}\rangle$  systems can be constructed as

$$|\mathcal{D}_0\bar{\mathcal{D}}_1\rangle = \sum_{m,m_L} C_{1m,Lm_L}^{J,M} \epsilon_m^\mu |Y_{L,m_L}\rangle, \quad (3.9)$$

$$|\mathcal{D}_0\bar{\mathcal{D}}_2\rangle = \sum_{m,m_L} C_{2m,Lm_L}^{J,M} \zeta_m^{\mu\nu} |Y_{L,m_L}\rangle, \quad (3.10)$$

$$|\mathcal{D}_1\bar{\mathcal{D}}_1\rangle = \sum_{m,m',m_S,m_L} C_{1m,1m'}^{S,m_S} C_{Sm_S,Lm_L}^{J,M} \epsilon_m^\mu \epsilon_{m'}^\nu |Y_{L,m_L}\rangle, \quad (3.11)$$

$$|\mathcal{D}_1\bar{\mathcal{D}}_2\rangle = \sum_{m,m',m_S,m_L} C_{1m,2m'}^{S,m_S} C_{Sm_S,Lm_L}^{J,M} \epsilon_m^\lambda \zeta_{m'}^{\mu\nu} |Y_{L,m_L}\rangle. \quad (3.12)$$

In the above expressions, the notations  $\mathcal{D}_0$ ,  $\mathcal{D}_1$ , and  $\mathcal{D}_2$  denote the charmed (charm-strange) mesons with the total angular momentum quantum numbers  $J = 0, 1$ , and  $2$ , respectively.  $C_{ab,cd}^{e,f}$  is the Clebsch-Gordan coefficient, and  $|Y_{L,m_L}\rangle$  is the spherical harmonics function. In Table 3, we summary the relevant spin-orbit wave functions  $|^{2S+1}L_J\rangle$  and the discussed channels under considering the coupled channel effect.

**Table 3.** The relevant quantum numbers  $J^P$  and possible channels  $|^{2S+1}L_J\rangle$  involved in this work. Here, ... means that the  $S$ -wave components for the corresponding channels do not exist.

$J^P$	$\mathcal{D}_0\bar{\mathcal{D}}_0$	$\mathcal{D}_0\bar{\mathcal{D}}_1$	$\mathcal{D}_0\bar{\mathcal{D}}_2$	$\mathcal{D}_1\bar{\mathcal{D}}_1$	$\mathcal{D}_1\bar{\mathcal{D}}_2$
$0^\pm$	$ ^1\mathbb{S}_0\rangle$	...	...	$ ^1\mathbb{S}_0\rangle/ ^5\mathbb{D}_0\rangle$	...
$1^\pm$	...	$ ^3\mathbb{S}_1\rangle/ ^3\mathbb{D}_1\rangle$	...	$ ^3\mathbb{S}_1\rangle/ ^3,5\mathbb{D}_1\rangle$	$ ^3\mathbb{S}_1\rangle/ ^3,5,7\mathbb{D}_1\rangle$
$2^\pm$	...	...	$ ^5\mathbb{S}_2\rangle/ ^5\mathbb{D}_2\rangle$	$ ^5\mathbb{S}_2\rangle/ ^1,3,5\mathbb{D}_2\rangle$	$ ^5\mathbb{S}_2\rangle/ ^3,5,7\mathbb{D}_2\rangle$
$3^\pm$	...	...	...	...	$ ^7\mathbb{S}_3\rangle/ ^3,5,7\mathbb{D}_3\rangle$

For the  $\mathcal{A}\bar{\mathcal{B}} \rightarrow \mathcal{A}\bar{\mathcal{B}}$  processes, there exist the direct channel and cross channel Feynman diagrams [23, 82], where  $\mathcal{A}$  and  $\mathcal{B}$  stand for two different charmed (charm-strange) mesons. The total effective potentials can be written as [41, 43, 82, 98]

$$\mathcal{V}_{Total}(\mathbf{r}) = \mathcal{V}_D(\mathbf{r}) + c\mathcal{V}_C(\mathbf{r}). \quad (3.13)$$

In Figure 6, we present the direct channel and cross channel Feynman diagrams. For the  $\mathcal{A}\bar{\mathcal{A}}$  systems, there exist the direct channel contribution.

With the standard procedures of the OBE model [78, 80–84], we can finally obtain the effective potentials in the coordinate space. In Appendix A, we collect the concrete expressions for all the OBE effective potentials. We estimate the coupling constants by fitting the reported experimental data and using several theoretical models [24, 80–82, 91, 95, 99–111]. In particular, we fix the phases between these coupling constants by the quark model [105]. In Table 4, we collect their values. In addition, we need to introduce

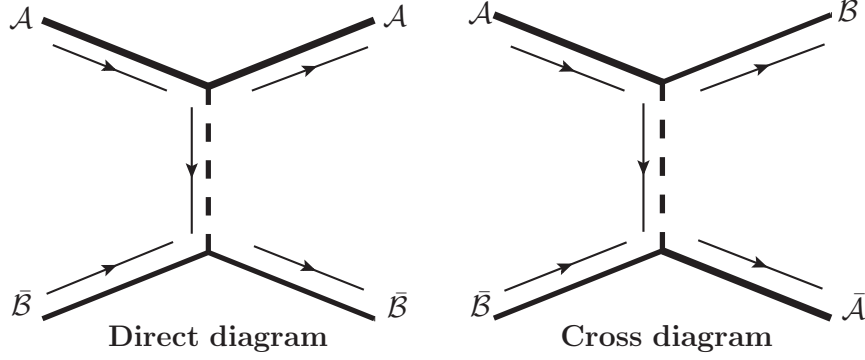


**Figure 6.** The direct channel and cross channel Feynman diagrams for the  $\mathcal{A}\bar{\mathcal{B}} \rightarrow \mathcal{A}\bar{\mathcal{B}}$  processes. Here, the notations  $\mathcal{A}$  and  $\mathcal{B}$  represent two different charmed (charmed-strange) mesons.

the following parameters of the hadron masses,  $m_\sigma = 600.00$  MeV,  $m_\pi = 137.27$  MeV,  $m_\eta = 547.86$  MeV,  $m_\rho = 775.49$  MeV,  $m_\omega = 782.65$  MeV,  $m_\phi = 1019.46$  MeV,  $m_D = 1867.24$  MeV,  $m_{D^*} = 2008.56$  MeV,  $m_{D_0^*} = 2324.50$  MeV,  $m_{D_1^*} = 2427.00$  MeV,  $m_{D_1} = 2422.00$  MeV,  $m_{D_2^*} = 2463.05$  MeV,  $m_{D_s} = 1968.34$  MeV,  $m_{D_s^*} = 2112.20$  MeV,  $m_{D_{s0}^*} = 2317.80$  MeV,  $m_{D_{s1}^*} = 2459.50$  MeV,  $m_{D_{s1}} = 2535.11$  MeV, and  $m_{D_{s2}^*} = 2569.10$  MeV [34].

**Table 4.** A summary of the coupling constants adopted in our calculations. Units of the coupling constants  $h' = (h_1 + h_2)/\Lambda_\chi$ ,  $\lambda$ ,  $\lambda'$ ,  $\lambda''$ ,  $\mu$ , and  $\mu_1$  are  $\text{GeV}^{-1}$ , and the coupling constant  $f_\pi$  is given in unit of GeV.

$g_\sigma$	$g'_\sigma$	$g''_\sigma$	$ h_\sigma $	$ h'_\sigma $	$g$	$\tilde{k}$	$k$	$ h $	$ \mu $	$ \zeta_1 $
-0.76	0.76	0.76	0.32	0.35	0.59	0.59	0.59	0.56	0.364	0.20
$ h' $	$f_\pi$	$\beta$	$\beta'$	$\beta''$	$\lambda$	$\lambda'$	$\lambda''$	$ \zeta $	$\mu_1$	$g_V$
0.55	0.132	-0.90	0.90	0.90	-0.56	0.56	0.56	0.727	0	5.83

### 3.1.2 Quark-interchange model

In this work, we adopt the quark-interchange model [29–32] to study the two-body hidden-charm decay behaviors for the possible charmonium-like molecules. The corresponding decay process reads as

$$A(c\bar{q}) + B(\bar{c}q) \rightarrow C(c\bar{c}) + D(q\bar{q}), \quad (3.14)$$

where  $A(c\bar{q})$  and  $B(\bar{c}q)$  are the components of the discussed charmonium-like molecule,  $q(\bar{q})$  stand for the light quarks (anti-quarks). The corresponding transition amplitudes can be decomposed as four concrete scattering processes in the molecular picture, as shown in Figure 7.

The interactions of the initial charmonium-like molecule can be expressed as

$$H = V_A^0 + V_B^0 + V_{AB}, \quad (3.15)$$

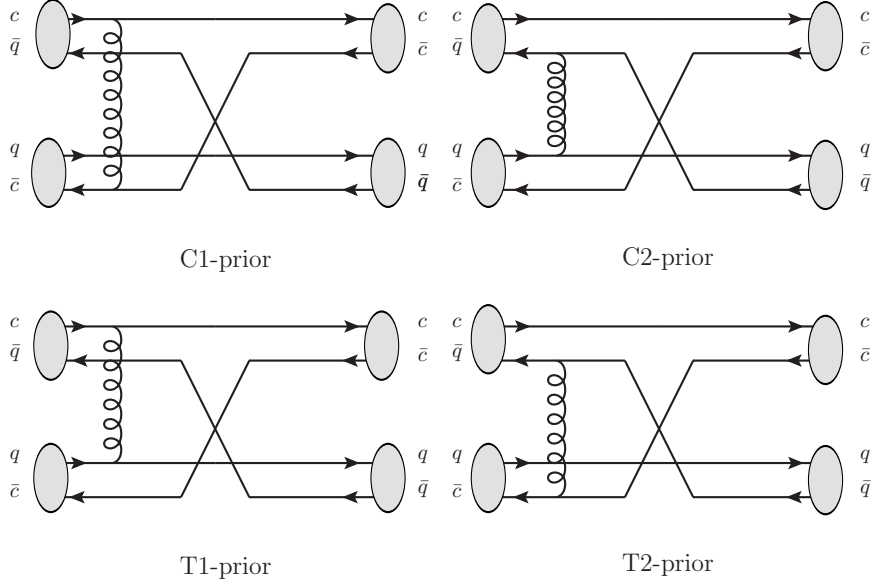


**Figure 7.** Quark-interchange diagrams for the scattering process  $A(c\bar{q}) + B(\bar{c}q) \rightarrow C(\bar{c}c) + D(q\bar{q})$  in the molecular picture. The curve line denotes the (anti-)quark-(anti-)quark interactions.

where  $V_A^0$  and  $V_B^0$  are the Hamiltonian of the free mesons A and B, respectively. The  $V_{AB}$  is the relevant scattering interaction between the mesons A and B, which has four parts according to the quark-interchange diagrams as showed in Figure 7. The two-body hidden-charm decay processes occur via very short range interactions, it is very different with the bound dynamic mechanism for the charmonium-like molecules. Perhaps, the one-gluon-exchange (OGE) potential  $V_{ij}(q^2)$  can be a good approximation to describe these interactions [74, 76, 112], i.e.,

$$V_{ij}(q^2) = \frac{\lambda_i}{2} \cdot \frac{\lambda_j}{2} \left( \frac{4\pi\alpha_s}{q^2} + \frac{6\pi b}{q^4} - \frac{8\pi\alpha_s}{3m_i m_j} e^{-\frac{q^2}{4\sigma^2}} \mathbf{s}_i \cdot \mathbf{s}_j \right),$$

$$\alpha_s(Q^2) = \frac{12\pi}{(32 - 2n_f) \ln \left( A + \frac{Q^2}{B^2} \right)}, \quad (3.16)$$

where  $Q^2$  is the square of the invariant masses of the interacting quarks, and  $\lambda_i(\lambda_j)$ ,  $m_i(m_j)$ , and  $\mathbf{s}_i(\mathbf{s}_j)$  represent the color generator, the mass, and the spin operator of the interacting quarks, respectively. For an anti-quark, the color generator  $\lambda_i$  is replaced by  $-\lambda_i^T$  in Eq. (3.16).

In addition, we need to construct the wave functions for all the discussed hadrons in the hidden-charm decay process. The total wave functions  $\psi_{\text{total}}$  can be respectively resolve into the color wave function  $\omega_{\text{color}}$ , the flavor wave function  $\chi_{\text{flavor}}$ , the spin wave function  $\chi_{\text{spin}}$ , and the space wave function  $\psi_{nLM_L}(\mathbf{p}_{\text{rel}})$ , i.e.,

$$\psi_{\text{total}} = \omega_{\text{color}} \chi_{\text{flavor}} \chi_{\text{spin}} \psi_{nLM_L}(\mathbf{p}_{\text{rel}}). \quad (3.17)$$

In our calculations, the space wave function  $\psi_{nLM_L}(\mathbf{p}_{\text{rel}})$  is estimated by the harmonic

oscillators wave function [113–115], which can be written as

$$\psi_{nLM_L}(\mathbf{P}_{\text{rel}}) = \frac{(-1)^n(-i)^L}{\beta^{3/2}} \sqrt{\frac{2n!}{\Gamma(n+L+\frac{3}{2})}} \left(\frac{p_{\text{rel}}}{\beta}\right)^L e^{-\frac{p_{\text{rel}}^2}{2\beta^2}} L_n^{L+\frac{1}{2}} \frac{p_{\text{rel}}^2}{\beta^2} Y_{LM_L}(\hat{\Omega}_{p_{\text{rel}}}). \quad (3.18)$$

Here,  $\mathbf{P}_{\text{rel}} = (m_{\bar{q}}\mathbf{p}_q + m_q\mathbf{p}_{\bar{q}})/(m_q + m_{\bar{q}})$  is the relative momentum,  $m_q$  ( $m_{\bar{q}}$ ) and  $\mathbf{p}_q$  ( $\mathbf{p}_{\bar{q}}$ ) are the masses and momenta of the quark (anti-quark), respectively.  $Y_{LM_L}(\hat{\Omega}_{p_{\text{rel}}})$ ,  $L_n^{L+1/2}(x)$ , and  $\beta$  denote the orbital angular function, the associated Laguerre polynomial, and the parameter of oscillator radial wave function, respectively.

Once the OGE potentials are sandwiched by the wave functions for the initial and final mesons, the effective interactions  $V_{\text{eff}}(\mathbf{P}_A, \mathbf{P}_C, \theta)$  can be decomposed as the product of the four relevant factors, i.e.,

$$V_{\text{eff}}(\mathbf{P}_A, \mathbf{P}_C, \theta) = I_{\text{color}} I_{\text{flavor}} I_{\text{spin}} I_{\text{space}}. \quad (3.19)$$

Here,  $I_i$  ( $i = \text{color, flavor, spin, space}$ ) correspond to the color, flavor, spin, and space factors, respectively. The color factor  $I_{\text{color}}$  is

$$I_{\text{color}} = \left\langle \omega_C \omega_D \left| \frac{\lambda_i}{2} \cdot \frac{\lambda_j}{2} \right| \omega_A \omega_B \right\rangle, \quad (3.20)$$

where  $\omega_i$  ( $i = A, B, C, D$ ) are the color functions. In the meson-meson hadronic molecular scenario,  $I_{\text{color}}$  is  $4/9$  and  $-4/9$  for the  $qq(\bar{q}\bar{q})$  and  $q\bar{q}$  interactions [74, 112], respectively. And  $I_{\text{flavor}} = 1$  for all quark-interchange processes. Meanwhile, we define the spin factor  $I_{\text{spin}}$  as

$$I_{\text{spin}} = \left\langle [\chi_C \chi_D]_{J'} \left| \hat{O}_s \right| [\chi_A \chi_B]_J \right\rangle, \quad (3.21)$$

where  $\chi_i$  ( $i = A, B, C, D$ ) are the spin functions, and  $J(J')$  represents the total spin of the initial (final) states. One can refer the detailed calculations in Ref. [112]. Moreover, we express the space factor  $I_{\text{space}}$  as follows, i.e.,

$$I_{\text{space}} = \int \int d\mathbf{k}_1 d\mathbf{k}_2 \psi_C(\mathbf{k}_C + \mathbf{K}_C) \psi_D(\mathbf{k}_D + \mathbf{K}_D) V(\mathbf{k}_1 - \mathbf{k}_2) \psi_A^*(\mathbf{k}_A + \mathbf{K}_A) \psi_B^*(\mathbf{k}_B + \mathbf{K}_B). \quad (3.22)$$

Here,  $\mathbf{k}_1$  and  $\mathbf{k}_2$  denote the three-momenta of the (anti-)quark in the initial and final states, respectively.  $\mathbf{k}_A$ ,  $\mathbf{k}_B$ ,  $\mathbf{k}_C$ , and  $\mathbf{k}_D$  are the three-momenta of the hadronic states A, B, C, and D, respectively. In the center-of-mass frame, we can obtain the relations  $\mathbf{k}_B = -\mathbf{k}_A$  and  $\mathbf{k}_D = -\mathbf{k}_C$ . In Table 5, we summarize the momenta substitutions for the different quark-interchange diagrams in Figure 7.

In general, a pair of charmed (charm-strange) meson and anti-charmed (anti-charm-strange) meson via the  $S$ -wave interaction can be easier to bind as loose charmonium-like molecules. For the higher orbit systems, there exist repulsive centrifugal force  $\ell(\ell+1)/2\mu r^2$ . Therefore, we only discuss the mass spectrum and two-body hidden-charm decay behaviors for the possible  $S$ -wave charmonium-like molecular candidates in this work. For an  $S$ -wave

**Table 5.** The momenta substitutions in Eq. (3.22) for the different quark-interchange diagrams. Here,  $a = \frac{m_c}{m_c+m_q}$ ,  $b = \frac{m_q}{m_c+m_q}$ ,  $m_c$  and  $m_q$  are the masses of the charm quark and light quark, respectively.

Diagrams	$\mathbf{k}_A$	$\mathbf{K}_A$	$\mathbf{k}_B$	$\mathbf{K}_B$	$\mathbf{k}_C$	$\mathbf{K}_C$	$\mathbf{k}_D$	$\mathbf{K}_D$
C1	$\mathbf{k}_1$	$-a\mathbf{P}_A$	$\mathbf{k}_1$	$-a\mathbf{P}_A - \mathbf{P}_C$	$\mathbf{k}_2$	$-\mathbf{P}_C$	$\mathbf{k}_1$	$-\mathbf{P}_C - \mathbf{P}_A$
C2	$\mathbf{k}_1$	$-b\mathbf{P}_A$	$\mathbf{k}_1$	$-b\mathbf{P}_A + \mathbf{P}_C$	$\mathbf{k}_1$	$\mathbf{P}_C - \mathbf{P}_A$	$\mathbf{k}_2$	$\mathbf{P}_C$
T1	$\mathbf{k}_1$	$-a\mathbf{P}_A$	$\mathbf{k}_2$	$-a\mathbf{P}_A - \mathbf{P}_C$	$\mathbf{k}_2$	$-\mathbf{P}_C$	$\mathbf{k}_1$	$-\mathbf{P}_C - \mathbf{P}_A$
T2	$\mathbf{k}_1$	$-b\mathbf{P}_A$	$\mathbf{k}_2$	$-b\mathbf{P}_A + \mathbf{P}_C$	$\mathbf{k}_1$	$\mathbf{P}_C - \mathbf{P}_A$	$\mathbf{k}_2$	$\mathbf{P}_C$

loosely bound state composed of hadrons A and B, we roughly define its momentum space wave function by the harmonic oscillators wave function [74, 76, 78, 79], i.e.,

$$\psi_{AB}(\mathbf{p}_{\text{rel}}) = \frac{1}{\beta^{\frac{3}{2}}\pi^{\frac{3}{4}}} e^{-\mathbf{p}_{\text{rel}}^2/2\beta^2}. \quad (3.23)$$

Here,  $\mathbf{p}_{\text{rel}} = (m_A\mathbf{p}_A + m_B\mathbf{p}_B)/(m_A + m_B)$  is the relative momentum of the discussed molecular state, and  $\beta = \sqrt{3\mu(m_A + m_B - m)}$  with its reduced mass  $\mu = \frac{m_A m_B}{m_A + m_B}$  [116, 117].

In the rest frame of the charmonium-like molecular states, the two-body strong decay widths satisfy

$$d\Gamma(M \rightarrow C + D) = \frac{|\mathbf{P}_C|}{32\pi^2 M^2} \int d\Omega |\mathcal{M}_{fi}|^2. \quad (3.24)$$

Here,  $M$  is the mass of the discussed initial molecule,  $M = m_A + m_B + E$  with  $E$  is the binding energy.  $\mathcal{M}_{fi}$  denotes the transition amplitude of the two-body scattering process, it can relate to the T-matrix, i. e.,

$$T = \langle \psi_D \psi_C | V_{fi} | \psi_X \rangle = \langle \psi_D \psi_C | V_{fi} | \psi_A \psi_B \psi_{AB} \rangle = \frac{\mathcal{M}_{fi}}{(2\pi)^{\frac{3}{2}} \sqrt{2M} \sqrt{2E_C} \sqrt{2E_D}}, \quad (3.25)$$

where  $\psi_C$  and  $\psi_D$  are the wave functions of the final mesons C and D,  $\psi_X$  is the normalized molecular wave function, it is a convolution by the component meson wave functions  $\psi_A$ ,  $\psi_B$ , and the wave function  $\psi_{AB}$  between two mesons A and B.  $V_{fi}$  represents the relevant scattering interaction, and  $E_C$  and  $E_D$  stand for the energies of the final mesons C and D. On the other hand, the T-matrix in the momentum space can be written as [74, 76]

$$\begin{aligned} T &= \frac{1}{(2\pi)^3} \int d\mathbf{P}_A \int d\mathbf{k} \delta^3(\mathbf{k} - \mathbf{P}_C) V_{\text{eff}}(\mathbf{P}_A, \mathbf{k}) \psi_{AB}(\mathbf{P}_A) \\ &= \frac{1}{(2\pi)^3} \int d\mathbf{P}_A V_{\text{eff}}(\mathbf{P}_A, \mathbf{P}_C) R_l(P_A) Y_{lm}(\mathbf{P}_A) = \frac{1}{(2\pi)^2} \mathcal{M}_l \end{aligned} \quad (3.26)$$

with

$$\mathcal{M}_l = \int d\theta \int dP_A P_A^2 \sin(\theta) V_{\text{eff}}(\mathbf{P}_A, \mathbf{P}_C, \theta) R_l(P_A) Y_{lm}(\mathbf{P}_A). \quad (3.27)$$



In the above expression, the wave function  $\psi_{AB}(\mathbf{P}_A)$  between mesons A and B is resolved to the radial wave function  $R_l(P_A)$  and the orbital angular function  $Y_{lm}(\mathbf{P}_A)$ , and  $\theta$  is the angle between the final momentum  $\mathbf{P}_C$  and initial momentum  $\mathbf{P}_A$ .

Finally, we obtain

$$\Gamma = |\mathbf{P}_C| \frac{E_C E_D}{(2\pi)^3 M} |\mathcal{M}_l|^2. \quad (3.28)$$

Here, we want to emphasize that the two-body hidden-charm decay widths depend on the relative momentum  $|\mathbf{P}_C|$  and the interactions  $|\mathcal{M}_l|^2$ , where the  $|\mathcal{M}_l|^2$  is determined by the wave functions for all the discussed mesons and the OGE potential. The parameters in the OGE potential [112] and the oscillating parameters used in the meson wave functions can be fixed with the mass spectrum of the mesons [34], and the corresponding numerical results are listed in Table 6.

**Table 6.** The parameters used in the quark model and the oscillating parameters (in units of GeV) used in the meson wave functions.

$b$ (GeV <sup>2</sup> )	$\sigma$ (GeV)	A	B (GeV)	$m_q$ (GeV)	$m_s$ (GeV)	$m_c$ (GeV)	$\beta_D$
0.180	0.897	10.000	0.310	0.334	0.575	1.776	0.394
$\beta_{D^*}$	$\beta_{D_1}$	$\beta_{D_2^*}$	$\beta_{D_s}$	$\beta_{D_s^*}$	$\beta_{D_{s0}^*}$	$\beta_{D_{s1}^{(\prime)}}$	$\beta_{D_{s2}^*}$
0.364	0.326	0.324	0.473	0.440	0.381	0.385	0.381
$\beta_{\eta_c}$	$\beta_{J/\psi}$	$\beta_{\chi_{cJ}(1P)}$	$\beta_\phi$	$\beta_{\eta^{(\prime)}}$	$\beta_\omega$		
0.618	0.595	0.500	0.370	0.465	0.293		

### 3.2 Numerical results and discussions

In this section, we firstly attempt to find the loosely bound state solutions for the charmed (charm-strange) meson and anti-charmed (anti-charm-strange) meson systems by solving the coupled channel Schrödinger equation. As the only one free parameter here, we vary the cutoff parameters in the range of 0.8-3.0 GeV. The loosely bound state with cutoff value around 1.0 GeV can be the prime hadronic molecular candidate, since this value range is widely accepted as a reasonable input parameter based on the experience of studying the deuteron [80, 87, 88]. As is well known, a reasonable loosely bound hadronic molecule should satisfy its binding energy is around several to several tens MeV, and its typical size should be larger than the size of all the component hadrons [10, 118].

In order to calculate the two-body hidden-charm decay widths for all the possible charmonium-like molecules, we simplify set their binding energies  $E$  from  $-1$  to  $-30$  MeV [10, 118]. In the following, we mainly focus on the  $S$ -wave and  $P$ -wave two-body hidden-charm decay processes. In Table 7, we collect the mass thresholds and allowed  $J^{PC}$  quantum numbers of the discussed final states with the isospin quantum number  $I = 0$ . Our results will be categorized into three corresponding cases:

1. The isoscalar charmonium-like molecular systems without hidden-strange quantum number,
2. The charmonium-like molecular systems with hidden-strange quantum number,
3. The isovector hidden-charm molecular tetraquark systems.

**Table 7.** The mass thresholds and allowed  $J^{PC}$  quantum numbers via the  $S(P)$ -wave decay models of these investigated isoscalar two-body hidden-charm decay channels.

Channels	$M_{th}$ (GeV)	$S$ -wave	$P$ -wave	Channels	$M_{th}$ (GeV)	$S$ -wave	$P$ -wave
$J/\psi\eta^{(\prime)}$	3.64(4.07)	$1^{+-}$	$0/1/2^{--}$	$\eta_c\eta^{(\prime)}$	3.53(3.94)	$0^{++}$	$1^{-+}$
$J/\psi\omega$	3.88	$0/1/2^{++}$	$0/1/2/3^{-+}$	$\eta_c\omega$	3.77	$1^{+-}$	$0/1/2^{--}$
$J/\psi\phi$	4.12	$0/1/2^{++}$	$0/1/2/3^{-+}$	$\eta_c\phi$	4.00	$1^{+-}$	$0/1/2^{--}$
$\chi_{c0}(1P)\eta^{(\prime)}$	3.96(4.37)	$0^{-+}$	$1^{++}$	$\chi_{c0}(1P)\omega$	4.20	$1^{--}$	$0/1/2^{+-}$
$\chi_{c0}(1P)\phi$	4.43	$1^{--}$	$0/1/2^{+-}$	$\chi_{c1}(1P)\eta^{(\prime)}$	4.06(4.47)	$1^{-+}$	$0/1/2^{++}$
$\chi_{c1}(1P)\omega$	4.29	$0/1/2^{--}$	$0/1/2/3^{+-}$	$\chi_{c1}(1P)\phi$	4.53	$0/1/2^{--}$	$0/1/2/3^{+-}$
$\chi_{c2}(1P)\eta^{(\prime)}$	4.10(4.51)	$2^{-+}$	$1/2/3^{++}$	$\chi_{c2}(1P)\omega$	4.34	$1/2/3^{--}$	$0/1/2/3^{+-}$
$\chi_{c2}(1P)\phi$	4.58	$1/2/3^{--}$	$0/1/2/3^{+-}$				

### 3.2.1 Isoscalar charmonium-like molecular systems without hidden-strange quantum number

**The isoscalar  $D^*\bar{D}^*$  system.** In Table 8, we present the corresponding bound state properties for the  $S$ -wave isoscalar  $D^*\bar{D}^*$  system. When cutoff values vary from 0.8 to 3.0 GeV, we can obtain bound state solutions for the  $S$ -wave isoscalar  $D^*\bar{D}^*$  states with  $J^{PC} = 0^{++}$ ,  $1^{+-}$ , and  $2^{++}$ . And we can obtain the relation of  $\Lambda[0(0^{++})] < \Lambda[0(1^{+-})] < \Lambda[0(2^{++})]$ . Suppose bound states with a smaller cutoff binds deeper when we set the same binding energy. We can find the isoscalar  $D^*\bar{D}^*$  interaction with  $I(J^{PC}) = 0(0^{++})$  is strongest attractive, followed by the states with  $I(J^{PC}) = 0(1^{+-})$  and  $0(2^{++})$ . Thus, we can conclude these three states are possible isoscalar hidden-charm molecular tetraquark candidates, and their masses satisfy  $M[0(0^{++})] < M[0(1^{+-})] < M[0(2^{++})]$ . Here, our results are also consistent with the conclusions in Refs. [19, 43, 119–129].

After that, we further discuss the two-body hidden-charm decay behaviors for these possible  $S$ -wave isoscalar  $D^*\bar{D}^*$  molecular candidates by using the heavy quark symmetry and the quark-interchange model, respectively. The two-body hidden-charm decay channels

**Table 8.** Bound state properties for the  $S$ -wave isoscalar  $D^*\bar{D}^*$  system. Cutoff  $\Lambda$ , binding energy  $E$ , and root-mean-square (RMS) radius  $r_{\text{RMS}}$  are in units of GeV, MeV, and fm, respectively. Here, we label the major probability for the corresponding channels in a bold manner.

Effect	Single channel			$S$ - $D$ wave mixing effect			
$J^{PC}$	$\Lambda$	$E$	$r_{\text{RMS}}$	$\Lambda$	$E$	$r_{\text{RMS}}$	$P(^1\text{S}_0/^5\text{D}_0)$
$0^{++}$	0.92	-0.56	3.98	0.91	-0.61	3.89	<b>99.56</b> /0.44
	0.99	-11.81	1.09	0.98	-10.80	1.15	<b>99.42</b> /0.58
$J^{PC}$	$\Lambda$	$E$	$r_{\text{RMS}}$	$\Lambda$	$E$	$r_{\text{RMS}}$	$P(^3\text{S}_1/^3\text{D}_1/^5\text{D}_1)$
$1^{+-}$	1.07	-0.38	4.54	1.05	-0.35	4.67	<b>99.49</b> /0.51/ $o(0)$
	1.16	-12.01	1.09	1.15	-12.35	1.10	<b>99.13</b> /0.87/ $o(0)$
$J^{PC}$	$\Lambda$	$E$	$r_{\text{RMS}}$	$\Lambda$	$E$	$r_{\text{RMS}}$	$P(^5\text{S}_2/^1\text{D}_2/^3\text{D}_2/^5\text{D}_2)$
$2^{++}$	2.06	-0.28	5.18	1.82	-0.33	5.05	<b>99.03</b> /0.07/ $o(0)$ /0.90
	3.00	-12.35	1.26	2.81	-12.45	1.28	<b>98.00</b> /0.15/ $o(0)$ /1.85

include the  $\eta_c\eta$ ,  $\eta_c\eta'$ ,  $\eta_c\omega$ ,  $J/\psi\eta$ , and  $J/\psi\omega$  channels. We can expand their spin wave functions in the heavy quark spin symmetry basis  $|S_{c\bar{c}}^{P_Q, C_Q}, L_{q\bar{q}}^{P_q, C_q}\rangle$ , i.e.,

$$|0^{++}\rangle = \frac{\sqrt{3}}{2} |0_{c\bar{c}}^{--}, 0_{q\bar{q}}^{--}, 0^{++}\rangle - \frac{1}{2} |1_{c\bar{c}}^{--}, 1_{q\bar{q}}^{--}, 0^{++}\rangle, \quad (3.29)$$

$$|1^{+-}\rangle = \frac{1}{\sqrt{2}} |0_{c\bar{c}}^{--}, 1_{q\bar{q}}^{--}, 1^{+-}\rangle + \frac{1}{\sqrt{2}} |1_{c\bar{c}}^{--}, 0_{q\bar{q}}^{--}, 1^{+-}\rangle, \quad (3.30)$$

$$|2^{++}\rangle = |1_{c\bar{c}}^{--}, 1_{q\bar{q}}^{--}, 2^{++}\rangle, \quad (3.31)$$

where  $S_{c\bar{c}}^{P_Q, C_Q}$  and  $L_{q\bar{q}}^{P_q, C_q}$  stand for the spin parities for the charmonium state and light-flavor meson, respectively. In the heavy quark symmetry, we can estimate that

- The isoscalar  $D^*\bar{D}^*$  molecular state with  $J^{PC} = 0^{++}$  can decay into the  $\eta_c\eta^{(\prime)}$  and  $J/\psi\omega$  channels through the  $S$ -wave interaction, the relative decay ratio  $\mathcal{B}_0 = \Gamma_0[J/\psi\omega]/\Gamma_0[\eta_c\eta^{(\prime)}]$  is roughly 1 : 3.
- For the isoscalar  $D^*\bar{D}^*$  molecular state with  $J^{PC} = 1^{+-}$ , it can decay into the  $J/\psi\eta^{(\prime)}$  and  $\eta_c\omega$ . The relative decay branching ratio for the  $J/\psi\eta^{(\prime)}$  and  $\eta_c\omega$  channels is  $\mathcal{B}_1 = \Gamma_1[J/\psi\eta]/\Gamma_1[\eta_c\omega] = 1 : 1$ . Since the phase space for the  $D^*\bar{D}^* \rightarrow J/\psi\eta$  is larger than that in the  $\eta_c\omega$  final state around 100 MeV, the partial decay widths for these two hidden-charm decay processes satisfy  $\Gamma_1[J/\psi\eta] > \Gamma_1[\eta_c\omega]$ , it leads to the  $J/\psi\eta$  channel is the prime decay channel to search for the isoscalar  $D^*\bar{D}^*$  molecular state with  $J^{PC} = 1^{+-}$ .

- For the isoscalar  $D^*\bar{D}^*$  molecular state with  $J^{PC} = 2^{++}$ , the  $\eta_c\eta^{(\prime)}$  is the only one dominant two-body hidden-charm decay mode.

When adopting the quark-interchange model, we can numerically give the two-body hidden-charm decay widths for these possible  $S$ -wave isoscalar  $D^*\bar{D}^*$  molecular candidates. In Figure 8, we present the binding energies  $E$  dependence of the partial decay widths. For the  $S$ -wave  $D^*\bar{D}^*$  bound state with  $I(J^{PC}) = 0(0^{++})$ , there exist  $\eta_c\eta$ ,  $\eta_c\eta'$ , and  $J/\psi\omega$  decay modes, and it prefers to decay into the  $\eta_c\eta'$  channel. Among to these three decay modes, the partial decay width for the  $J/\psi\omega$  decay mode is the smallest, this is also consistent with our above analysis based on the heavy quark symmetry. Here, we also find that the partial decay width for the  $D^*\bar{D}^*[0(0^{++})] \rightarrow \eta_c\eta'$  is much larger than the partial decay width in the  $\eta_c\eta$  final state, although the phase space in the  $\eta_c\eta'$  final state is smaller. As we previously emphasized, the two-body hidden-charm decay width depends on the relative momentum  $|\mathbf{P}_C|$  in the final state and the interactions  $|\mathcal{M}_l|^2$ , where the  $|\mathcal{M}_l|^2$  corresponds to the overlap of the wave functions for the interactive hadrons. The large phase space leads to suppress the product of the wave functions in an exponential type  $|\mathcal{M}_l|^2 \sim \text{Exp}[-\mathbf{p}^2]V(\mathbf{p}^2)$  [112]. In Table 9, we present three groups of numerical results of the  $|\mathcal{M}_0|^2$  and the relative momentum  $|\mathbf{P}_C|$  in the final state for the  $D^*\bar{D}^*$  bound state with  $I^G(J^{PC}) = 0^+(0^{++})$ , and the bound energies are taken three typical values  $E = -5, -15$ , and  $-30$  MeV, respectively. It is obvious that the  $|\mathcal{M}_0|^2$  of the  $\eta_c\eta$  channel is significant less than the  $\eta_c\eta'$  channel, although the relative momentum  $|\mathbf{P}_C|$  in the  $\eta_c\eta$  channel is almost two to three times more than that in the  $\eta_c\eta'$  channel. We can also find the competitive relation between the phase space and the interaction term in the following results.

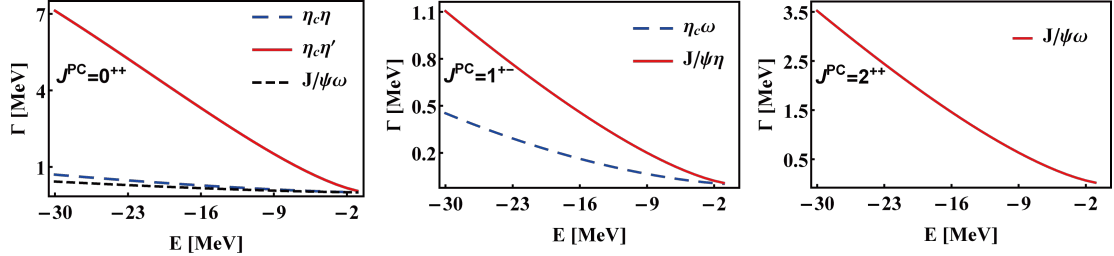


**Figure 8.** The binding energies  $E$  dependence of the decay widths for these possible  $S$ -wave isoscalar  $D^*\bar{D}^*$  molecular candidates.

For the  $D^*\bar{D}^*$  molecular state with  $I(J^{PC}) = 0(1^{+-})$ , we consider the  $J/\psi\eta$  and  $\eta_c\omega$  hidden-charm decay modes. As we previously analyzed, the decay ratio between these two channels is around 1 in the heavy quark symmetry. Here, the relative momentum  $|\mathbf{P}_C|$  in the  $J/\psi\eta$  and  $\eta_c\omega$  final states are around 655 MeV and 590 MeV, respectively. Therefore, the products of the wave functions in these two decay modes should be very close. Therefore, the partial decay width for the  $J/\psi\eta$  channel is a little larger as the larger relative momentum  $|\mathbf{P}_C|$ , as presented in Figure 8. Finally, the  $J/\psi\eta$  can be the suitable final states to search for the  $D^*\bar{D}^*$  molecular state with  $I(J^{PC}) = 0(1^{+-})$ .

**Table 9.** The bound energy  $E$  dependence of the relative momentum  $|\mathbf{P}_C|$  in the final state and the  $|\mathcal{M}_0|^2$  for the  $D^*\bar{D}^*$  bound state with  $I^G(J^{PC}) = 0^+(0^{++})$ . Here, we take three typical bound energies  $E = -5, -15$ , and  $-30$  MeV, respectively.

$( \mathbf{P}_C ,  \mathcal{M}_0 ^2)$	$E = -5$ MeV	$E = -15$ MeV	$E = -30$ MeV
$\eta_c\eta'$	(0.322, 0.845)	(0.298, 4.258)	(0.258, 11.593)
$\eta_c\eta$	(0.756, 0.033)	(0.746, 0.172)	(0.732, 0.485)

For the  $D^*\bar{D}^*$  bound state with  $I(J^{PC}) = 0(2^{++})$ , the  $J/\psi\omega$  is a significant two-body hidden-charm decay channel as presented in Figure 8. In addition, the isoscalar  $D^*\bar{D}^*$  molecular state with  $J^{PC} = 0^{++}$  can strongly couple to the  $D\bar{D}$  channel via the  $S$ -wave coupling, and the  $D^*\bar{D}^*[0(2^{++})]$  can decay into the  $D\bar{D}^*$  and  $D\bar{D}$  channels through the  $D$ -wave interactions, which indicate that the two-body open-charm decay widths satisfy  $\Gamma_{\text{Open}}[0(0^{++})] > \Gamma_{\text{Open}}[0(2^{++})]$ . Thus, we can estimate that the strong decay width for the  $D^*\bar{D}^*$  molecule with  $I(J^{PC}) = 0(0^{++})$  is larger than that for the  $D^*\bar{D}^*$  molecule with  $I(J^{PC}) = 0(2^{++})$ <sup>5</sup>. To summarize, if both the  $D^*\bar{D}^*$  states with  $I(J^{PC}) = 0(0^{++})$  and  $0(2^{++})$  are the possible charmonium-like molecular candidates, their mass and decay width satisfy  $M[0(0^{++})] < M[0(2^{++})]$  and  $\Gamma[0(0^{++})] > \Gamma[0(2^{++})]$ , respectively. These important characters on their mass spectrum and two-body strong decay behaviors provided here can help us to search and further identify the  $D^*\bar{D}^*$  charmonium-like molecules.

According to the above analysis, the  $J/\psi\omega$  final state has the potential to observe the possible  $D^*\bar{D}^*$  charmonium-like molecules with  $I(J^{PC}) = 0(0^{++})$  and  $0(2^{++})$ . Recalling the BaBar data presented in Figure 2, we can find possible evidence of the existence of two enhancement structures below the  $D^*\bar{D}^*$  threshold by analyzing the  $J/\psi\omega$  invariant mass spectrum of the  $B \rightarrow J/\psi\omega K$  [51, 52]. In Figure 9, we label the possible positions of the  $D^*\bar{D}^*$  charmonium-like molecules with  $I(J^{PC}) = 0(0^{++})$  and  $0(2^{++})$  in the  $J/\psi\omega$  invariant mass spectrum in the  $B \rightarrow J/\psi\omega K$  [51, 52]. We look forward the future experiments with higher precision data can test our theoretical predictions.

Meanwhile, it is interesting to note that the  $S$ -wave  $D^*\bar{D}^*$  state with  $I(J^{PC}) = 0(1^{+-})$  is favored to be the possible charmonium-like molecular candidate. As presented in Figure 8, the  $J/\psi\eta$  channel is the important two-body hidden-charm decay mode, and the corresponding decay width is around 1 MeV. Experimentally, we may find an enhancement structure around 3.9 GeV in the  $J/\psi\eta$  invariant mass spectrum of the  $B \rightarrow J/\psi\eta K$  [53], which may correspond to the  $S$ -wave isoscalar  $D^*\bar{D}^*$  molecular state with  $J^{PC} = 1^{+-}$  (see Figure 9 (b)). In addition, we notice that the BESIII Collaboration [130] and the Belle Collaboration [131] respectively analyzed the  $J/\psi\eta$  invariant mass spectrum in the  $e^+e^-$  annihilation process and the  $B \rightarrow J/\psi\eta K$  process, unfortunately, no significant signal around 3.9 GeV was found. This could be because there are only several dozen events or less

<sup>5</sup>Here, we neglect the other decay modes with very small contribution, like the three-body decay modes, the two-body decay modes via the  $D$ -wave interaction.

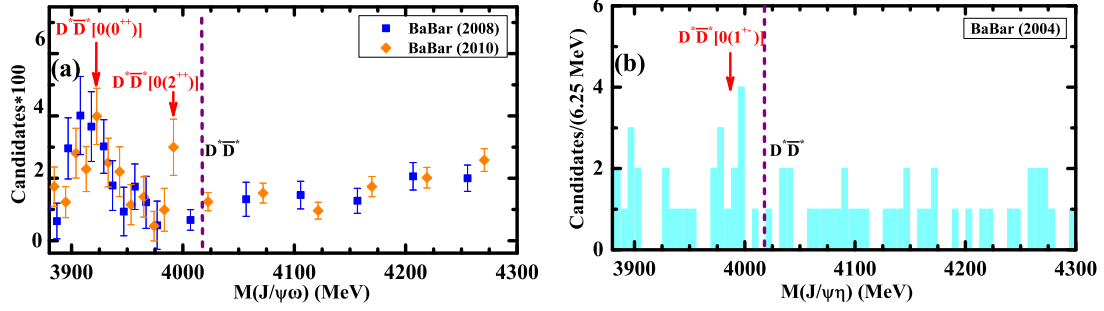


**Figure 9.** The  $J/\psi\omega$  and  $J/\psi\eta$  invariant mass spectrum around the  $D^*\bar{D}^*$  threshold in the  $B \rightarrow J/\psi\omega K$  [51, 52] and  $B \rightarrow J/\psi\eta K$  [53], respectively.

in the  $J/\psi\eta$  invariant mass spectrum [53, 130, 131], in comparison with the observations of the  $J/\psi\omega$  invariant mass spectrum [17, 51, 52], we expect more precision experimental data to further check the structure around 3.9 GeV in the  $J/\psi\eta$  invariant mass spectrum.

In short, due to the lack of the sufficiently accurate experimental results, the present data sample from the  $B$  meson decays was not large enough to analyze these possible charmonium-like molecular tetraquark structures in the  $J/\psi\omega$  and  $J/\psi\eta$  invariant mass spectrum [17, 51–53, 131], and the study of these possible charmonium-like molecular tetraquark candidates will become an important research field at the precision frontier in future experiments. Thus, we strongly expect experimental colleagues to focus on the detailed structures around 3.9 GeV in the  $J/\psi\omega$  and  $J/\psi\eta$  invariant mass spectrum with more precise experimental data, like the LHCb, Belle II, and BESIII, it will provide strong evidence of existing charmonium-like molecular tetraquark states if these possible enhancement structures can be confirmed in future experiments.

**The isoscalar  $D\bar{D}$  systems with their masses around 4.3 GeV.** In this section, we try to understand very broad structure around 4.3 GeV in the  $J/\psi\omega$  invariant mass spectrum of the  $B \rightarrow J/\psi\omega K$  process [17, 51, 52]. The mass thresholds of the  $D^*\bar{D}_1$ ,  $D^*\bar{D}_2^*$ ,  $D\bar{D}_2^*$ , and  $D\bar{D}_1$  systems locate around this energy region. In general, the pion exchange interaction usually plays a crucial role in forming the hadronic molecular states [10]. In the following, we discuss these  $S$ -wave isoscalar charmonium-like molecular tetraquark systems with three different groups, i.e., the  $S$ -wave isoscalar charmonium-like molecular tetraquark systems with the pion exchange contribution occurring in the direct channel effective potentials, the  $S$ -wave isoscalar charmonium-like molecular tetraquark systems with the pion exchange contribution occurring in the cross channel effective potentials, and the  $S$ -wave isoscalar charmonium-like molecular tetraquark systems without the pion exchange process.

(i). The  $S$ -wave isoscalar  $D^*\bar{D}_1$  and  $D^*\bar{D}_2^*$  systems.

By performing numerical calculations, we can obtain the loosely bound state solutions for the  $S$ -wave isoscalar  $D^*\bar{D}_1$  and  $D^*\bar{D}_2^*$  systems when the cutoff values are tuned from 0.8 to 3.0 GeV. In Table 10, we present the corresponding bound state solutions. Compared to the high spin states, we find that the low spin states can be easier to bind as charmonium-like molecular candidates for the  $S$ -wave isoscalar  $D^*\bar{D}_1$  and  $D^*\bar{D}_2^*$  systems. Here, we also

consider the coupled channel effect, and find the coupled channel effect plays a minor role in the above discussed systems. In fact, there are several papers on the predictions of the possible  $S$ -wave isoscalar  $D^*\bar{D}_1$  and  $D^*\bar{D}_2^*$  charmonium-like molecular tetraquark states [69, 132–136].

**Table 10.** Bound state solutions for the  $S$ -wave isoscalar  $D^*\bar{D}_1$  and  $D^*\bar{D}_2^*$  systems. Conventions are the same as Table 8.

Effect	Single channel			$S$ - $D$ wave mixing effect			
$D^*\bar{D}_1[J^{PC}]$	$\Lambda$	$E$	$r_{\text{RMS}}$	$\Lambda$	$E$	$r_{\text{RMS}}$	$P(^1S_0/^5D_0)$
$0^{--}$	0.96	-0.59	3.73	0.95	-0.52	3.92	<b>99.70</b> /0.30
	1.03	-11.12	1.07	1.03	-12.40	1.03	<b>99.59</b> /0.41
$0^{-+}$	0.92	-0.56	3.91	0.91	-0.55	3.96	<b>99.53</b> /0.47
	0.99	-11.42	1.08	0.99	-12.82	1.05	<b>99.41</b> /0.59
$D^*\bar{D}_1[J^{PC}]$	$\Lambda$	$E$	$r_{\text{RMS}}$	$\Lambda$	$E$	$r_{\text{RMS}}$	$P(^3S_1/^3D_1/^5D_1)$
$1^{--}$	1.10	-0.48	4.11	1.08	-0.33	4.61	<b>99.64</b> /0.35/0.01
	1.20	-12.57	1.03	1.19	-12.74	1.03	<b>99.38</b> /0.61/0.01
$1^{-+}$	1.06	-0.45	4.25	1.04	-0.34	4.68	<b>99.47</b> /0.52/0.01
	1.15	-11.80	1.07	1.14	-11.75	1.09	<b>99.13</b> /0.86/0.01
$D^*\bar{D}_1[J^{PC}]$	$\Lambda$	$E$	$r_{\text{RMS}}$	$\Lambda$	$E$	$r_{\text{RMS}}$	$P(^5S_2/^1D_2/^3D_2/^5D_2)$
$2^{--}$	2.56	-0.32	4.89	2.60	-0.33	4.90	<b>98.90</b> /0.05/ $o(0)$ /1.05
	2.58	-9.86	1.16	2.74	-8.65	1.33	<b>93.06</b> /4.18/ $o(0)$ /2.75
$2^{-+}$	1.73	-0.81	3.68	1.59	-0.34	4.90	<b>99.30</b> /0.08/ $o(0)$ /0.62
	2.14	-12.16	1.24	2.07	-12.74	1.24	<b>98.77</b> /0.27/ $o(0)$ /0.93
$D^*\bar{D}_2^*[J^{PC}]$	$\Lambda$	$E$	$r_{\text{RMS}}$	$\Lambda$	$E$	$r_{\text{RMS}}$	$P(^3S_1/^3D_1/^5D_1/^7D_1)$
$1^{--}$	0.97	-0.27	4.80	0.97	-0.51	4.00	<b>99.81</b> /0.09/ $o(0)$ /0.10
	1.05	-10.92	1.09	1.05	-11.81	1.06	<b>99.71</b> /0.19/ $o(0)$ /0.09
$1^{-+}$	0.94	-0.28	4.78	0.94	-0.56	3.90	<b>99.77</b> /0.07/ $o(0)$ /0.16
	1.02	-12.82	1.01	1.02	-13.86	0.99	<b>99.69</b> /0.05/ $o(0)$ /0.26
$D^*\bar{D}_2^*[J^{PC}]$	$\Lambda$	$E$	$r_{\text{RMS}}$	$\Lambda$	$E$	$r_{\text{RMS}}$	$P(^5S_2/^3D_2/^5D_2/^7D_2)$
$2^{--}$	1.11	-0.31	4.77	1.10	-0.28	4.84	<b>99.78</b> / $o(0)$ /0.22/ $o(0)$
	1.21	-11.55	1.08	1.21	-12.66	1.04	<b>99.59</b> /0.01/0.40/ $o(0)$
$2^{-+}$	1.21	-0.67	3.68	1.19	-0.28	4.84	<b>99.67</b> / $o(0)$ /0.33/ $o(0)$
	1.36	-12.76	1.04	1.35	-12.82	1.05	<b>99.38</b> /0.01/0.60/0.01
$D^*\bar{D}_2^*[J^{PC}]$	$\Lambda$	$E$	$r_{\text{RMS}}$	$\Lambda$	$E$	$r_{\text{RMS}}$	$P(^7S_3/^3D_3/^5D_3/^7D_3)$
$3^{--}$	1.97	-0.32	4.94	1.77	-0.33	4.91	<b>99.03</b> /0.04/ $o(0)$ /0.93
	2.74	-12.49	1.21	2.51	-12.41	1.24	<b>97.70</b> /0.19/0.03/2.07
$3^{-+}$	1.90	-0.32	4.94	1.73	-0.31	4.98	<b>99.21</b> /0.07/ $o(0)$ /0.72
	2.87	-12.26	1.23	2.64	-12.24	1.25	<b>98.36</b> /0.39/0.03/1.22

After analyzing the mass spectrum for these  $S$ -wave isoscalar  $D^*\bar{D}_1$  and  $D^*\bar{D}_2^*$  systems, we further study two-body hidden-charm decay behaviors of these possible  $S$ -wave isoscalar  $D^*\bar{D}_1$  and  $D^*\bar{D}_2^*$  molecular candidates. For the  $S$ -wave  $D^*\bar{D}_1$  bound state with  $I(J^{PC}) = 0(0^{-+})$ , the allowed two-body hidden-charm decay modes include  $J/\psi\omega$ ,  $\chi_{c0}(1P)\eta$ , and  $\chi_{c0}(1P)\eta'$ , the  $S$ -wave  $D^*\bar{D}_1$  bound state with  $I(J^{PC}) = 0(1^{-+})$  can decay into  $\eta_c\eta$ ,  $\eta_c\eta'$ ,  $J/\psi\omega$ , and  $\chi_{c1}(1P)\eta$  channels, and the  $S$ -wave  $D^*\bar{D}_1$  bound state with  $I(J^{PC}) = 0(2^{-+})$  exists the  $J/\psi\omega$  and  $\chi_{c2}(1P)\eta$  decay channels. In Figure 10, we present the binding energies  $E$  dependence of the decay widths for these possible  $S$ -wave isoscalar  $D^*\bar{D}_1$  and  $D^*\bar{D}_2^*$  molecular candidates. Here, we neglect several two-body hidden-charm strong decay modes with very small widths in Figure 10. Our results indicate that the total two-body hidden-charm strong decay widths of the  $S$ -wave isoscalar  $D^*\bar{D}_1$  molecular candidates with positive  $C$ -parity are a little small. All the  $S$ -wave  $D^*\bar{D}_1$  bound states with  $I(J^{PC}) = 0[(0^{-+}), (1^{-+}), (2^{-+})]$  can decay into the  $J/\psi\omega$  channel. The  $\chi_{c0}(1P)\eta^{(\prime)}$ ,  $\chi_{c1}(1P)\eta$ , and  $\chi_{c2}(1P)\eta$  are the important decay channels for the  $S$ -wave isoscalar  $D^*\bar{D}_1$  bound states with  $J^{PC} = 0^{-+}$ ,  $1^{-+}$ , and  $2^{-+}$ , respectively. With the increasing of the binding energy, the  $J/\psi\omega$  decay mode becomes more and more important. Therefore, it may be possible to search for the  $D^*\bar{D}_1$  molecular candidates with  $I(J^{PC}) = 0[(0^{-+}), (1^{-+}), (2^{-+})]$  in the  $J/\psi\omega$  invariant mass spectrum from the  $B \rightarrow J/\psi\omega K$ .

Different from these discussed  $S$ -wave isoscalar  $D^*\bar{D}_1$  molecular candidates with positive  $C$ -parity, the  $S$ -wave isoscalar  $D^*\bar{D}_1$  molecular candidates with negative  $C$ -parity have abundant two-body hidden-charm decay channels. For the isoscalar  $D^*\bar{D}_1$  molecular candidates with  $J^{PC} = 0^{--}$ ,  $1^{--}$ , and  $2^{--}$ , their allowed two-body hidden-charm decay modes include  $[\eta_c\omega, J/\psi\eta, J/\psi\eta', \chi_{c1}(1P)\omega]$ ,  $[\eta_c\omega, J/\psi\eta, J/\psi\eta', \chi_{c0}(1P)\omega, \chi_{c1}(1P)\omega, \chi_{c2}(1P)\omega]$ , and  $[\eta_c\omega, J/\psi\eta, J/\psi\eta', \chi_{c1}(1P)\omega, \chi_{c2}(1P)\omega]$ , respectively. In Figure 10, we only present the important two-body hidden-charm decay modes for the isoscalar  $D^*\bar{D}_1$  molecular candidates with  $J^{PC} = 0^{--}$ ,  $1^{--}$ , and  $2^{--}$ , their partial decay widths for the  $\chi_{cJ}(1P)\omega$  channels are all around several MeV. For the  $D^*\bar{D}_1$  bound state with  $I(J^{PC}) = 0(0^{--})$ , the  $\chi_{c1}(1P)\omega$  is the most important two-body hidden-charm decay channel in our calculations. For the  $D^*\bar{D}_1$  bound state with  $I(J^{PC}) = 0(1^{--})$ , it prefers to decay into the  $\chi_{c2}(1P)\omega$  channel, and the remaining  $\chi_{c0}(1P)\omega$  and  $\chi_{c1}(1P)\omega$  final channels are also important. For the  $D^*\bar{D}_1$  bound state with  $I(J^{PC}) = 0(2^{--})$ , the  $\chi_{c2}(1P)\omega$  and  $\chi_{c1}(1P)\omega$  channels are the main two-body hidden-charm decay channels, especially the  $\chi_{c2}(1P)\omega$  channel.

As shown in Figure 10, we also calculate the two-body hidden-charm decay behaviors of these possible  $S$ -wave isoscalar  $D^*\bar{D}_2^*$  molecular candidates, the allowed two-body hidden-



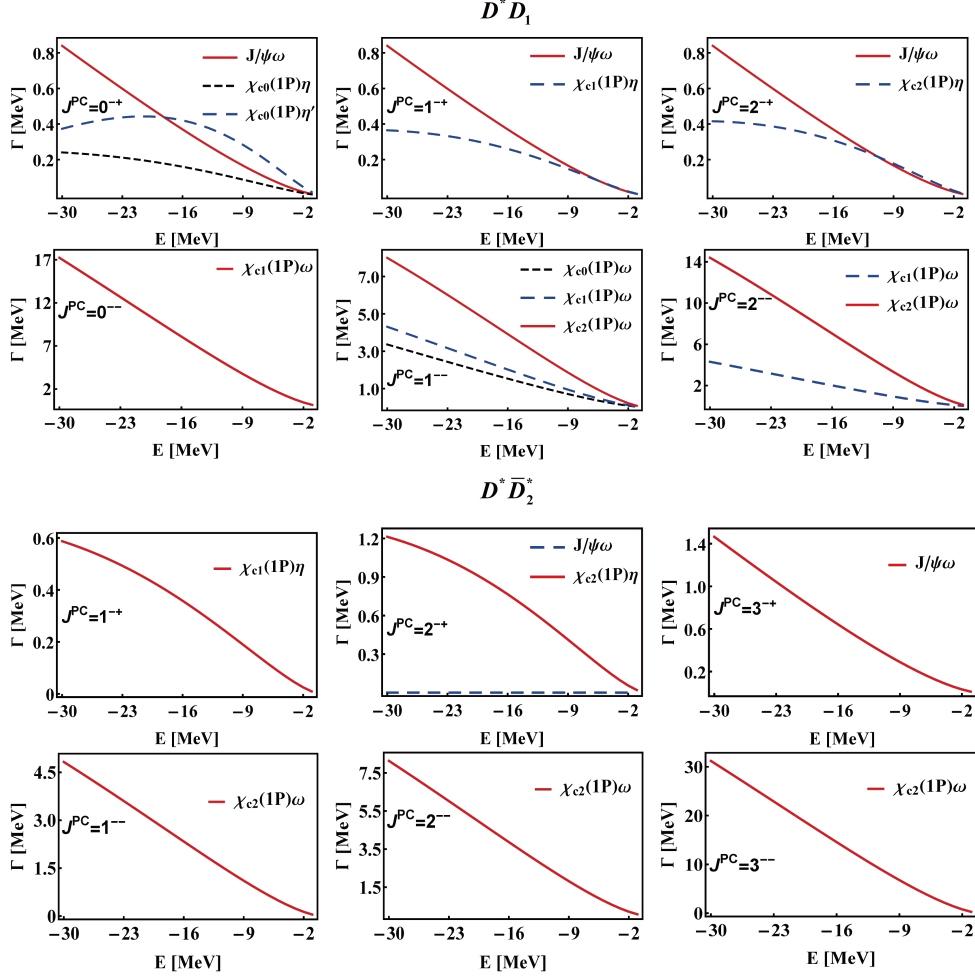


**Figure 10.** The binding energies  $E$  dependence of the decay widths for these possible  $S$ -wave isoscalar  $D^*\bar{D}_1$  and  $D^*\bar{D}_2^*$  molecular candidates.

charm decay channels include

$$\begin{aligned}
D^*\bar{D}_2^*[0(1^{++})] &: \eta_c\eta, \eta_c\eta', J/\psi\omega, \chi_{c1}(1P)\eta, \chi_{c1}(1P)\eta', \\
D^*\bar{D}_2^*[0(2^{++})] &: J/\psi\omega, \chi_{c2}(1P)\eta, \\
D^*\bar{D}_2^*[0(3^{++})] &: J/\psi\omega, \\
D^*\bar{D}_2^*[0(1^{--})] &: \eta_c\omega, J/\psi\eta, J/\psi\eta', \chi_{c0}(1P)\omega, \chi_{c1}(1P)\omega, \chi_{c2}(1P)\omega, \\
D^*\bar{D}_2^*[0(2^{--})] &: \eta_c\omega, J/\psi\eta, J/\psi\eta', \chi_{c1}(1P)\omega, \chi_{c2}(1P)\omega, \\
D^*\bar{D}_2^*[0(3^{--})] &: \chi_{c2}(1P)\omega.
\end{aligned} \tag{3.32}$$

Finally, we find that

- For the  $D^*\bar{D}_2^*$  bound state with  $I(J^{PC}) = 0(1^{++})$ , it dominantly decay into the  $\chi_{c1}(1P)\eta$  channel. For the  $D^*\bar{D}_2^*$  bound state with  $I(J^{PC}) = 0(2^{++})$ , we calculate

two decay final states, the  $J/\psi\omega$  and  $\chi_{c2}(1P)\eta$ , where the decay width of the  $\chi_{c2}(1P)\eta$  channel is significantly larger than the  $J/\psi\omega$  channel, even if we increase the binding energies  $E$  from  $-1$  to  $-30$  MeV,  $\Gamma(J/\psi\omega)$  is approximate 0 MeV. In other words, it may be a little hard to observe the  $D^*\bar{D}_2^*$  molecular state with  $I(J^{PC}) = 0(2^{-+})$  in the  $J/\psi\omega$  decay channel, and the  $\chi_{c2}(1P)\eta$  can be the prime channel to search for the possible  $D^*\bar{D}_2^*$  molecular candidate with  $I(J^{PC}) = 0(2^{-+})$ . However, the  $J/\psi\omega$  may be the one of important decay channel to search for the possible  $D^*\bar{D}_2^*$  molecular candidate with  $I(J^{PC}) = 0(3^{-+})$ , as it is the dominantly two-body hidden-charm decay channel with the corresponding partial decay width around 1 MeV.

- The  $\chi_{c2}(1P)\omega$  is the dominant two-body hidden-charm decay channel for all the  $S$ -wave isoscalar  $D^*\bar{D}_2^*$  bound states with negative  $C$ -parity. Especially, the partial decay width  $\Gamma(D^*\bar{D}_2^*[0(3^{--})] \rightarrow \chi_{c2}(1P)\omega)$  can reach several tens MeV when the binding energy is taken around several tens MeV.

All in all, the  $S$ -wave isoscalar  $D^*\bar{D}_1$  and  $D^*\bar{D}_2^*$  states can be good charmonium-like molecular candidates. We can summary the dominant two-body hidden-charm decay channels for the corresponding isoscalar charmonium-like molecular candidates as follows, i.e.,

$$\begin{aligned}
J/\psi\omega &: D^*\bar{D}_1[(0, 1, 2)^{-+}], D^*\bar{D}_2^*[3^{-+}], \\
\chi_{c1}(1P)\omega &: D^*\bar{D}_1[0^{--}], \\
\chi_{c2}(1P)\omega &: D^*\bar{D}_1[(1, 2)^{--}], \quad D^*\bar{D}_2^*[(1, 2, 3)^{--}], \\
\chi_{c1}(1P)\eta &: D^*\bar{D}_2^*[1^{-+}], \\
\chi_{c2}(1P)\eta &: D^*\bar{D}_2^*[2^{-+}].
\end{aligned} \tag{3.33}$$

(ii). The  $S$ -wave isoscalar  $D\bar{D}_2^*$  system.

For the  $D\bar{D}_2^*$  system, the  $\pi$  exchange occurs in the  $D\bar{D}_2^* \rightarrow D_2^*\bar{D}$  process, and the interaction Feynman diagram corresponds to the Cross diagram in Figure 6. In Table 11, we collect the bound state solutions for the  $S$ -wave isoscalar  $D\bar{D}_2^*$  system. It is obvious that these  $S$ -wave isoscalar  $D\bar{D}_2^*$  states can be possible charmonium-like molecular candidates as their bound state solutions satisfy the typical characters for a loosely bound hadronic molecule<sup>6</sup> [133, 135].

For the  $D\bar{D}_2^*$  bound state with  $I(J^{PC}) = 0(2^{-+})$ , the allowed two-body hidden-charm decay channels include  $J/\psi\omega$  and  $\chi_{c2}(1P)\eta$ . For the  $D\bar{D}_2^*$  bound state with  $I(J^{PC}) = 0(2^{--})$ , it can decay into  $\eta_c\omega$ ,  $J/\psi\eta$ ,  $J/\psi\eta'$ , and  $\chi_{c1}(1P)\omega$  channels. In Figure 11, we present the binding energies  $E$  dependence of the corresponding decay widths. For the  $D\bar{D}_2^*$  bound state with  $I(J^{PC}) = 0(2^{-+})$ , the  $\chi_{c2}(1P)\eta$  is the dominant two-body hidden-charm decay channel, and the partial decay width for the  $J/\psi\omega$  channel is relatively small

<sup>6</sup>When the cutoff  $\Lambda$  is taken around 1 GeV, the binding energy is around several to several tens MeV, and the size of bound state is larger than the size of its component.

**Table 11.** Bound state solutions for the  $S$ -wave isoscalar  $D\bar{D}_2^*$  system. Conventions are the same as Table 8.

Effect	Single channel			$S$ - $D$ wave mixing effect			
$D\bar{D}_2^*[J^{PC}]$	$\Lambda$	$E$	$r_{\text{RMS}}$	$\Lambda$	$E$	$r_{\text{RMS}}$	$P(^5S_2/^5D_2)$
$2^{--}$	1.46	-0.25	5.08	1.46	-0.34	4.74	<b>99.99</b> /0.01
	1.85	-12.22	1.11	1.82	-12.40	1.11	<b>99.91</b> /0.09
$2^{-+}$	1.30	-0.36	4.69	1.29	-0.24	5.17	<b>99.99</b> /0.01
	1.47	-12.03	1.11	1.47	-12.89	1.08	<b>99.93</b> /0.07

around 1 MeV. For the  $D\bar{D}_2^*$  bound state with  $I(J^{PC}) = 0(2^{--})$ , the partial decay width for the  $\chi_{c1}(1P)\omega$  channel is around several MeV, perhaps one can search for the possible  $D\bar{D}_2^*$  molecular state with  $I(J^{PC}) = 0(2^{--})$  in the  $\chi_{c1}(1P)\omega$  invariant mass spectrum from the  $B$  meson weak decay.

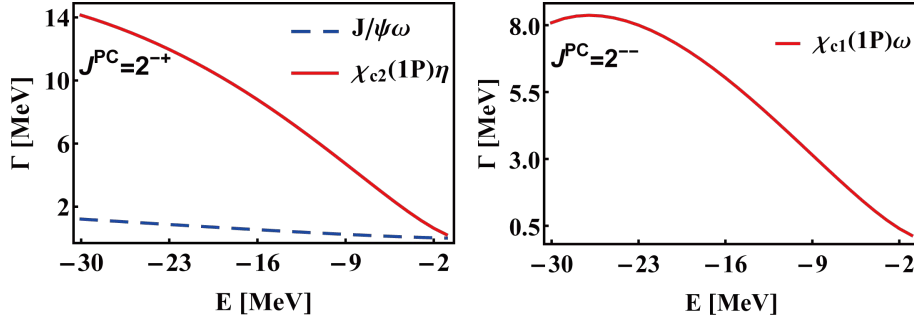


**Figure 11.** The binding energies  $E$  dependence of the decay widths for these possible  $S$ -wave isoscalar  $D\bar{D}_2^*$  molecular candidates.

(iii). The  $S$ -wave isoscalar  $D\bar{D}_1$  system.

Despite the  $\pi$  exchange does not contribute to the effective potentials for the  $S$ -wave  $D\bar{D}_1$  system as the parity forbidden, the scalar and vector mesons exchange interactions may be strong enough to generate an bound state [80, 137]. As shown in Table 12, our numerical results suggest the isoscalar  $D\bar{D}_1$  states with  $I(J^{PC}) = 0[(1^{--}), (1^{-+})]$  can be possible charmonium-like molecular candidates. In fact, the  $S$ -wave isoscalar  $D\bar{D}_1$  molecular states were intensively discussed in Refs. [69, 89, 102, 104, 132, 133, 135], which may be related to the  $Y(4260)$ <sup>7</sup> [139].

The binding energies  $E$  dependence of the decay widths for the isoscalar  $D\bar{D}_1$  molecular candidates with  $J^{PC} = 1^{-+}$  and  $1^{--}$  are given in Figure 12. The  $D\bar{D}_1$  bound state with

<sup>7</sup>In 2017, the BESIII gave more precise data of the  $e^+e^- \rightarrow J/\psi\pi^+\pi^-$  [138], which shows that the  $Y(4260)$  [139] is split into two resonances  $Y(4220)$  and  $Y(4320)$ .

**Table 12.** Bound state solutions for the  $S$ -wave isoscalar  $D\bar{D}_1$  system. Conventions are the same as Table 8.

Effect	Single channel			$S$ - $D$ wave mixing effect			
$D\bar{D}_1[J^{PC}]$	$\Lambda$	$E$	$r_{\text{RMS}}$	$\Lambda$	$E$	$r_{\text{RMS}}$	$P(^3\mathbb{S}_1/^3\mathbb{D}_1)$
$1^{--}$	1.38	-0.29	4.92	1.38	-0.32	4.80	<b>99.98</b> /0.02
	1.63	-12.63	1.09	1.63	-12.89	1.08	<b>99.93</b> /0.07
$1^{-+}$	1.39	-0.36	4.72	1.39	-0.39	4.60	<b>99.98</b> /0.02
	1.67	-12.13	1.14	1.67	-12.42	1.13	<b>99.92</b> /0.08

$I(J^{PC}) = 0(1^{-+})$  prefers to decay into the  $J/\psi\omega$  channel, and the partial decay widths for the remaining two-body hidden-charm decay channels are very small, they are less than 0.5 MeV by varying the binding energies  $E$  from -1 to -30 MeV. Moreover, the  $\chi_{c0}(1P)\omega$  is the dominant two-body hidden-charm decay channel for the  $D\bar{D}_1$  bound state with  $I(J^{PC}) = 0(1^{--})$ .

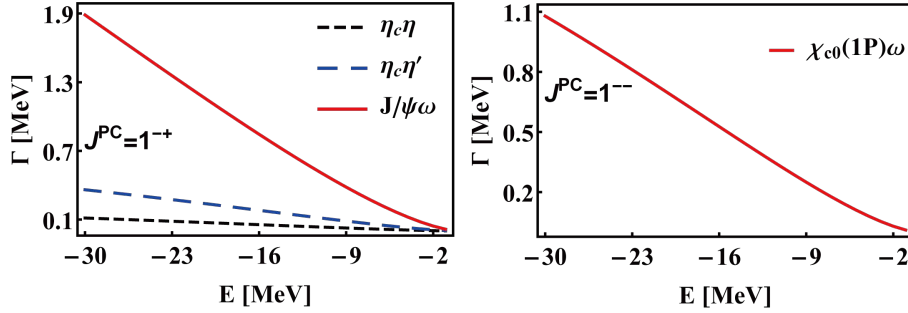


**Figure 12.** The binding energies  $E$  dependence of the decay widths for the  $S$ -wave isoscalar  $D\bar{D}_1$  molecular candidates with  $J^{PC} = 1^{-+}$  and  $1^{--}$ .

Let's give a short summary, we can predict a serial of possible charmonium-like molecules composed by the  $S$ -wave isoscalar  $D^*\bar{D}_1$ ,  $D^*\bar{D}_2^*$ ,  $D\bar{D}_2^*$ , and  $D\bar{D}_1$  systems. In Table 13, we summary their two-body hidden-charm decay information, including the important two-body hidden-charm decay channels and the order of the decay widths. The relevant results of the two-body hidden-charm decay properties can be very helpful to search for these possible charmonium-like molecules. For example, the  $J/\psi\omega$  channel is the dominant two-body hidden-charm decay mode for the isoscalar  $D^*\bar{D}_1[(0, 1, 2)^{-+}]$ ,  $D^*\bar{D}_2^*[3^{-+}]$ , and  $D\bar{D}_1[1^{-+}]$  bound states, perhaps, it is possible to observe the experimental signal of these possible charmonium-like molecules in the  $J/\psi\omega$  final state. When we recall the experimental data of the  $B \rightarrow J/\psi\omega K$  [17, 51, 52], our predictions of these possible charmonium-like molecules also reflect the complexity of the structures in the  $J/\psi\omega$  invariant mass spectrum around 4.3 GeV. At present, it is a little difficult to definitely identify these possible charmonium-like

molecules, we hope further experiments can provide more precise measurement of the  $B$  meson decay into a charmonium state plus a light-flavor meson. In addition, the  $\chi_{cJ}(1P)\omega$  are the important two-body hidden-charm decay channels for the possible  $S$ -wave isoscalar  $D^*\bar{D}_1$ ,  $D^*\bar{D}_2^*$ ,  $D\bar{D}_2^*$ , and  $D\bar{D}_1$  systems of negative  $C$ -parity in our calculations.

**Table 13.** A summary of the important two-body hidden-charm decay channels and the order of the decay widths for all the possible  $S$ -wave isoscalar  $D^*\bar{D}_1$ ,  $D^*\bar{D}_2^*$ ,  $D\bar{D}_2^*$ , and  $D\bar{D}_1$  charmonium-like molecules. Here,  $\mathcal{O}(x)$  stands for the partial decay widths in the order of  $x$  MeV with the binding energies around 5 to 20 MeV. We label the dominant two-body hidden-charm decay modes in the bold manner.

States	Two-body hidden-charm decay channels	$\mathcal{O}(\Gamma)$
$D^*\bar{D}_1[0^{-+}]$	$\mathbf{J/\psi\omega}$ , $\chi_{c0}(1P)\eta$ , $\chi_{c0}(1P)\eta'$	0.10, 0.10, 0.10
$D^*\bar{D}_1[0^{--}]$	$\chi_{c1}(\mathbf{1P})\omega$	1.00
$D^*\bar{D}_1[1^{-+}]$	$\mathbf{J/\psi\omega}$ , $\chi_{c1}(1P)\eta$	0.10, 0.10
$D^*\bar{D}_1[1^{--}]$	$\chi_{c2}(\mathbf{1P})\omega$ , $\chi_{c1}(1P)\omega$ , $\chi_{c0}(1P)\omega$	1.00, 1.00, 1.00
$D^*\bar{D}_1[2^{-+}]$	$\mathbf{J/\psi\omega}$ , $\chi_{c2}(1P)\eta$	0.10, 0.10
$D^*\bar{D}_1[2^{--}]$	$\chi_{c2}(\mathbf{1P})\omega$ , $\chi_{c1}(1P)\omega$	10.00, 1.00
$D^*\bar{D}_2^*[1^{-+}]$	$\chi_{c1}(\mathbf{1P})\eta$	0.10
$D^*\bar{D}_2^*[1^{--}]$	$\chi_{c2}(\mathbf{1P})\omega$	1.00
$D^*\bar{D}_2^*[2^{-+}]$	$\chi_{c2}(\mathbf{1P})\eta$ , $J/\psi\omega$	1.00, 0.10
$D^*\bar{D}_2^*[2^{--}]$	$\chi_{c2}(\mathbf{1P})\omega$	1.00
$D^*\bar{D}_2^*[3^{-+}]$	$\mathbf{J/\psi\omega}$	0.10
$D^*\bar{D}_2^*[3^{--}]$	$\chi_{c2}(\mathbf{1P})\omega$	10.00
$D\bar{D}_2^*[2^{-+}]$	$\chi_{c2}(\mathbf{1P})\eta$ , $J/\psi\omega$	10.00, 1.00
$D\bar{D}_2^*[2^{--}]$	$\chi_{c1}(\mathbf{1P})\omega$	1.00
$D\bar{D}_1[1^{-+}]$	$\mathbf{J/\psi\omega}$ , $\eta_c\eta'$ , $\eta_c\eta$	1.00, 0.10, 0.10
$D\bar{D}_1[1^{--}]$	$\chi_{c0}(\mathbf{1P})\omega$	0.10

For the sake of completeness, we also discuss the mass spectrum and the two-body hidden-charm decay behaviors for the  $S$ -wave isoscalar  $D\bar{D}$  and  $D\bar{D}^*$  systems, the relevant results are given in the Appendix B.

### 3.2.2 Charmonium-like molecular tetraquark systems with hidden-strange quantum number

With the help of the  $SU(3)$  flavor symmetry, we can further study the interactions between the charm-strange meson and anti-charm-strange meson, in this section, we analyze the existence probability of the charmonium-like molecules with hidden-strange quantum number and study their two-body hidden-charm decay behaviors.

**The  $D_s^* \bar{D}_s^*$  system.** For the  $D_s^* \bar{D}_s^*$  system, the  $\eta$  and  $\phi$  exchanges contribute to the effective potentials in the OBE model. The relevant numerical results for the  $S$ -wave  $D_s^* \bar{D}_s^*$  system are given in Table 14, and the cutoff parameters are taken in the range from 1.0 to 3.0 GeV.

**Table 14.** Bound state solutions for the  $S$ -wave  $D_s^* \bar{D}_s^*$  system. Conventions are the same as Table 8.

Effect	Single channel			$S$ - $D$ wave mixing effect			
$J^{PC}$	$\Lambda$	$E$	$r_{\text{RMS}}$	$\Lambda$	$E$	$r_{\text{RMS}}$	$P(^1\text{S}_0/^5\text{D}_0)$
$0^{++}$	1.59	-0.72	3.49	1.58	-0.23	4.98	<b>99.98</b> /0.02
	1.65	-11.09	0.98	1.65	-11.34	0.97	<b>99.95</b> /0.05
$J^{PC}$	$\Lambda$	$E$	$r_{\text{RMS}}$	$\Lambda$	$E$	$r_{\text{RMS}}$	$P(^3\text{S}_1/^3\text{D}_1/^5\text{D}_1)$
$1^{+-}$	1.89	-0.52	4.00	1.88	-0.26	4.89	<b>99.98</b> /0.02/ $o(0)$
	2.00	-12.37	0.95	2.00	-12.52	0.94	<b>99.96</b> /0.04/ $o(0)$

For the  $S$ -wave  $D_s^* \bar{D}_s^*$  states with  $J^{PC} = 0^{++}$  and  $1^{+-}$ , we can obtain the loosely bound state solutions for these states when the cutoff values are taken to be around 1.6 GeV and 1.9 GeV, respectively. Thus, the  $S$ -wave  $D_s^* \bar{D}_s^*$  states with  $J^{PC} = 0^{++}$  and  $1^{+-}$  can be the possible hidden-charm and hidden-strange molecular tetraquark candidates, especially the  $D_s^* \bar{D}_s^*$  molecular state with  $J^{PC} = 0^{++}$  [140, 141]. If taking a large cutoff  $\Lambda > 3.0$  GeV, there exist the loosely bound state solutions for the  $D_s^* \bar{D}_s^*$  state with  $J^{PC} = 2^{++}$  in Ref. [19]. However, such cutoff parameter is far from the usual value around 1.0 GeV [80, 87, 88], which is consistent with our numerical results.

In the following, we calculate the two-body hidden-charm strong decay behaviors for the possible  $S$ -wave  $D_s^* \bar{D}_s^*$  bound states with  $J^{PC} = 0^{++}$ ,  $1^{+-}$ , and  $2^{++}$ . The binding energies  $E$  dependence of the partial decay widths for the possible  $S$ -wave  $D_s^* \bar{D}_s^*$  bound states with  $J^{PC} = 0^{++}$ ,  $1^{+-}$ , and  $2^{++}$  are presented in Figure 13. The two-body hidden-charm decay behaviors for the  $S$ -wave  $D_s^* \bar{D}_s^*$  bound states are very similar to those in the  $S$ -wave  $D^* \bar{D}^*$  bound states, i.e., the  $D_s^* \bar{D}_s^*$  bound state with  $J^{PC} = 0^{++}$  can decay into the  $\eta_c \eta^{(\prime)}$  and  $J/\psi \phi$  channels, and the  $\eta_c \eta'$  is the dominant channel. Here, the partial decay width for the  $\eta_c \eta$  channel is very small, as we mentioned in the last section, although the

phase space in the  $\eta_c\eta$  final state is larger than that in the  $\eta_c\eta'$ , the partial decay width is strongly suppressed by the product of the wave functions for the interaction mesons. For the  $J/\psi\phi$  decay mode, its final state momentum  $|\mathbf{P}_C(\phi)|$  is very close to  $|\mathbf{P}_C(\eta')|$ , therefore, the production between the wave functions in the  $J/\psi\phi$  and  $\eta_c\eta'$  should be comparative, the OGE interaction plays an important role in their partial decay widths. Here, the branching ratio of  $\mathcal{B}_0 = \Gamma_0(\eta_c\eta')/\Gamma_0(J/\psi\phi)$  is around 2.5 when the binding energy is taken from  $-1$  to  $-30$  MeV, this result is roughly consistent with the analysis from the heavy quark symmetry.

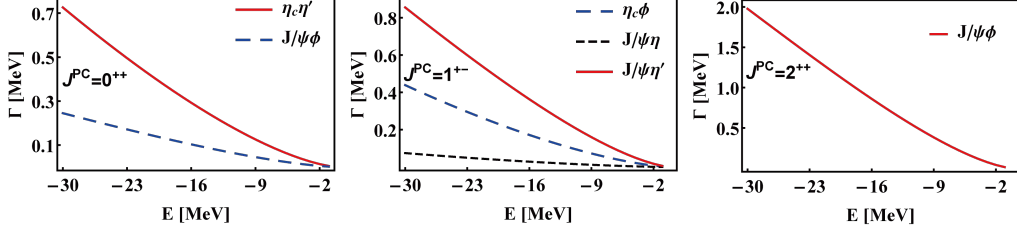


**Figure 13.** The binding energies  $E$  dependence of the decay widths for the possible  $S$ -wave  $D_s^*\bar{D}_s^*$  bound states with  $J^{PC} = 0^{++}$ ,  $1^{+-}$ , and  $2^{++}$ .

For the  $S$ -wave  $D_s^*\bar{D}_s^*$  bound state with  $J^{PC} = 1^{+-}$ , the  $J/\psi\eta^{(\prime)}$  and  $\eta_c\phi$  are the important two-body hidden-charm decay channels, and  $\Gamma(J/\psi\eta') > \Gamma(\eta_c\phi) > \Gamma(J/\psi\eta)$ . For the  $S$ -wave  $D_s^*\bar{D}_s^*$  bound state with  $J^{PC} = 2^{++}$ , there only exists the  $J/\psi\phi$  decay channel, and its partial decay width is in the order around 1 MeV.

**The  $D_s\bar{D}_s$ ,  $D_s\bar{D}_s^*$ ,  $D_s\bar{D}_{s0}^*$ ,  $D_s\bar{D}_{s1}'$ ,  $D_s^*\bar{D}_{s0}^*$ , and  $D_s^*\bar{D}_{s1}'$  systems.** Besides the  $S$ -wave  $D_s^*\bar{D}_s^*$  system, we also investigate the bound state properties of the  $S$ -wave  $D_s\bar{D}_s$ ,  $D_s\bar{D}_s^*$ ,  $D_s\bar{D}_{s0}^*$ ,  $D_s\bar{D}_{s1}'$ ,  $D_s^*\bar{D}_{s0}^*$ , and  $D_s^*\bar{D}_{s1}'$  systems by tuning the cutoff values  $\Lambda$  from 1.0 to 3.0 GeV, and the corresponding numerical results are listed in Table 15. If we still adopt the general criterion of the loosely hadron-hadron molecule [80, 82, 87, 88], we can find

- There may exist several possible charmonium-like molecular tetraquark candidates with hidden-strange quantum number, such as the  $D_s\bar{D}_s^*$  state with  $J^{PC} = 1^{+-}$  [120, 141], the  $D_s\bar{D}_{s0}^*$  state with  $J^{PC} = 0^{-\mp}$  [96, 108–110], the  $D_s\bar{D}_{s1}'$  state with  $J^{PC} = 1^{-+}$ , the  $D_s^*\bar{D}_{s1}'$  states with  $J^{PC} = 0^{-\mp}$  and  $1^{-+}$ . In particular, the coupled channel effect plays an important role in generating these loosely bound states, i.e., the  $D_s\bar{D}_s^*$  state with  $J^{PC} = 1^{+-}$ , the  $D_s\bar{D}_{s0}^*$  state with  $J^{PC} = 0^{-\mp}$ , and the  $D_s\bar{D}_{s1}'$  state with  $J^{PC} = 1^{-+}$ .
- If we increase the cutoff value around 2.0 GeV, we can obtain loosely bound state solutions for the  $D_s\bar{D}_s^*$  state with  $J^{PC} = 1^{++}$ , the  $D_s^*\bar{D}_{s0}^*$  state with  $J^{PC} = 1^{--}$ , and the  $D_s^*\bar{D}_{s1}'$  state with  $J^{PC} = 1^{--}$ . They may be the possible charmonium-like molecular candidates with hidden-strange quantum number.
- In addition, we don't obtain bound state solutions for the  $D_s\bar{D}_s$  state with  $J^{PC} = 0^{++}$ , the  $D_s\bar{D}_{s1}'$  state with  $J^{PC} = 1^{--}$ , and the  $D_s^*\bar{D}_{s1}'$  state with  $J^{PC} = 2^{-\mp}$  by tuning cutoff values from 1.0 to 3.0 GeV.

**Table 15.** Bound state solutions for the  $S$ -wave  $D_s\bar{D}_s^*$ ,  $D_s\bar{D}_{s0}^*$ ,  $D_s\bar{D}'_{s1}$ ,  $D_s^*\bar{D}_{s0}^*$ , and  $D_s^*\bar{D}'_{s1}$  systems. Conventions are the same as Table 8.

Effect	Single channel			$S$ - $D$ wave mixing effect				Coupled channel effect			
States[ $J^{PC}$ ]	$\Lambda$	$E$	$r_{\text{RMS}}$	$\Lambda$	$E$	$r_{\text{RMS}}$	$P(^3\mathbb{S}_1/^3\mathbb{D}_1)$	$\Lambda$	$E$	$r_{\text{RMS}}$	$P(D_s\bar{D}_s^*/D_s^*\bar{D}_s^*)$
$D_s\bar{D}_s^*[1^{+-}]$	2.65	-0.26	4.96	2.27	-0.43	4.39	<b>99.25</b> /0.75	1.63	-0.13	5.41	<b>96.64</b> /3.36
	2.85	-11.95	0.98	2.43	-11.85	1.03	<b>96.56</b> /3.44	1.66	-8.92	0.99	<b>78.85</b> /21.15
$D_s\bar{D}_s^*[1^{++}]$	$\times$	$\times$	$\times$	2.71	-0.27	4.99	<b>99.46</b> /0.54				
	$\times$	$\times$	$\times$	3.00	-5.69	1.49	<b>97.69</b> /2.31				
States[ $J^{PC}$ ]	$\Lambda$	$E$	$r_{\text{RMS}}$					$\Lambda$	$E$	$r_{\text{RMS}}$	$P(D_s\bar{D}_{s0}^*/D_s^*\bar{D}'_{s1})$
$D_s\bar{D}_{s0}^*[0^{--}]$	2.83	-0.28	4.93					1.49	-0.43	4.27	<b>96.97</b> /3.03
	3.00	-0.92	3.32					1.52	-10.05	1.00	<b>81.81</b> /18.19
$D_s\bar{D}_{s0}^*[0^{-+}]$	$\times$	$\times$	$\times$					1.87	-2.52	1.77	<b>85.11</b> /14.89
	$\times$	$\times$	$\times$					1.88	-8.21	0.94	<b>75.72</b> /24.48
State[ $J^{PC}$ ]	$\Lambda$	$E$	$r_{\text{RMS}}$	$\Lambda$	$E$	$r_{\text{RMS}}$	$P(^3\mathbb{S}_1/^3\mathbb{D}_1)$	$\Lambda$	$E$	$r_{\text{RMS}}$	$P(D_s\bar{D}'_{s1}/D_s^*\bar{D}_{s0}^*/D_s^*\bar{D}'_{s1})$
$D_s\bar{D}'_{s1}[1^{-+}]$	2.17	-0.33	4.65	2.15	-0.29	4.79	<b>99.98</b> /0.02	1.87	-0.31	4.69	<b>98.76</b> /1.24/ $o(0)$
	2.55	-12.60	1.00	2.51	-12.35	1.00	<b>99.82</b> /0.18	1.99	-12.64	0.92	<b>87.08</b> /12.92/ $o(0)$
State[ $J^{PC}$ ]	$\Lambda$	$E$	$r_{\text{RMS}}$	$\Lambda$	$E$	$r_{\text{RMS}}$	$P(^3\mathbb{S}_1/^3\mathbb{D}_1)$	$\Lambda$	$E$	$r_{\text{RMS}}$	$P(D_s^*\bar{D}_{s0}^*/D_s^*\bar{D}'_{s1})$
$D_s^*\bar{D}_{s0}^*[1^{--}]$	2.17	-0.31	4.73	2.17	-0.31	4.72	<b>100.00</b> / $o(0)$	2.17	-0.31	4.72	<b>100.00</b> / $o(0)$
	2.53	-12.42	1.00	2.53	-12.42	1.00	<b>100.00</b> / $o(0)$	2.53	-12.42	1.00	<b>100.00</b> / $o(0)$
States[ $J^{PC}$ ]	$\Lambda$	$E$	$r_{\text{RMS}}$	$\Lambda$	$E$	$r_{\text{RMS}}$	$P(^1\mathbb{S}_0/^5\mathbb{D}_0)$				
$D_s^*\bar{D}'_{s1}[0^{--}]$	1.37	-0.41	4.33	1.37	-0.52	3.99	<b>99.96</b> /0.04				
	1.45	-12.34	0.98	1.45	-12.82	0.97	<b>99.90</b> /0.10				
$D_s^*\bar{D}'_{s1}[0^{-+}]$	1.87	-0.33	4.24	1.87	-0.36	4.13	<b>99.99</b> /0.01				
	1.91	-10.27	0.85	1.91	-10.40	0.85	<b>99.99</b> /0.01				
States[ $J^{PC}$ ]	$\Lambda$	$E$	$r_{\text{RMS}}$	$\Lambda$	$E$	$r_{\text{RMS}}$	$P(^3\mathbb{S}_1/^3\mathbb{D}_1/^5\mathbb{D}_1)$				
$D_s^*\bar{D}'_{s1}[1^{--}]$	2.29	-0.59	3.53	2.28	-0.47	3.87	<b>99.97</b> /0.03/ $o(0)$				
	2.37	-13.38	0.78	2.36	-13.47	0.79	<b>99.88</b> /0.12/ $o(0)$				
$D_s^*\bar{D}'_{s1}[1^{-+}]$	1.55	-0.22	5.10	1.55	-0.36	4.52	<b>99.95</b> /0.05/ $o(0)$				
	1.68	-11.38	1.02	1.68	-12.17	1.00	<b>99.84</b> /0.16/ $o(0)$				



In the following, we also focus on two-body hidden-charm decay behaviors of these possible charmonium-like molecular candidates with hidden-strange quantum number. In Figure 14, we present the binding energies  $E$  dependence of the decay widths for these possible  $S$ -wave  $D_s\bar{D}_s^*$ ,  $D_s\bar{D}_{s0}^*$ ,  $D_s\bar{D}_{s1}'$ ,  $D_s^*\bar{D}_{s0}^*$ , and  $D_s^*\bar{D}_{s1}'$  molecular candidates. We can conclude that

1. The  $D_s\bar{D}_s^*$  bound states with  $J^{PC} = 1^{++}$  and  $1^{+-}$  mainly decay into the  $\chi_{c0}(1P)\eta$  and  $\eta_c\phi$  channels, respectively. The  $J/\psi\eta$  is the other important decay mode for the  $D_s\bar{D}_s^*$  bound state with  $J^{PC} = 1^{+-}$ . Their corresponding partial decay widths are less than 0.5 MeV when their binding energies are around  $-1$  to  $-30$  MeV.
2. For the  $D_s\bar{D}_{s0}^*$  bound state with  $J^{PC} = 0^{-+}$ , there are two two-body hidden-charm decay channels, the  $J/\psi\phi$  and  $\chi_{c0}(1P)\eta$ . Their partial decay widths are around 0.1 MeV. For its negative  $C$ -parity partner, there exist the  $J/\psi\eta^{(\prime)}$  and  $\eta_c\phi$  decay modes, among these three two-body hidden-charm decay channels, the  $\eta_c\phi$  is the most important, which has the largest partial decay width.
3. For the  $S$ -wave  $D_s\bar{D}_{s1}'$  bound state with  $J^{PC} = 1^{-+}$ , the dominant two-body hidden-charm decay channel is the  $J/\psi\phi$ . It also can decay into the  $\chi_{c1}(1P)\eta$  final state with small partial decay width.
4. For the  $S$ -wave  $D_s^*\bar{D}_{s0}^*$  bound state with  $J^{PC} = 1^{--}$ , the largest two-body hidden-charm decay width is given by the  $\eta_c\phi$  channel, and it also can decay into the  $J/\psi\eta$  and  $J/\psi\eta'$  channels.
5. For these possible  $S$ -wave  $D_s^*\bar{D}_{s1}'$  molecular candidates, the two-body hidden-charm decay behaviors for the positive  $C$ -parity bound states are a little complicated, the  $J/\psi\phi$  channel is very important for both the  $D_s^*\bar{D}_{s1}'$  molecular candidates with  $J^{PC} = 0^{-+}$  and  $1^{-+}$ . In addition, the  $\chi_{c1}(1P)\phi$  channel has sizable contributions for the  $D_s^*\bar{D}_{s1}'$  bound state with  $J^{PC} = 0^{--}$ , and the  $D_s^*\bar{D}_{s1}'$  bound state with  $J^{PC} = 1^{--}$  mainly decay into the  $\chi_{c0}(1P)\phi$  and  $\chi_{c1}(1P)\phi$  channels.

**The  $D_s^{(*)}\bar{D}_{s1}$  and  $D_s^{(*)}\bar{D}_{s2}^*$  systems.** In our previous work [82], we systematic study the interactions between a pair of charm-strange meson and anti-charm-strange meson in the  $H$ -doublet or  $T$ -doublet by using the OBE model and considering the  $S$ - $D$  wave mixing and the coupled channel effect, and we can predict several possible  $H\bar{T}$ -type charmonium-like molecular states, i.e., the  $D_s^*\bar{D}_{s1}$  molecular states with  $J^{PC} = 0^{-\pm}/1^{-\pm}$  and the  $D_s^*\bar{D}_{s2}^*$  molecular states with  $J^{PC} = 1^{-\pm}/2^{-\pm}$ . In the following, we just estimate two-body hidden-charm decay behaviors for those predicted charmonium-like molecules. According to the selection rules from the parity and angular momentum conservation, the possible two-body hidden-charm decay channels include the  $J/\psi\phi$  and  $\chi_{c0,1,2}(1P)\eta^{(\prime)}$  channels for the  $D_s^*\bar{D}_{s1}$  and  $D_s^*\bar{D}_{s2}^*$  bound states with positive  $C$ -parity. For their negative  $C$  parity partners, they can decay into the  $\chi_{c0,1,2}(1P)\phi$  channels. In Figure 14, we present the binding energies  $E$  dependence of the corresponding partial decay widths for these possible  $S$ -wave  $D_s^*\bar{D}_{s1}$

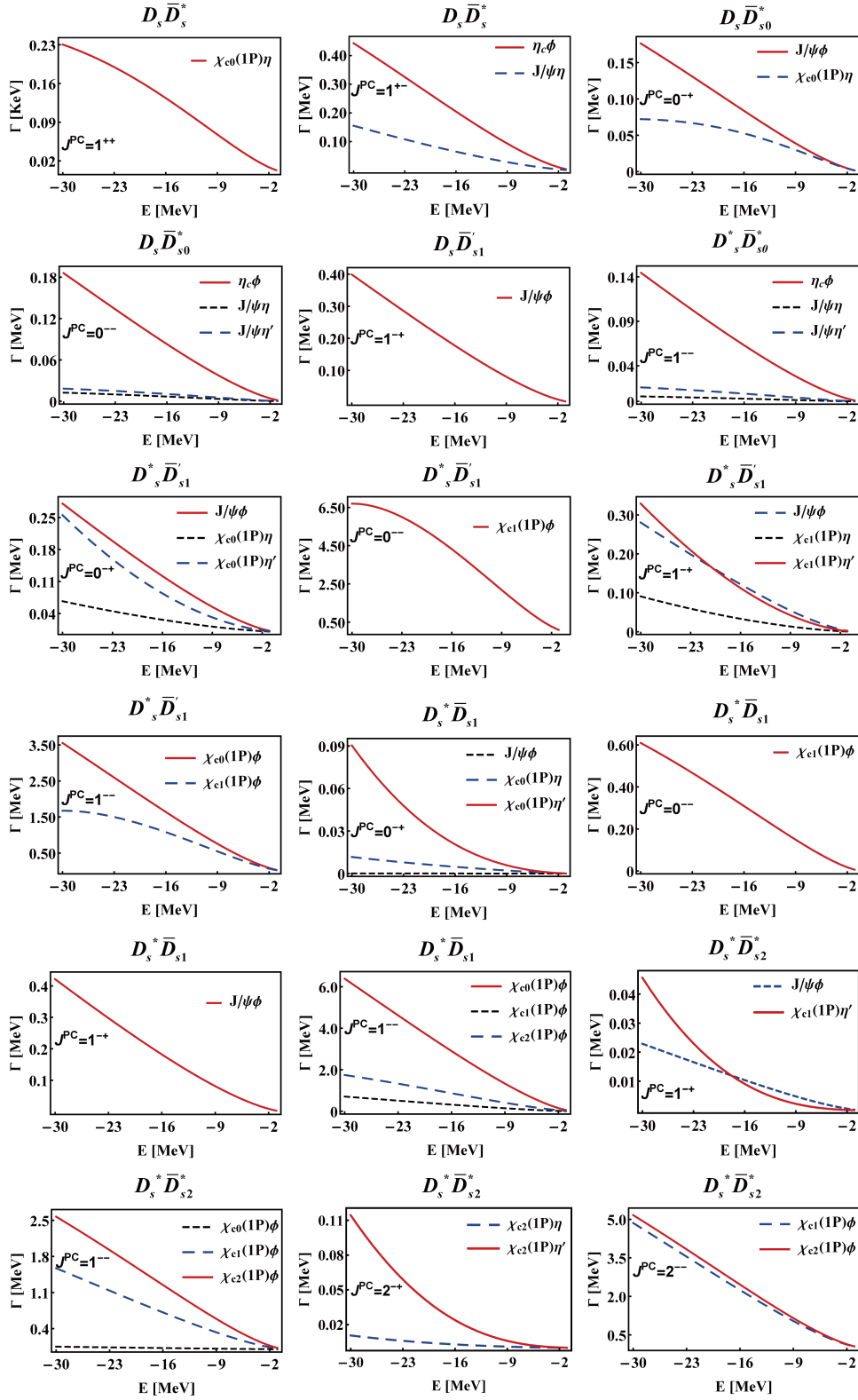


**Figure 14.** The binding energies  $E$  dependence of the decay widths for these possible  $S$ -wave  $D_s\bar{D}_s^*$ ,  $D_s\bar{D}_{s0}^*$ ,  $D_s\bar{D}_{s1}^*$ ,  $D_s^*\bar{D}_{s0}$ ,  $D_s^*\bar{D}_{s1}$ ,  $D_s^*\bar{D}_{s1}'$  and  $D_s^*\bar{D}_{s2}^*$  molecular candidates.

and  $D_s^* \bar{D}_{s2}^*$  molecular candidates. Here, we only present the two-body hidden-charm decay widths for the important decay modes.

As we see in Figure 14, the two-body hidden-charm decay widths for these possible  $D_s^* \bar{D}_{s1}$  and  $D_s^* \bar{D}_{s2}^*$  molecular candidates with negative  $C$ -parity are much larger than those corresponding bound states with positive  $C$ -parity. The  $\chi_{c1}(1P)\phi$  channel is the dominant two-body hidden-charm decay channel for the  $D_s^* \bar{D}_{s1}$  bound state with  $J^{PC} = 0^{--}$  and the  $D_s^* \bar{D}_{s2}^*$  bound states with  $J^{PC} = 1^{--}$  and  $2^{--}$ , the corresponding partial decay widths are around several MeV when we take the binding energies in the range from  $-1$  to  $-30$  MeV. For the  $D_s^* \bar{D}_{s1}$  bound state with  $J^{PC} = 1^{--}$ , the  $\chi_{c0}(1P)\phi$  channel is the dominant two-body hidden-charm decay channel. In addition, the  $\chi_{c2}(1P)\phi$  can be the other important decay mode for the  $D_s^* \bar{D}_{s2}^*$  bound state with  $J^{PC} = 2^{--}$ .

In Table 16, we summary their bound properties and two-body hidden-charm decay information, including the bound properties, the important two-body hidden-charm decay channels, and the order of the decay widths. Here, notations  $\surd$  and  $\nexists$  are marked the charmonium-like molecular candidates with their bound state solutions with the cutoff  $\Lambda$  in the regions of 1 to 2 GeV and 2 to 3 GeV, respectively.

The obtained results are theoretic reference to search for possible charmonium-like molecular tetraquark with hidden-strange quantum number. So far, many charmonium-like structures have been observed in the  $J/\psi\phi$  invariant mass spectrum. In particular, the recent LHCb Collaboration updated the amplitude analysis of the  $B^+ \rightarrow J/\psi\phi K^+$  decay with the combined data set collected in Run I plus Run II [59], and they reported several enhancement structures, some of them locate close to the mass thresholds of our investigated charmonium-like molecular tetraquark systems with hidden-strange quantum number, our study of the mass spectrum and two-body hidden-charm decay behaviors for these charmonium-like molecules with hidden-strange quantum number may provide hints to understand the nature of the reported charmonium-like states, i.e.,

1. The masses of the  $X(4140)$  with  $J^{PC} = 1^{++}$  and the  $X(4150)$  with  $J^{PC} = 2^{-+}$  [59] are close to the  $D_s^* \bar{D}_s^*$  threshold. It is obvious that their quantum configurations do not fit into the  $S$ -wave  $D_s^* \bar{D}_s^*$  molecules. If their resonance parameters and quantum numbers can be further confirmed in the future, the assignment of these complicated structures as the  $S$ -wave  $D_s^* \bar{D}_s^*$  molecular states will be facing great challenge.
2. When we recall the other charmonium-like structure  $Y(4274)$  [18, 20, 54] (see Figure 3 for more details), its mass are close to the  $D_s \bar{D}_{s0}^*$  threshold, its spin-parity is favored as  $J^{PC} = 1^{++}$  by the LHCb Collaboration [20, 59], the similar situation happens, our results do not support the  $Y(4274)$  with  $J^{PC} = 1^{++}$  as the  $S$ -wave  $D_s \bar{D}_{s0}^*$  molecular state.
3. In the mass region from 4.5 GeV to 4.7 GeV, the recent LHCb Collaboration reported the four enhancement structures  $X(4500)$ ,  $X(4630)$ ,  $X(4685)$ , and  $X(4700)$  in the  $J/\psi\phi$  mass spectrum from the  $B \rightarrow J/\psi\phi K$  decay [59]. Our results indicate there can exist six possible charmonium-like molecular tetraquark candidates with hidden-strange quantum number with positive  $C$ -parity. Some of them can mainly decay to

**Table 16.** A summary of the bound properties, the important two-body hidden-charm decay channels, and the order of the decay widths for all the possible  $S$ -wave charmonium-like molecules with hidden-strange quantum number. Here, notations  $\checkmark$  and  $\ncheckmark$  are marked the charmonium-like molecular candidates with their bound state solutions with the cutoff  $\Lambda$  around 1 to 2 GeV and around 2 to 3 GeV, respectively. The  $\mathcal{O}(x)$  stands for the partial decay widths in the order of  $x$  MeV with the binding energies around 5 to 20 MeV. We label the dominant two-body hidden-charm decay modes in the bold manner.

States	Bound properties	Decay channels	$\mathcal{O}(\Gamma)$
$D_s^* \bar{D}_s^*[0^{++}]$	$\checkmark$	<b><math>\eta_c \eta'</math>, <math>J/\psi \phi</math></b>	0.10, 0.10
$D_s^* \bar{D}_s^*[1^{+-}]$	$\checkmark$	<b><math>J/\psi \eta'</math>, <math>\eta_c \phi</math>, <math>J/\psi \eta</math></b>	0.10, 0.10, 0.01
$D_s^* \bar{D}_s^*[2^{++}]$	$\ncheckmark$	<b><math>J/\psi \phi</math></b>	1.00
$D_s \bar{D}_s^*[1^{++}]$	$\checkmark$	<b><math>\chi_{c0}(1P) \eta</math></b>	0.10
$D_s \bar{D}_s^*[1^{+-}]$	$\ncheckmark$	<b><math>\eta_c \phi</math>, <math>J/\psi \eta</math></b>	0.10, 0.01
$D_s \bar{D}_{s0}^*[0^{-+}]$	$\checkmark$	<b><math>J/\psi \phi</math>, <math>\chi_{c0}(1P) \eta</math></b>	0.10, 0.01
$D_s \bar{D}_{s0}^*[0^{--}]$	$\checkmark$	<b><math>\eta_c \phi</math>, <math>J/\psi \eta'</math>, <math>J/\psi \eta</math></b>	0.10, 0.01, 0.01
$D_s \bar{D}'_{s1}[1^{-+}]$	$\checkmark$	<b><math>J/\psi \phi</math></b>	0.10
$D_s^* \bar{D}_{s0}^*[1^{--}]$	$\ncheckmark$	<b><math>\eta_c \phi</math>, <math>J/\psi \eta'</math>, <math>J/\psi \eta</math></b>	0.01, 0.001, 0.001
$D_s^* \bar{D}'_{s1}[0^{-+}]$	$\checkmark$	<b><math>J/\psi \phi</math>, <math>\chi_{c0}(1P) \eta'</math>, <math>\chi_{c0}(1P) \eta</math></b>	0.10, 0.10, 0.01
$D_s^* \bar{D}'_{s1}[0^{--}]$	$\checkmark$	<b><math>\chi_{c1}(1P) \phi</math></b>	1.00
$D_s^* \bar{D}'_{s1}[1^{-+}]$	$\ncheckmark$	<b><math>\chi_{c1}(1P) \eta'</math>, <math>J/\psi \phi</math>, <math>\chi_{c1}(1P) \eta</math></b>	0.10, 0.10, 0.01
$D_s^* \bar{D}'_{s1}[1^{--}]$	$\checkmark$	<b><math>\chi_{c0}(1P) \phi</math>, <math>\chi_{c1}(1P) \phi</math></b>	1.00, 1.00
$D_s^* \bar{D}_{s1}[0^{-+}]$	$\checkmark$	<b><math>\chi_{c0}(1P) \eta'</math>, <math>\chi_{c0}(1P) \eta</math>, <math>J/\psi \phi</math></b>	0.01, 0.001, 0.001
$D_s^* \bar{D}_{s1}[0^{--}]$	$\checkmark$	<b><math>\chi_{c1}(1P) \phi</math></b>	0.10
$D_s^* \bar{D}_{s1}[1^{-+}]$	$\checkmark$	<b><math>J/\psi \phi</math></b>	0.10
$D_s^* \bar{D}_{s1}[1^{--}]$	$\checkmark$	<b><math>\chi_{c0}(1P) \phi</math>, <math>\chi_{c2}(1P) \phi</math>, <math>\chi_{c1}(1P) \phi</math></b>	1.00, 1.00, 0.10
$D_s^* \bar{D}_{s2}^*[1^{-+}]$	$\checkmark$	<b><math>\chi_{c1}(1P) \eta'</math>, <math>J/\psi \phi</math></b>	0.01, 0.01
$D_s^* \bar{D}_{s2}^*[1^{--}]$	$\checkmark$	<b><math>\chi_{c2}(1P) \phi</math>, <math>\chi_{c1}(1P) \phi</math>, <math>\chi_{c0}(1P) \phi</math></b>	1.00, 1.00, 0.01
$D_s^* \bar{D}_{s2}^*[2^{-+}]$	$\ncheckmark$	<b><math>\chi_{c2}(1P) \eta'</math>, <math>\chi_{c2}(1P) \eta</math></b>	0.01, 0.01
$D_s^* \bar{D}_{s2}^*[2^{--}]$	$\checkmark$	<b><math>\chi_{c2}(1P) \phi</math>, <math>\chi_{c1}(1P) \phi</math></b>	1.00, 1.00

the  $J/\psi\phi$  final state. In our former work [79], the  $X(4630)$  can be assigned as the  $D_s^*\bar{D}_{s1}$  charmonium-like molecule with  $J^{PC} = 1^{-+}$ . If these six predicted charmoniumlike molecules really exist, it is a big challenge to search and further identify separately by using the data from the  $B \rightarrow J/\psi\phi K$  process.

4. In addition, our calculations can predict several possible charmonium-like molecular candidates with negative  $C$ -parity, which deserve to attract the experiment's attentions. Because their two-body hidden-charm decay channels are the  $\chi_{c0,1,2}(1P)\phi$ , the  $B \rightarrow \chi_{c0,1,2}(1P)\phi + K \rightarrow J/\psi\gamma\phi + K$  may be the prime decay process to search for these possible charmonium-like molecules.

In fact, the phenomena in high mass region are very complicated, beside these possible charmonium-like molecular structures, there can exist several traditional charmonium states with their masses around these discussed thresholds. For example, the Lanzhou group indicated that the masses for the  $\chi_{c0}(3^3P_0)$ ,  $\chi_{c1}(3^3P_1)$ , and  $\chi_{c2}(3^3P_2)$  states are around 4177 MeV, 4197 MeV, and 4213 MeV [142, 143], which is close to the  $D_s^*\bar{D}_s^*$  thresholds. Both the theoretical side and the experimental side will make many efforts to clarify this puzzling phenomenon in the future.

### 3.2.3 Isovector charmonium-like molecular tetraquark systems

In this section, let us discuss the final proposal whether there exist isovector charmonium-like molecules from a charmed meson and an anti-charmed meson interactions, where the charmed (anti-charmed) mesons are in the  $H/T$  doublets. In comparison with the isoscalar  $\mathcal{D}\bar{\mathcal{D}}$  systems, the OBE effective potentials for the  $S$ -wave isovector  $\mathcal{D}\bar{\mathcal{D}}$  systems are very different. Since the  $\pi$  and  $\rho$  exchanges couple to the isospin charge, their properties in the isovector  $\mathcal{D}\bar{\mathcal{D}}$  systems are contrary to those in the isoscalar  $\mathcal{D}\bar{\mathcal{D}}$  systems, and the corresponding effective potentials are three times weaker (see Eqs. (A.3)-(A.6) for details). Therefore, the OBE effective potentials for the  $S$ -wave isovector  $\mathcal{D}\bar{\mathcal{D}}$  systems may be not strong enough to bind isovector charmonium-like molecular states.

When we input the corresponding OBE effective potentials, only the  $S$ -wave isovector  $D^*\bar{D}_1$  state with  $J^{PC} = 2^{-+}$  can generate the loosely bound state with the cutoff parameter  $\Lambda$  around 3.0 GeV. Even though we consider the  $S$ - $D$  wave mixing and the coupled channel effect, the cutoff  $\Lambda$  is still much larger than 1.0 GeV [87, 88]. If we take the cutoff value from the deuteron as the reasonable input, the interactions from a pair of charmed meson and anti-charmed meson are not strong enough to bind  $S$ -wave isovector charmonium-like molecular tetraquark states.

Experimentally, there have accumulated abundant experimental observations of the charged charmonium-like states from the  $B$  meson decays as introduced in the section 2.3. If they are real particles, they cannot be traditional mesons but the multiquark matters. As shown in Figure 15, their masses are all above the mass thresholds of the corresponding  $\mathcal{D}\bar{\mathcal{D}}$  systems. Obviously, they cannot be assigned as the isovector charmonium-like molecular states. In short, our results exclude the charged charmonium-like states as the isovector meson-meson molecular states, which perfectly match the experimental observations. In

fact, the other groups also support our conclusions [13, 23, 43, 45, 50, 89, 120, 122, 123, 144–150].

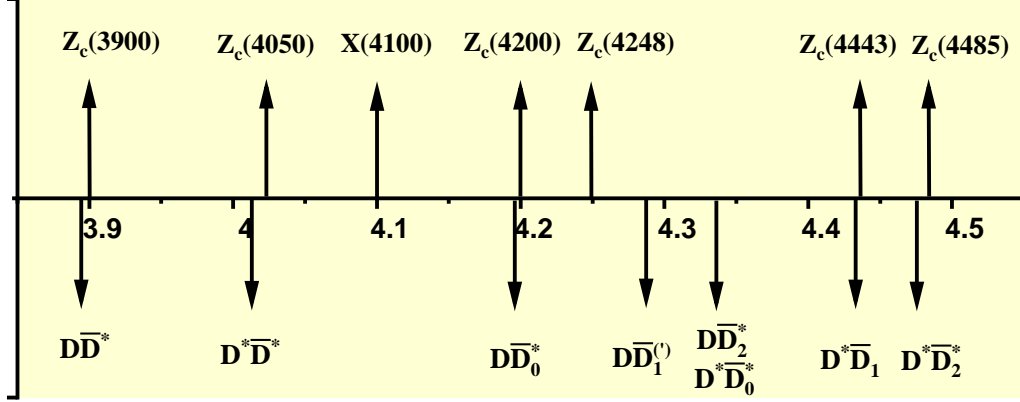


**Figure 15.** The masses comparison between the charged charmonium-like states [10–16] and the  $D\bar{D}$  thresholds.

Before closing our discussion on the isovector charmonium-like systems, we would like to emphasize that we only analyze whether the charged charmonium-like states can be the isovector charmonium-like molecular states composed of a pair of charmed meson and anti-charmed meson. In fact, many theoretical groups propose other different explanations on the nature of the charged charmonium-like states, like the compact tetraquark configurations, the meson-meson scattering states, and the kinematical effect (including the coupled channel cusp effect, the reflection mechanism, the interference effect, the initial single pion emission mechanism, the triangle singularities, the rescattering effect, and so on), people can refer articles [10, 13, 16, 151–165] for more details.

## 4 Summary

Exploration of the hadronic molecular states is an interesting and important research topics in the hadron physics. Since 2003, serials of charmonium-like structures have been reported by different experiments in different beams, different reactions, and different energy regions, some of them are very close to a pair of charmed meson and anti-charmed meson thresholds, which inspired theorists to explain them in the hadronic molecular scenario. Although the charmonium-like hadronic molecular states are not forbidden by the Quantum Chromodynamics (QCD), one cannot give a precisely conclusion whether the charmonium-like hadronic molecular states exist or not up to now.

The perfect match between experimental observations and the theoretical predictions on the three  $P_c$  states provides a strong evidence of the existence of hidden-charm meson-baryon molecular pentaquark states. If replacing  $ud$  quarks of  $\Lambda_b$  by an antiquark  $\bar{q}$ , the production mechanisms of the  $P_c$  states from  $\Lambda_b$  baryon decays and the  $XYZ$  states from  $B$  meson decays are very similar. The  $B \rightarrow XYZ + K$  decay should be the ideal process to produce charmonium-like molecular states.

In such a situation, we firstly focus on the isoscalar  $D^*\bar{D}^*$  systems with  $J^{PC} = 0^{++}$ ,  $1^{+-}$ , and  $2^{++}$ . And we find their interactions are attractive enough to generate bound charmonium-like molecular states. After performing a qualitative calculation on their two-body hidden-charm decay behaviors, we find that the  $J/\psi\omega$  and  $J/\psi\eta$  channels are the essential decay modes for the isoscalar  $D^*\bar{D}^*$  molecular states with  $J^{PC} = 0^{++}/2^{++}$  and  $1^{+-}$ , respectively. If checking the data from the  $J/\psi\omega$  invariant mass distribution in the  $B \rightarrow J/\psi\omega K$  and the  $J/\psi\eta$  invariant mass distribution in the  $B \rightarrow J/\psi\eta K$ , one can roughly find double enhancement structures in  $J/\psi\omega$  invariant mass distribution and single structure in  $J/\psi\eta$  invariant mass distribution, their masses are just below the  $D^*\bar{D}^*$  threshold, which may correspond to the isoscalar  $D^*\bar{D}^*$  charmonium-like molecules with  $J^P = 0^{++}/2^{++}$  and  $1^{+-}$ , respectively. The behavior of the double enhancement structures around 3.9 GeV below the  $D^*\bar{D}^*$  threshold from the  $B \rightarrow J/\psi\omega K$  and the single structure in the same energy region from the  $B \rightarrow J/\psi\eta K$  can provide crucial information to identify the charmonium-like molecule. Thus, we suggest to systematically check the correlation of charmonium-like molecular states and charmonium-like structures existing in the  $XYZ$  data of the  $B \rightarrow XYZ + K$  decay.

After that, we promote our study to the interactions between a charmed (charm-strange) meson and an anti-charmed (anti-charm-strange) meson, including the  $D^{(*)}\bar{D}^{(*)}$ ,  $\bar{D}^{(*)}\bar{D}_1$ ,  $D^{(*)}\bar{D}_2^*$ ,  $D_s^{(*)}\bar{D}_s^{(*)}$ ,  $D_s^{(*)}\bar{D}_{s0}^*$ ,  $D_s^{(*)}\bar{D}'_{s1}$ ,  $D_s^{(*)}\bar{D}_{s1}$ ,  $D_s^{(*)}\bar{D}_{s2}^*$  systems. After input the OBE effective potentials, we can find a series of promising isoscalar charmonium-like molecular tetraquark candidates as summarized in Tables 13. Our results exclude these discussed  $S$ -wave isovector charmonium-like tetraquark states as the hadronic molecular candidates in the OBE model. Besides analyzing the mass spectrum, we also discuss their two-body hidden-charm decay behaviors of these possible molecular tetraquark candidates with the quark-interchange model. In Table 13, we collect the important two-body hidden-charm decay channels and the order for the corresponding partial decay widths for these promising charmonium-like molecular candidates. These obtained decay properties can be very helpful to search and identify these discussed molecular tetraquark candidates.

In this work, our results indicate that the underlying phenomena behind the wide structure around 4.3 GeV in the  $B \rightarrow J/\psi\omega K$  is very complicated. There can exist five possible isoscalar charmonium-like molecular candidates, such as the  $D^*\bar{D}_1$  bound states with  $I(J^{PC}) = 0(0^{-+})$ ,  $0(1^{-+})$ ,  $0(2^{-+})$ , the  $D^*\bar{D}_2^*$  bound state with  $I(J^{PC}) = 0(3^{-+})$ , and the  $D\bar{D}_1$  bound state with  $I(J^{PC}) = 0(1^{-+})$ . The  $J/\psi\omega$  channel is their dominant two-body hidden-charm decay channel. In addition, we can predict many isoscalar charmonium-like molecular states with negative  $C$ -parity in the same mass region. Their dominant two-body hidden-charm decay modes are the  $\chi_{cJ}(1P)\omega$  with  $J = 0, 1, 2$ . The  $B \rightarrow \chi_{cJ}(1P)\omega + K \rightarrow J/\psi\gamma\omega + K$  may be the good production process to search for these predicted isoscalar charmonium-like molecular states with  $C = -$ .

Meanwhile, we also study the mass spectrum and two-body hidden-charm decay behaviors for the possible charmonium-like  $\mathcal{D}_s\bar{\mathcal{D}}_s$  molecular states with hidden-strange quantum number summarized in Table 16, where  $\mathcal{D}_s$  stands for the charm-strange meson. The  $J/\psi\phi$  channel is the dominant two-body hidden-charm decay channel for most of the possible  $\mathcal{D}_s\bar{\mathcal{D}}_s$  molecular states. In order to further distinguish these structures, one need more

precision experimental data, and more analysis on the other decay channel could be also useful. The two-body hidden-charm decay widths for the possible  $\mathcal{D}_s\bar{\mathcal{D}}_s$  molecular states with negative  $C$  parity are much larger than the corresponding decay widths for the positive  $C$  parity partners.

Finding the charmonium-like states has been going on for around 20 years. With the running of Belle II [27] and the accumulation of Run II and Run III data at LHCb [28], the study of the charmonium-like states will step into a new area, here, we suggest to systematically check the correlation of charmonium-like molecular states and charmonium-like structures existing in the  $XYZ$  data of the  $B \rightarrow XYZ + K$  decay. The present work provides a good start point and new insight for identifying charmonium-like molecule. We expect more theoretical and experimental efforts in exploring this important and intriguing research topic in the coming golden decade.

## A Relevant subpotentials

Before presenting the effective potentials for these investigated tetraquark systems, we first define several operators  $\mathcal{O}_k^{(j)}$  involved in this work, which include

$$\begin{aligned}
\mathcal{O}_1 &= \epsilon_3^\dagger \cdot \epsilon_1, & \mathcal{O}_2 &= \epsilon_4^\dagger \cdot \epsilon_1, & \mathcal{O}_3 &= T(\epsilon_4^\dagger, \epsilon_1), & \mathcal{O}_4 &= (\epsilon_3^\dagger \cdot \epsilon_1) (\epsilon_4^\dagger \cdot \epsilon_2), \\
\mathcal{O}_5 &= (\epsilon_3^\dagger \times \epsilon_1) \cdot (\epsilon_4^\dagger \times \epsilon_2), & \mathcal{O}_6 &= T(\epsilon_3^\dagger \times \epsilon_1, \epsilon_4^\dagger \times \epsilon_2), \\
\mathcal{O}_7 &= \mathcal{S}(\epsilon_{4m}^\dagger \cdot \epsilon_{2a}) (\epsilon_{4n}^\dagger \cdot \epsilon_{2b}), & \mathcal{O}_8 &= \frac{2}{27} \mathcal{S}(\epsilon_{3m}^\dagger \cdot \epsilon_{2a}) (\epsilon_{3n}^\dagger \cdot \epsilon_{2b}), \\
\mathcal{O}_9 &= \frac{1}{27} \mathcal{S}T(\epsilon_{3m}^\dagger, \epsilon_{3n}^\dagger) T(\epsilon_{2a}, \epsilon_{2b}) + \frac{2}{27} \mathcal{S}T(\epsilon_{3m}^\dagger, \epsilon_{2a}) T(\epsilon_{3n}^\dagger, \epsilon_{2b}), \\
\mathcal{O}_{10} &= \frac{2}{27} \mathcal{S}(\epsilon_{3m}^\dagger \cdot \epsilon_{2a}) T(\epsilon_{3n}^\dagger, \epsilon_{2b}), & \mathcal{O}_{11} &= -\frac{1}{3} (\epsilon_3^\dagger \cdot \epsilon_1) (\epsilon_4^\dagger \cdot \epsilon_2) + \frac{1}{3} (\epsilon_3^\dagger \cdot \epsilon_4^\dagger) (\epsilon_1 \cdot \epsilon_2), \\
\mathcal{O}_{12} &= \frac{2}{3} T(\epsilon_3^\dagger, \epsilon_1) T(\epsilon_4^\dagger, \epsilon_2) + \frac{1}{3} T(\epsilon_3^\dagger, \epsilon_4^\dagger) T(\epsilon_1, \epsilon_2), \\
\mathcal{O}_{13} &= \frac{1}{6} (\epsilon_3^\dagger \cdot \epsilon_4^\dagger) T(\epsilon_1, \epsilon_2) + \frac{1}{6} (\epsilon_1 \cdot \epsilon_2) T(\epsilon_3^\dagger, \epsilon_4^\dagger) - \frac{1}{3} (\epsilon_3^\dagger \cdot \epsilon_1) T(\epsilon_4^\dagger, \epsilon_2), \\
\mathcal{O}_{14} &= \mathcal{S}(\epsilon_3^\dagger \cdot \epsilon_1) (\epsilon_{4m}^\dagger \cdot \epsilon_{2a}) (\epsilon_{4n}^\dagger \cdot \epsilon_{2b}), & \mathcal{O}'_{14} &= \mathcal{S}(\epsilon_4^\dagger \cdot \epsilon_2) (\epsilon_{3m}^\dagger \cdot \epsilon_{1a}) (\epsilon_{3n}^\dagger \cdot \epsilon_{1b}), \\
\mathcal{O}_{15} &= \mathcal{S}(\epsilon_{4m}^\dagger \cdot \epsilon_{2a}) (\epsilon_3^\dagger \times \epsilon_1) \cdot (\epsilon_{4n}^\dagger \times \epsilon_{2b}), \\
\mathcal{O}'_{15} &= \mathcal{S}(\epsilon_{3m}^\dagger \cdot \epsilon_{1a}) (\epsilon_4^\dagger \times \epsilon_2) \cdot (\epsilon_{3n}^\dagger \times \epsilon_{1b}), \\
\mathcal{O}_{16} &= \mathcal{S}(\epsilon_{4m}^\dagger \cdot \epsilon_{2a}) T(\epsilon_3^\dagger \times \epsilon_1, \epsilon_{4n}^\dagger \times \epsilon_{2b}), & \mathcal{O}'_{16} &= \mathcal{S}(\epsilon_{3m}^\dagger \cdot \epsilon_{1a}) T(\epsilon_4^\dagger \times \epsilon_2, \epsilon_{3n}^\dagger \times \epsilon_{1b}), \\
\mathcal{O}_{17} &= \mathcal{S}(\epsilon_{3m}^\dagger \cdot \epsilon_1) (\epsilon_4^\dagger \cdot \epsilon_{2a}) (\epsilon_{3n}^\dagger \cdot \epsilon_{2b}), & \mathcal{O}'_{17} &= \mathcal{S}(\epsilon_{4m}^\dagger \cdot \epsilon_2) (\epsilon_3^\dagger \cdot \epsilon_{1a}) (\epsilon_{4n}^\dagger \cdot \epsilon_{1b}), \\
\mathcal{O}_{18} &= \mathcal{S}(\epsilon_{3m}^\dagger \cdot \epsilon_1) (\epsilon_4^\dagger \cdot \epsilon_{2a}) T(\epsilon_{3n}^\dagger, \epsilon_{2b}), & \mathcal{O}'_{18} &= \mathcal{S}(\epsilon_{4m}^\dagger \cdot \epsilon_2) (\epsilon_3^\dagger \cdot \epsilon_{1a}) T(\epsilon_{4n}^\dagger, \epsilon_{1b}), \\
\mathcal{O}_{19} &= \frac{1}{27} \mathcal{S} \left[ (\epsilon_{3m}^\dagger \times \epsilon_1) \cdot (\epsilon_4^\dagger \times \epsilon_{2a}) (\epsilon_{3n}^\dagger \cdot \epsilon_{2b}) + [(\epsilon_{3m}^\dagger \times \epsilon_1) \cdot \epsilon_{2b}] [\epsilon_{3n}^\dagger \cdot (\epsilon_4^\dagger \times \epsilon_{2a})] \right], \\
\mathcal{O}'_{19} &= \frac{1}{27} \mathcal{S} \left[ (\epsilon_{4m}^\dagger \times \epsilon_2) \cdot (\epsilon_3^\dagger \times \epsilon_{1a}) (\epsilon_{4n}^\dagger \cdot \epsilon_{1b}) + [(\epsilon_{4m}^\dagger \times \epsilon_2) \cdot \epsilon_{1b}] [\epsilon_{4n}^\dagger \cdot (\epsilon_3^\dagger \times \epsilon_{1a})] \right],
\end{aligned}$$



$$\begin{aligned}
\mathcal{O}_{20} &= \frac{1}{27} \mathcal{S} T(\epsilon_{3m}^\dagger \times \epsilon_1, \epsilon_{3n}^\dagger) T(\epsilon_4^\dagger \times \epsilon_{2a}, \epsilon_{2b}) + \frac{1}{27} \mathcal{S} T(\epsilon_{3m}^\dagger \times \epsilon_1, \epsilon_4^\dagger \times \epsilon_{2a}) T(\epsilon_{3n}^\dagger, \epsilon_{2b}) \\
&\quad + \frac{1}{27} \mathcal{S} T(\epsilon_{3m}^\dagger \times \epsilon_1, \epsilon_{2b}) T(\epsilon_{3n}^\dagger, \epsilon_4^\dagger \times \epsilon_{2a}), \\
\mathcal{O}'_{20} &= \frac{1}{27} \mathcal{S} T(\epsilon_{4m}^\dagger \times \epsilon_2, \epsilon_{4n}^\dagger) T(\epsilon_3^\dagger \times \epsilon_{1a}, \epsilon_{1b}) + \frac{1}{27} \mathcal{S} T(\epsilon_{4m}^\dagger \times \epsilon_2, \epsilon_3^\dagger \times \epsilon_{1a}) T(\epsilon_{4n}^\dagger, \epsilon_{1b}) \\
&\quad + \frac{1}{27} \mathcal{S} T(\epsilon_{4m}^\dagger \times \epsilon_2, \epsilon_{1b}) T(\epsilon_{4n}^\dagger, \epsilon_3^\dagger \times \epsilon_{1a}), \\
\mathcal{O}_{21} &= \frac{1}{54} \mathcal{S} \left[ \left[ (\epsilon_{3m}^\dagger \times \epsilon_1) \cdot (\epsilon_4^\dagger \times \epsilon_{2a}) \right] T(\epsilon_{3n}^\dagger, \epsilon_{2b}) + \left[ (\epsilon_{3m}^\dagger \times \epsilon_1) \cdot \epsilon_{2b} \right] T(\epsilon_{3n}^\dagger, \epsilon_4^\dagger \times \epsilon_{2a}) \right] \\
&\quad + \frac{1}{54} \mathcal{S} \left[ (\epsilon_{3n}^\dagger \cdot \epsilon_{2b}) T(\epsilon_{3m}^\dagger \times \epsilon_1, \epsilon_4^\dagger \times \epsilon_{2a}) + \left[ \epsilon_{3n}^\dagger \cdot (\epsilon_4^\dagger \times \epsilon_{2a}) \right] T(\epsilon_{3m}^\dagger \times \epsilon_1, \epsilon_{2b}) \right], \\
\mathcal{O}'_{21} &= \frac{1}{54} \mathcal{S} \left[ \left[ (\epsilon_{4m}^\dagger \times \epsilon_2) \cdot (\epsilon_3^\dagger \times \epsilon_{1a}) \right] T(\epsilon_{4n}^\dagger, \epsilon_{1b}) + \left[ (\epsilon_{4m}^\dagger \times \epsilon_2) \cdot \epsilon_{1b} \right] T(\epsilon_{4n}^\dagger, \epsilon_3^\dagger \times \epsilon_{1a}) \right] \\
&\quad + \frac{1}{54} \mathcal{S} \left[ (\epsilon_{4n}^\dagger \cdot \epsilon_{1b}) T(\epsilon_{4m}^\dagger \times \epsilon_2, \epsilon_3^\dagger \times \epsilon_{1a}) + \left[ \epsilon_{4n}^\dagger \cdot (\epsilon_3^\dagger \times \epsilon_{1a}) \right] T(\epsilon_{4m}^\dagger \times \epsilon_2, \epsilon_{1b}) \right].
\end{aligned} \tag{A.1}$$

Here, we define  $\mathcal{S} = \sum_{m,n,a,b} C_{1m,1n}^{2,m+n} C_{1a,1b}^{2,a+b}$ , and  $T(\mathbf{x}, \mathbf{y}) = 3(\hat{\mathbf{r}} \cdot \mathbf{x})(\hat{\mathbf{r}} \cdot \mathbf{y}) - \mathbf{x} \cdot \mathbf{y}$  is the tensor force operator. For these operators  $\mathcal{O}_k^{(\prime)}$ , they should be sandwiched by the relevant spin-orbital wave functions  $|^{2S+1}L_J\rangle$  for these investigated tetraquark systems, such as  $\langle D\bar{D}^*(^3\mathbb{S}_1) | \mathcal{O}_1 | D\bar{D}^*(^3\mathbb{S}_1) \rangle = 1$ . The obtained operator matrix elements  $\mathcal{O}_k^{(\prime)}[J]$  are summarized in Tables 17 and 18, which will be used in our calculations.

In addition, the function  $Y(\Lambda_i, m_i, r)$  is defined as

$$Y_i \equiv \begin{cases} |q_i| \leq m, & \frac{e^{-m_i r} - e^{-\Lambda_i^2 r}}{4\pi r} - \frac{\Lambda_i^2 - m_i^2}{8\pi\Lambda_i} e^{-\Lambda_i r}; \\ |q_i| > m, & \frac{\cos(m'_i r) - e^{-\Lambda_i r}}{4\pi r} - \frac{\Lambda_i^2 + m_i'^2}{8\pi\Lambda_i} e^{-\Lambda_i r}; \end{cases} \tag{A.2}$$

where  $m_i = \sqrt{m^2 - q_i^2}$ ,  $m'_i = \sqrt{q_i^2 - m^2}$ , and  $\Lambda_i = \sqrt{\Lambda^2 - q_i^2}$ .

### A.1 Hidden-charm molecular tetraquark systems without hidden-strange quantum number

For convenience, we define two functions  $\mathcal{H}(I)Y(\Lambda, m_P, r)$  and  $\mathcal{G}(I)Y(\Lambda, m_V, r)$  for these investigated hidden-charm tetraquark systems, i.e.,

$$\mathcal{H}(0)Y(\Lambda, m_P, r) = \frac{3}{2}Y(\Lambda, m_\pi, r) + \frac{1}{6}Y(\Lambda, m_\eta, r), \tag{A.3}$$

$$\mathcal{H}(1)Y(\Lambda, m_P, r) = -\frac{1}{2}Y(\Lambda, m_\pi, r) + \frac{1}{6}Y(\Lambda, m_\eta, r), \tag{A.4}$$

$$\mathcal{G}(0)Y(\Lambda, m_V, r) = \frac{3}{2}Y(\Lambda, m_\rho, r) + \frac{1}{2}Y(\Lambda, m_\omega, r), \tag{A.5}$$

$$\mathcal{G}(1)Y(\Lambda, m_V, r) = -\frac{1}{2}Y(\Lambda, m_\rho, r) + \frac{1}{2}Y(\Lambda, m_\omega, r). \tag{A.6}$$

Here,  $\mathcal{H}(I)$  and  $\mathcal{G}(I)$  are the isospin factors for these investigated hidden-charm tetraquark systems, and  $I$  denote the isospin quantum numbers.

**Table 17.** The relevant operator matrix elements  $\mathcal{O}_k^{(i)}[J] = \langle f | \mathcal{O}_k^{(i)} | i \rangle$  in the effective potentials.

$\mathcal{O}_1[1] = \text{diag}(1, 1)$	$\mathcal{O}_3[1] = \begin{pmatrix} 0 & -\sqrt{2} \\ -\sqrt{2} & 1 \end{pmatrix}$	$\mathcal{O}_4[0] = \text{diag}(1, 1)$	$\mathcal{O}_6[0] = \begin{pmatrix} 0 & \sqrt{2} \\ \sqrt{2} & 2 \end{pmatrix}$
$\mathcal{O}_2[1] = \text{diag}(1, 1)$		$\mathcal{O}_5[0] = \text{diag}(2, -1)$	
$\mathcal{O}_4[1] = \text{diag}(1, 1, 1)$	$\mathcal{O}_6[1] = \begin{pmatrix} 0 & -\sqrt{2} & 0 \\ -\sqrt{2} & 1 & 0 \\ 0 & 0 & 1 \end{pmatrix}$	$\mathcal{O}_4[2] = \text{diag}(1, 1, 1, 1)$	$\mathcal{O}_7[2] = \text{diag}(1, 1)$
$\mathcal{O}_5[1] = \text{diag}(1, 1, -1)$		$\mathcal{O}_5[2] = \text{diag}(-1, 2, 1, -1)$	$\mathcal{O}_8[2] = \text{diag}(\frac{2}{27}, \frac{2}{27})$
$\mathcal{O}_6[2] = \begin{pmatrix} 0 & \frac{\sqrt{2}}{\sqrt{5}} & 0 & -\frac{\sqrt{14}}{\sqrt{5}} \\ \frac{\sqrt{2}}{\sqrt{5}} & 0 & 0 & -\frac{2}{\sqrt{7}} \\ 0 & 0 & -1 & 0 \\ -\frac{\sqrt{14}}{\sqrt{5}} & -\frac{2}{\sqrt{7}} & 0 & -\frac{3}{7} \end{pmatrix}$		$\mathcal{O}_9[2] = \begin{pmatrix} \frac{8}{135} & -\frac{4\sqrt{2}}{27\sqrt{35}} \\ -\frac{4\sqrt{2}}{27\sqrt{35}} & \frac{4}{27} \end{pmatrix}$	
$\mathcal{O}_{10}[2] = \begin{pmatrix} 0 & -\frac{\sqrt{7}}{27\sqrt{10}} \\ -\frac{\sqrt{7}}{27\sqrt{10}} & -\frac{1}{126} \end{pmatrix}$		$\mathcal{O}_{11}[0] = \text{diag}(\frac{2}{3}, -\frac{1}{3})$	
$\mathcal{O}_{12}[0] = \begin{pmatrix} \frac{4}{3} & -\frac{2\sqrt{2}}{3} \\ -\frac{2\sqrt{2}}{3} & 4 \end{pmatrix}$		$\mathcal{O}_{11}[1] = \text{diag}(-\frac{1}{3}, -\frac{1}{3}, -\frac{1}{3})$	
$\mathcal{O}_{12}[1] = \begin{pmatrix} -\frac{2}{3} & -\frac{2\sqrt{2}}{3} & 0 \\ -\frac{2\sqrt{2}}{3} & 0 & 0 \\ 0 & 0 & -\frac{4}{3} \end{pmatrix}$		$\mathcal{O}_{11}[2] = \text{diag}(-\frac{1}{3}, \frac{2}{3}, -\frac{1}{3}, -\frac{1}{3})$	
$\mathcal{O}_{12}[2] = \begin{pmatrix} \frac{8}{15} & -\frac{2\sqrt{2}}{3\sqrt{5}} & 0 & -\frac{4\sqrt{2}}{3\sqrt{35}} \\ -\frac{2\sqrt{2}}{3\sqrt{5}} & \frac{4}{3} & 0 & \frac{4}{3\sqrt{7}} \\ 0 & 0 & -\frac{4}{3} & 0 \\ -\frac{4\sqrt{2}}{3\sqrt{35}} & \frac{4}{3\sqrt{7}} & 0 & \frac{4}{3} \end{pmatrix}$		$\mathcal{O}_{13}[0] = \begin{pmatrix} 0 & \frac{\sqrt{2}}{15} \\ -\frac{8\sqrt{2}}{15} & -\frac{1}{15} \end{pmatrix}$	
$\mathcal{O}_{14}^{(i)}[1] = \text{diag}(1, 1, 1, 1)$		$\mathcal{O}_{13}[1] = \begin{pmatrix} 0 & -\frac{1}{30\sqrt{2}} & \frac{\sqrt{3}}{10\sqrt{2}} \\ -\frac{1}{30\sqrt{2}} & \frac{4}{105} & \frac{3\sqrt{3}}{70} \\ \frac{\sqrt{3}}{10\sqrt{2}} & \frac{3\sqrt{3}}{70} & -\frac{1}{105} \end{pmatrix}$	
$\mathcal{O}_{15}^{(i)}[1] = \text{diag}(\frac{3}{2}, \frac{3}{2}, \frac{1}{2}, -1)$		$\mathcal{O}_{13}[2] = \begin{pmatrix} 0 & -\frac{1}{\sqrt{10}} & 0 & \frac{\sqrt{2}}{3\sqrt{35}} \\ 0 & 0 & 0 & -\frac{4}{21\sqrt{7}} \\ 0 & 0 & -\frac{1}{14} & \frac{1}{14\sqrt{7}} \\ \frac{\sqrt{2}}{3\sqrt{35}} & \frac{23}{21\sqrt{7}} & \frac{1}{14\sqrt{7}} & \frac{13}{294} \end{pmatrix}$	
$\mathcal{O}_{17}^{(i)}[1] = \text{diag}(\frac{1}{6}, \frac{1}{6}, \frac{1}{2}, 1)$		$\mathcal{O}_{16}[1] = \begin{pmatrix} 0 & \frac{3}{5\sqrt{2}} & \frac{\sqrt{6}}{\sqrt{5}} & \frac{\sqrt{21}}{5\sqrt{2}} \\ \frac{3}{5\sqrt{2}} & -\frac{3}{10} & \frac{\sqrt{3}}{\sqrt{5}} & -\frac{\sqrt{3}}{5\sqrt{7}} \\ \frac{\sqrt{6}}{\sqrt{5}} & \frac{\sqrt{3}}{\sqrt{5}} & \frac{1}{2} & \frac{2}{\sqrt{35}} \\ \frac{\sqrt{21}}{5\sqrt{2}} & -\frac{\sqrt{3}}{5\sqrt{7}} & \frac{2}{\sqrt{35}} & \frac{48}{35} \end{pmatrix}$	
$\mathcal{O}_{19}^{(i)}[1] = \text{diag}(\frac{1}{18}, \frac{1}{18}, \frac{5}{54}, -\frac{1}{27})$		$\mathcal{O}_{18}[1] = \begin{pmatrix} 0 & -\frac{23}{15\sqrt{2}} & -\frac{2\sqrt{2}}{\sqrt{15}} & -\frac{\sqrt{7}}{5\sqrt{6}} \\ -\frac{23}{15\sqrt{2}} & \frac{23}{30} & -\frac{2}{\sqrt{15}} & \frac{1}{5\sqrt{21}} \\ \frac{2\sqrt{2}}{\sqrt{15}} & \frac{2}{\sqrt{15}} & \frac{1}{2} & -\frac{2}{\sqrt{35}} \\ -\frac{\sqrt{7}}{5\sqrt{6}} & \frac{1}{5\sqrt{21}} & \frac{2}{\sqrt{35}} & \frac{24}{35} \end{pmatrix}$	
$\mathcal{O}'_{16}[1] = \begin{pmatrix} 0 & \frac{3}{5\sqrt{2}} & -\frac{\sqrt{6}}{\sqrt{5}} & \frac{\sqrt{21}}{5\sqrt{2}} \\ \frac{3}{5\sqrt{2}} & -\frac{3}{10} & -\frac{\sqrt{3}}{\sqrt{5}} & -\frac{\sqrt{3}}{5\sqrt{7}} \\ -\frac{\sqrt{6}}{\sqrt{5}} & -\frac{\sqrt{3}}{\sqrt{5}} & \frac{1}{2} & -\frac{2}{\sqrt{35}} \\ \frac{\sqrt{21}}{5\sqrt{2}} & -\frac{\sqrt{3}}{5\sqrt{7}} & -\frac{2}{\sqrt{35}} & \frac{48}{35} \end{pmatrix}$			

Through the above preparation, we can write the effective potentials in the coordinate space for all of the investigated hidden-charm tetraquark systems, which include

1. The  $D\bar{D}$  system:

$$\mathcal{V} = -g_\sigma^2 Y_\sigma - \frac{1}{2} \beta^2 g_V^2 \mathcal{G}(I) Y_V. \quad (\text{A.7})$$

2. The  $D\bar{D}^*$  system:

$$\begin{aligned} \mathcal{V}_D &= -g_\sigma^2 \mathcal{O}_1 Y_\sigma - \frac{1}{2} \beta^2 g_V^2 \mathcal{O}_1 \mathcal{G}(I) Y_V, \\ \mathcal{V}_C &= -\frac{g^2}{3f_\pi^2} (\mathcal{O}_2 \mathcal{Z} + \mathcal{O}_3 \mathcal{T}) \mathcal{H}(I) Y_{P0} + \frac{2}{3} \lambda^2 g_V^2 (2\mathcal{O}_2 \mathcal{Z} - \mathcal{O}_3 \mathcal{T}) \mathcal{G}(I) Y_{V0}. \end{aligned} \quad (\text{A.8})$$

3. The  $D^* \bar{D}^*$  system:

$$\mathcal{V} = -g_\sigma^2 \mathcal{O}_4 Y_\sigma + \frac{g^2}{3f_\pi^2} (\mathcal{O}_5 \mathcal{Z} + \mathcal{O}_6 \mathcal{T}) \mathcal{H}(I) Y_P$$

**Table 18.** The relevant operator matrix elements  $\mathcal{O}_k^{(i)}[J] = \langle f | \mathcal{O}_k^{(i)} | i \rangle$  in the effective potentials.

$\mathcal{O}'_{18}[1] = \begin{pmatrix} 0 & -\frac{23}{15\sqrt{2}} & -\frac{2\sqrt{2}}{\sqrt{15}} & \frac{\sqrt{7}}{5\sqrt{6}} \\ -\frac{23}{15\sqrt{2}} & \frac{23}{30} & \frac{2}{\sqrt{15}} & \frac{1}{5\sqrt{21}} \\ -\frac{2\sqrt{2}}{\sqrt{15}} & -\frac{2}{\sqrt{15}} & \frac{1}{2} & \frac{2}{\sqrt{35}} \\ -\frac{\sqrt{7}}{5\sqrt{6}} & \frac{1}{5\sqrt{21}} & -\frac{2}{\sqrt{35}} & \frac{24}{35} \end{pmatrix}$	$\mathcal{O}_{20}[1] = \begin{pmatrix} \frac{2}{45} & -\frac{\sqrt{2}}{45} & 0 & \frac{\sqrt{2}}{15\sqrt{21}} \\ -\frac{\sqrt{2}}{45} & \frac{1}{15} & 0 & -\frac{8}{15\sqrt{21}} \\ 0 & 0 & -\frac{1}{9} & -\frac{2\sqrt{5}}{27\sqrt{7}} \\ \frac{\sqrt{2}}{15\sqrt{21}} & -\frac{8}{15\sqrt{21}} & \frac{2\sqrt{5}}{27\sqrt{7}} & \frac{92}{945} \end{pmatrix}$
$\mathcal{O}'_{20}[1] = \begin{pmatrix} \frac{2}{45} & -\frac{7}{45} & 0 & \frac{\sqrt{2}}{15\sqrt{21}} \\ -\frac{7}{45} & \frac{1}{15} & 0 & -\frac{15\sqrt{21}}{15\sqrt{21}} \\ 0 & 0 & -\frac{1}{9} & \frac{2\sqrt{5}}{27\sqrt{7}} \\ \frac{\sqrt{2}}{15\sqrt{21}} & -\frac{8}{15\sqrt{21}} & -\frac{2\sqrt{5}}{27\sqrt{7}} & \frac{92}{945} \end{pmatrix}$	$\mathcal{O}_{21}[1] = \begin{pmatrix} 0 & -\frac{7}{90\sqrt{2}} & 0 & \frac{\sqrt{7}}{30\sqrt{6}} \\ -\frac{7}{90\sqrt{2}} & \frac{7}{180} & 0 & -\frac{1}{30\sqrt{21}} \\ 0 & 0 & \frac{1}{108} & \frac{\sqrt{5}}{27\sqrt{7}} \\ \frac{\sqrt{7}}{30\sqrt{6}} & -\frac{1}{30\sqrt{21}} & -\frac{\sqrt{5}}{27\sqrt{7}} & \frac{4}{315} \end{pmatrix}$
$\mathcal{O}'_{21}[1] = \begin{pmatrix} 0 & -\frac{7}{90\sqrt{2}} & 0 & \frac{\sqrt{7}}{30\sqrt{6}} \\ -\frac{7}{90\sqrt{2}} & \frac{7}{180} & 0 & -\frac{1}{30\sqrt{21}} \\ 0 & 0 & \frac{1}{108} & \frac{\sqrt{5}}{27\sqrt{7}} \\ \frac{\sqrt{7}}{30\sqrt{6}} & -\frac{1}{30\sqrt{21}} & -\frac{\sqrt{5}}{27\sqrt{7}} & \frac{4}{315} \end{pmatrix}$	$\mathcal{O}_{14}^{(i)}[2] = \text{diag}(1, 1, 1, 1)$
$\mathcal{O}_{16}[2] = \begin{pmatrix} 0 & -\frac{3\sqrt{2}}{5} & -\frac{\sqrt{7}}{\sqrt{10}} & \frac{\sqrt{7}}{5} \\ -\frac{3\sqrt{2}}{5} & \frac{3}{10} & \frac{3}{\sqrt{35}} & -\frac{3\sqrt{2}}{5\sqrt{7}} \\ -\frac{\sqrt{7}}{\sqrt{10}} & \frac{3}{\sqrt{35}} & -\frac{3}{14} & \frac{4\sqrt{2}}{7\sqrt{5}} \\ \frac{\sqrt{7}}{5} & -\frac{3\sqrt{2}}{5\sqrt{7}} & \frac{4\sqrt{2}}{7\sqrt{5}} & \frac{12}{35} \end{pmatrix}$	$\mathcal{O}_{15}^{(i)}[2] = \text{diag}(\frac{1}{2}, \frac{3}{2}, \frac{1}{2}, -1)$
$\mathcal{O}'_{18}[2] = \begin{pmatrix} 0 & \frac{2\sqrt{2}}{5} & -\frac{\sqrt{7}}{\sqrt{10}} & \frac{\sqrt{7}}{5} \\ -\frac{2\sqrt{2}}{5} & -\frac{23}{30} & \frac{2}{\sqrt{35}} & \frac{3\sqrt{2}}{5\sqrt{7}} \\ -\frac{\sqrt{7}}{\sqrt{10}} & -\frac{2}{\sqrt{35}} & -\frac{3}{14} & -\frac{4\sqrt{2}}{7\sqrt{5}} \\ -\frac{\sqrt{7}}{5} & \frac{\sqrt{2}}{5\sqrt{7}} & -\frac{4\sqrt{2}}{7\sqrt{5}} & \frac{12}{35} \end{pmatrix}$	$\mathcal{O}_{17}^{(i)}[2] = \text{diag}(\frac{1}{2}, \frac{1}{6}, \frac{1}{2}, 1)$
$\mathcal{O}_{20}[2] = \begin{pmatrix} \frac{2}{27} & 0 & -\frac{\sqrt{2}}{27\sqrt{35}} & \frac{2}{27\sqrt{7}} \\ 0 & \frac{1}{45} & 0 & \frac{\sqrt{2}}{15\sqrt{7}} \\ -\frac{\sqrt{2}}{27\sqrt{35}} & 0 & \frac{29}{189} & \frac{5\sqrt{10}}{189} \\ -\frac{2}{27\sqrt{7}} & \frac{\sqrt{2}}{15\sqrt{7}} & -\frac{5\sqrt{10}}{189} & -\frac{28}{135} \end{pmatrix}$	$\mathcal{O}_{19}^{(i)}[2] = \text{diag}(\frac{5}{54}, \frac{1}{18}, \frac{5}{54}, -\frac{1}{27})$
$\mathcal{O}_{21}[2] = \begin{pmatrix} 0 & 0 & -\frac{\sqrt{7}}{54\sqrt{10}} & \frac{\sqrt{7}}{54} \\ 0 & -\frac{7}{180} & 0 & -\frac{1}{15\sqrt{14}} \\ -\frac{\sqrt{7}}{54\sqrt{10}} & 0 & -\frac{252}{189} & \frac{2\sqrt{10}}{189} \\ -\frac{\sqrt{7}}{54} & -\frac{1}{15\sqrt{14}} & -\frac{2\sqrt{10}}{189} & \frac{1}{135} \end{pmatrix}$	$\mathcal{O}_{18}[2] = \begin{pmatrix} 0 & -\frac{2\sqrt{2}}{5} & -\frac{\sqrt{7}}{\sqrt{10}} & -\frac{\sqrt{7}}{5} \\ \frac{2\sqrt{2}}{5} & -\frac{23}{30} & -\frac{2}{\sqrt{35}} & \frac{\sqrt{2}}{5\sqrt{7}} \\ -\frac{\sqrt{7}}{\sqrt{10}} & \frac{2}{\sqrt{35}} & -\frac{3}{14} & \frac{4\sqrt{2}}{7\sqrt{5}} \\ \frac{\sqrt{7}}{5} & -\frac{2\sqrt{2}}{5\sqrt{7}} & \frac{4\sqrt{2}}{7\sqrt{5}} & \frac{6}{35} \end{pmatrix}$
$\mathcal{O}'_{16}[3] = \begin{pmatrix} 0 & -\frac{1}{5\sqrt{2}} & -\frac{1}{\sqrt{5}} & -\frac{2\sqrt{3}}{5} \\ -\frac{1}{5\sqrt{2}} & \frac{23}{105} & -\frac{4\sqrt{2}}{7\sqrt{5}} & \frac{2\sqrt{6}}{35} \\ -\frac{1}{\sqrt{5}} & \frac{4\sqrt{2}}{7\sqrt{5}} & -\frac{4}{7} & \frac{\sqrt{3}}{7\sqrt{5}} \\ -\frac{2\sqrt{3}}{5} & \frac{2\sqrt{6}}{35} & -\frac{\sqrt{3}}{7\sqrt{5}} & -\frac{11}{35} \end{pmatrix}$	$\mathcal{O}'_{16}[2] = \begin{pmatrix} \frac{3\sqrt{2}}{5} & \frac{3}{10} & -\frac{3}{\sqrt{35}} & -\frac{3\sqrt{2}}{5\sqrt{7}} \\ -\frac{3\sqrt{2}}{5} & -\frac{23}{30} & \frac{2}{\sqrt{35}} & \frac{3\sqrt{2}}{5\sqrt{7}} \\ -\frac{\sqrt{7}}{\sqrt{10}} & -\frac{2}{\sqrt{35}} & -\frac{3}{14} & -\frac{4\sqrt{2}}{7\sqrt{5}} \\ -\frac{\sqrt{7}}{5} & \frac{\sqrt{2}}{5\sqrt{7}} & -\frac{4\sqrt{2}}{7\sqrt{5}} & \frac{12}{35} \end{pmatrix}$
$\mathcal{O}'_{18}[3] = \begin{pmatrix} 0 & -\frac{1}{5\sqrt{2}} & -\frac{1}{\sqrt{5}} & -\frac{2\sqrt{3}}{5} \\ -\frac{1}{5\sqrt{2}} & \frac{23}{105} & -\frac{4\sqrt{2}}{7\sqrt{5}} & \frac{2\sqrt{6}}{35} \\ -\frac{1}{\sqrt{5}} & \frac{4\sqrt{2}}{7\sqrt{5}} & -\frac{4}{7} & \frac{\sqrt{3}}{7\sqrt{5}} \\ -\frac{2\sqrt{3}}{5} & \frac{2\sqrt{6}}{35} & -\frac{\sqrt{3}}{7\sqrt{5}} & -\frac{11}{35} \end{pmatrix}$	$\mathcal{O}'_{20}[2] = \begin{pmatrix} \frac{2}{27} & 0 & -\frac{\sqrt{2}}{27\sqrt{35}} & \frac{2}{27\sqrt{7}} \\ 0 & \frac{1}{45} & 0 & \frac{\sqrt{2}}{15\sqrt{7}} \\ -\frac{\sqrt{2}}{27\sqrt{35}} & 0 & \frac{29}{189} & \frac{5\sqrt{10}}{189} \\ -\frac{2}{27\sqrt{7}} & \frac{\sqrt{2}}{15\sqrt{7}} & -\frac{5\sqrt{10}}{189} & -\frac{28}{135} \end{pmatrix}$
$\mathcal{O}'_{20}[3] = \begin{pmatrix} -\frac{4}{135} & \frac{\sqrt{2}}{105} & -\frac{2\sqrt{5}}{189} & -\frac{4}{315\sqrt{3}} \\ \frac{\sqrt{2}}{105} & \frac{16}{315} & 0 & -\frac{\sqrt{2}}{35\sqrt{3}} \\ \frac{2\sqrt{5}}{189} & 0 & \frac{1}{21} & \frac{\sqrt{5}}{63\sqrt{3}} \\ -\frac{4}{315\sqrt{3}} & -\frac{\sqrt{2}}{35\sqrt{3}} & -\frac{\sqrt{5}}{63\sqrt{3}} & \frac{82}{945} \end{pmatrix}$	$\mathcal{O}'_{21}[2] = \begin{pmatrix} 0 & 0 & -\frac{\sqrt{7}}{54\sqrt{10}} & \frac{\sqrt{7}}{54} \\ 0 & -\frac{7}{180} & 0 & -\frac{1}{15\sqrt{14}} \\ -\frac{\sqrt{7}}{54\sqrt{10}} & 0 & -\frac{252}{189} & \frac{2\sqrt{10}}{189} \\ -\frac{\sqrt{7}}{54} & -\frac{1}{15\sqrt{14}} & -\frac{2\sqrt{10}}{189} & \frac{1}{135} \end{pmatrix}$
$\mathcal{O}'_{21}[3] = \begin{pmatrix} 0 & \frac{1}{30\sqrt{2}} & -\frac{\sqrt{5}}{54} & -\frac{1}{45\sqrt{3}} \\ \frac{1}{30\sqrt{2}} & \frac{1}{90} & 0 & -\frac{\sqrt{2}}{35\sqrt{3}} \\ \frac{\sqrt{5}}{54} & 0 & -\frac{2}{189} & -\frac{\sqrt{5}}{126\sqrt{3}} \\ -\frac{1}{45\sqrt{3}} & -\frac{\sqrt{2}}{35\sqrt{3}} & \frac{\sqrt{5}}{126\sqrt{3}} & -\frac{11}{1890} \end{pmatrix}$	$\mathcal{O}_{16}[3] = \begin{pmatrix} 0 & \frac{3}{5\sqrt{2}} & -\frac{1}{\sqrt{5}} & -\frac{4\sqrt{3}}{5} \\ \frac{3}{5\sqrt{2}} & -\frac{3}{35} & -\frac{6\sqrt{2}}{7\sqrt{5}} & -\frac{6\sqrt{6}}{35} \\ -\frac{1}{\sqrt{5}} & -\frac{6\sqrt{2}}{7\sqrt{5}} & -\frac{4}{7} & \frac{\sqrt{3}}{7\sqrt{5}} \\ -\frac{4\sqrt{3}}{5} & -\frac{6\sqrt{6}}{35} & \frac{\sqrt{3}}{7\sqrt{5}} & -\frac{22}{35} \end{pmatrix}$
	$\mathcal{O}_{18}[3] = \begin{pmatrix} 0 & -\frac{1}{5\sqrt{2}} & \frac{1}{\sqrt{5}} & -\frac{2\sqrt{3}}{5} \\ -\frac{1}{5\sqrt{2}} & \frac{23}{105} & \frac{4\sqrt{2}}{7\sqrt{5}} & \frac{2\sqrt{6}}{35} \\ \frac{1}{\sqrt{5}} & -\frac{4\sqrt{2}}{7\sqrt{5}} & -\frac{4}{7} & -\frac{\sqrt{3}}{7\sqrt{5}} \\ -\frac{2\sqrt{3}}{5} & \frac{2\sqrt{6}}{35} & \frac{\sqrt{3}}{7\sqrt{5}} & -\frac{11}{35} \end{pmatrix}$
	$\mathcal{O}_{20}[3] = \begin{pmatrix} -\frac{4}{135} & \frac{\sqrt{2}}{105} & \frac{2\sqrt{5}}{189} & -\frac{4}{315\sqrt{3}} \\ \frac{\sqrt{2}}{105} & \frac{16}{315} & 0 & -\frac{\sqrt{2}}{35\sqrt{3}} \\ -\frac{2\sqrt{5}}{189} & 0 & \frac{1}{21} & -\frac{\sqrt{5}}{63\sqrt{3}} \\ -\frac{4}{315\sqrt{3}} & -\frac{\sqrt{2}}{35\sqrt{3}} & \frac{\sqrt{5}}{63\sqrt{3}} & \frac{82}{945} \end{pmatrix}$
	$\mathcal{O}_{21}[3] = \begin{pmatrix} 0 & \frac{1}{30\sqrt{2}} & \frac{\sqrt{5}}{54} & -\frac{1}{45\sqrt{3}} \\ \frac{1}{30\sqrt{2}} & \frac{1}{90} & 0 & -\frac{\sqrt{2}}{35\sqrt{3}} \\ -\frac{\sqrt{5}}{54} & 0 & -\frac{2}{189} & -\frac{\sqrt{5}}{126\sqrt{3}} \\ -\frac{1}{45\sqrt{3}} & -\frac{\sqrt{2}}{35\sqrt{3}} & \frac{\sqrt{5}}{126\sqrt{3}} & -\frac{11}{1890} \end{pmatrix}$

$$-\frac{1}{2}\beta^2 g_V^2 \mathcal{O}_4 \mathcal{G}(I) Y_V + \frac{2}{3} \lambda^2 g_V^2 (2\mathcal{O}_5 \mathcal{Z} - \mathcal{O}_6 \mathcal{T}) \mathcal{G}(I) Y_V. \quad (\text{A.9})$$

4. The  $D\bar{D}_1$  system:

$$\begin{aligned} \mathcal{V}_D &= g_\sigma g_\sigma'' \mathcal{O}_1 Y_\sigma + \frac{1}{2} \beta \beta'' g_V^2 \mathcal{O}_2 \mathcal{G}(I) Y_V, \\ \mathcal{V}_C &= \frac{2h_\sigma'^2}{9f_\pi^2} (\mathcal{O}_2 \mathcal{Z} + \mathcal{O}_3 \mathcal{T}) Y_{\sigma 1} + \frac{\zeta_1^2 g_V^2}{3} \mathcal{O}_2 \mathcal{G}(I) Y_{V1}. \end{aligned} \quad (\text{A.10})$$

5. The  $D\bar{D}_2^*$  system:

$$\begin{aligned} \mathcal{V}_D &= g_\sigma g_\sigma'' \mathcal{O}_7 Y_\sigma + \frac{1}{2} \beta \beta'' g_V^2 \mathcal{O}_7 \mathcal{G}(I) Y_V, \\ \mathcal{V}_C &= \frac{h'^2}{f_\pi^2} [\mathcal{O}_8 \mathcal{Z} \mathcal{Z} + \mathcal{O}_9 \mathcal{T} \mathcal{T} + \mathcal{O}_{10} \{\mathcal{T}, \mathcal{Z}\}] \mathcal{H}(I) Y_{P2}. \end{aligned} \quad (\text{A.11})$$

6. The  $D^* \bar{D}_1$  system:

$$\begin{aligned} \mathcal{V}_D &= g_\sigma g_\sigma'' \mathcal{O}_4 Y_\sigma + \frac{5gk}{18f_\pi^2} (\mathcal{O}_5 \mathcal{Z} + \mathcal{O}_6 \mathcal{T}) \mathcal{H}(I) Y_P \\ &\quad + \frac{1}{2} \beta \beta'' g_V^2 \mathcal{O}_4 \mathcal{G}(I) Y_V - \frac{5}{9} \lambda \lambda'' g_V^2 (2\mathcal{O}_5 \mathcal{Z} - \mathcal{O}_6 \mathcal{T}) \mathcal{G}(I) Y_V, \\ \mathcal{V}_C &= \frac{h_\sigma'^2}{18\pi_\pi^2} (\mathcal{O}_5 \mathcal{Z} + \mathcal{O}_6 \mathcal{T}) Y_{\sigma 3} + \frac{\zeta_1^2 g_V^2}{12} \mathcal{O}_5 \mathcal{G}(I) Y_{V3} \\ &\quad + \frac{h'^2}{6f_\pi^2} [\mathcal{O}_{11} \mathcal{Z} \mathcal{Z} + \mathcal{O}_{12} \mathcal{T} \mathcal{T} + \mathcal{O}_{13} \{\mathcal{T}, \mathcal{Z}\}] \mathcal{H}(I) Y_{P3}. \end{aligned} \quad (\text{A.12})$$

7. The  $D^* \bar{D}_2^*$  system:

$$\begin{aligned} \mathcal{V}_D &= g_\sigma g_\sigma'' \frac{\mathcal{O}_{14} + \mathcal{O}'_{14}}{2} Y_\sigma + \frac{gk}{3f_\pi^2} \left( \frac{\mathcal{O}_{15} + \mathcal{O}'_{15}}{2} \mathcal{Z} + \frac{\mathcal{O}_{16} + \mathcal{O}'_{16}}{2} \mathcal{T} \right) \mathcal{H}(I) Y_P \\ &\quad + \frac{1}{2} \beta \beta'' g_V^2 \frac{\mathcal{O}_{14} + \mathcal{O}'_{14}}{2} \mathcal{G}(I) Y_V - \frac{2}{3} \lambda \lambda'' g_V^2 \left( 2 \frac{\mathcal{O}_{15} + \mathcal{O}'_{15}}{2} \mathcal{Z} - \frac{\mathcal{O}_{16} + \mathcal{O}'_{16}}{2} \mathcal{T} \right) \mathcal{G}(I) Y_V, \\ \mathcal{V}_C &= \frac{h_\sigma'^2}{3f_\pi^2} \left( \frac{\mathcal{O}_{17} + \mathcal{O}'_{17}}{2} \mathcal{Z} + \frac{\mathcal{O}_{18} + \mathcal{O}'_{18}}{2} \mathcal{T} \right) Y_{\sigma 4} + \frac{\zeta_1^2 g_V^2}{2} \frac{\mathcal{O}_{17} + \mathcal{O}'_{17}}{2} \mathcal{G}(I) Y_{V4} \\ &\quad + \frac{h'^2}{f_\pi^2} \left[ \frac{\mathcal{O}_{19} + \mathcal{O}'_{19}}{2} \mathcal{Z} \mathcal{Z} + \frac{\mathcal{O}_{20} + \mathcal{O}'_{20}}{2} \mathcal{T} \mathcal{T} + \frac{\mathcal{O}_{21} + \mathcal{O}'_{21}}{2} \{\mathcal{T}, \mathcal{Z}\} \right] \mathcal{H}(I) Y_{P4}. \end{aligned} \quad (\text{A.13})$$

In the above expressions, the operators are defined as  $\mathcal{Z} = \frac{1}{r^2} \frac{\partial}{\partial r} r^2 \frac{\partial}{\partial r}$ ,  $\mathcal{T} = r \frac{\partial}{\partial r} \frac{1}{r} \frac{\partial}{\partial r}$ , and  $\{\mathcal{T}, \mathcal{Z}\} = \mathcal{T} \mathcal{Z} + \mathcal{Z} \mathcal{T}$ . Additionally, the variables  $q_i$  are written as  $q_0 = m_{D^*} - m_D$ ,  $q_1 = m_{D_1} - m_D$ ,  $q_2 = m_{D_2^*} - m_D$ ,  $q_3 = m_{D_1} - m_{D^*}$ , and  $q_4 = m_{D_2^*} - m_{D^*}$ .

## A.2 Hidden-charm tetraquark systems with hidden-strange quantum number

For these discussed hidden-charm tetraquark systems with hidden-strange quantum number, we consider the effective potentials from the  $\eta$  and  $\phi$  exchanges [82]. In the following, we collect the expressions of the effective potentials for these discussed systems.

- The  $D_s \bar{D}_s$  system:

$$\mathcal{V} = -\frac{1}{2}\beta^2 g_V^2 Y_\phi. \quad (\text{A.14})$$

- The  $D_s \bar{D}_s^*$  system:

$$\begin{aligned} \mathcal{V}_D &= -\frac{1}{2}\beta^2 g_V^2 \mathcal{O}_1 Y_\phi, \\ \mathcal{V}_C &= -\frac{2g^2}{9f_\pi^2} (\mathcal{O}_2 \mathcal{Z} + \mathcal{O}_3 \mathcal{T}) Y_{\eta 5} + \frac{2}{3}\lambda^2 g_V^2 (2\mathcal{O}_2 \mathcal{Z} - \mathcal{O}_3 \mathcal{T}) Y_{\phi 5}. \end{aligned} \quad (\text{A.15})$$

- The  $D_s^* \bar{D}_s^*$  system:

$$\mathcal{V} = \frac{2g^2}{9f_\pi^2} (\mathcal{O}_5 \mathcal{Z} + \mathcal{O}_6 \mathcal{T}) Y_\eta - \frac{1}{2}\beta^2 g_V^2 \mathcal{O}_4 Y_\phi + \frac{2}{3}\lambda^2 g_V^2 (2\mathcal{O}_5 \mathcal{Z} - \mathcal{O}_6 \mathcal{T}) Y_\phi. \quad (\text{A.16})$$

- The  $D_s \bar{D}_{s0}^*$  system:

$$\begin{aligned} \mathcal{V}_D &= \frac{1}{2}\beta\beta' g_V^2 Y_\phi, \\ \mathcal{V}_C &= -\frac{2h^2 q_6^2}{3f_\pi^2} Y_{\eta 6}. \end{aligned} \quad (\text{A.17})$$

- The  $D_s \bar{D}'_{s1}$  system:

$$\begin{aligned} \mathcal{V}_D &= \frac{1}{2}\beta\beta' g_V^2 \mathcal{O}_1 Y_\phi, \\ \mathcal{V}_C &= \frac{1}{2} (\zeta^2 g_V^2 - 4\mu^2 g_V^2 q_7^2) \mathcal{O}_2 Y_{\phi 7} - \frac{2}{3}\mu^2 g_V^2 (\mathcal{O}_2 \mathcal{Z} + \mathcal{O}_3 \mathcal{T}) Y_{\phi 7}. \end{aligned} \quad (\text{A.18})$$

- The  $D_s^* \bar{D}_{s0}^*$  system:

$$\begin{aligned} \mathcal{V}_D &= \frac{1}{2}\beta\beta' g_V^2 \mathcal{O}_1 Y_\phi, \\ \mathcal{V}_C &= -\frac{1}{2} (\zeta^2 g_V^2 - 4\mu^2 g_V^2 q_8^2) \mathcal{O}_2 Y_{\phi 8} + \frac{2}{3}\mu^2 g_V^2 (\mathcal{O}_2 \mathcal{Z} + \mathcal{O}_3 \mathcal{T}) Y_{\phi 8}. \end{aligned} \quad (\text{A.19})$$

- The  $D_s^* \bar{D}'_{s1}$  system:

$$\begin{aligned} \mathcal{V}_D &= \frac{2g\tilde{k}}{9f_\pi^2} (\mathcal{O}_5 \mathcal{Z} + \mathcal{O}_6 \mathcal{T}) Y_\eta + \frac{1}{2}\beta\beta' g_V^2 \mathcal{O}_4 Y_\phi - \frac{2}{3}\lambda\lambda' g_V^2 (2\mathcal{O}_5 \mathcal{Z} - \mathcal{O}_6 \mathcal{T}) Y_\phi, \\ \mathcal{V}_C &= -\frac{2h^2 q_9^2}{3f_\pi^2} \mathcal{O}_4 Y_{\eta 9} - \frac{1}{2} (\zeta^2 g_V^2 - 4\mu^2 g_V^2 q_9^2) \mathcal{O}_6 Y_{\phi 9} + \frac{2}{3}\mu^2 g_V^2 (\mathcal{O}_5 \mathcal{Z} + \mathcal{O}_6 \mathcal{T}) Y_{\phi 9}. \end{aligned} \quad (\text{A.20})$$

Here, the variables  $q_i$  are defined as  $q_5 = m_{D_s^*} - m_{D_s}$ ,  $q_6 = m_{D_{s0}^*} - m_{D_s}$ ,  $q_7 = m_{D'_{s1}} - m_{D_s}$ ,  $q_8 = m_{D_{s0}^*} - m_{D_s^*}$ , and  $q_9 = m_{D'_{s1}} - m_{D_s^*}$ . When performing the numerical calculations, the operators  $\mathcal{O}_k$  will be replaced by the corresponding numerical matrixes, which are summarized in Table 17.

## B $D\bar{D}$ and $D\bar{D}^*$ systems

In Table 19, we collect the corresponding bound state solutions for the  $S$ -wave isoscalar  $D\bar{D}$  and  $D\bar{D}^*$  systems. And our numerical results suggest that there exist possible charmonium-like molecular candidates for the  $S$ -wave  $D\bar{D}$  state with  $I(J^{PC}) = 0(0^{++})$  and the  $S$ -wave  $D\bar{D}^*$  states with  $I(J^{PC}) = 0[(1^{+-}), (1^{++})]$ . In Refs. [43, 120, 123, 127–129], the  $S$ -wave  $D\bar{D}$  bound state with  $I(J^{PC}) = 0(0^{++})$  was estimated. After the observation of the  $X(3872)$  by the Belle Collaboration [37], the  $S$ -wave isoscalar  $D\bar{D}^*$  molecular states have been extensively studied in Refs. [38–50, 119, 122, 127–129, 166–168].

**Table 19.** Bound state solutions for the  $S$ -wave isoscalar  $D\bar{D}$  and  $D\bar{D}^*$  systems. Conventions are the same as Table 8.

Effect	Single channel			$S$ - $D$ wave mixing effect			
State[ $J^{PC}$ ]	$\Lambda$	$E$	$r_{\text{RMS}}$				
$D\bar{D}[0^{++}]$	1.46	-0.29	5.08				
	1.76	-12.55	1.15				
States[ $J^{PC}$ ]	$\Lambda$	$E$	$r_{\text{RMS}}$	$\Lambda$	$E$	$r_{\text{RMS}}$	$P(^3S_1/^3D_1)$
$D\bar{D}^*[1^{+-}]$	1.62	-0.36	4.70	1.36	-0.39	4.71	<b>97.38</b> /2.62
	1.77	-12.51	1.07	1.49	-12.32	1.19	<b>92.15</b> /7.85
$D\bar{D}^*[1^{++}]$	1.18	-0.27	5.15	1.08	-0.27	5.22	<b>99.05</b> /0.95
	1.53	-12.39	1.19	1.30	-12.09	1.23	<b>96.99</b> /3.01

In Figure 16, we present the binding energies  $E$  dependence of the decay widths for the  $S$ -wave isoscalar  $D\bar{D}$  with  $J^{PC} = 0^{++}$  and  $D\bar{D}^*$  with  $J^{PC} = 1^{+-}$  molecular candidates. Here, the  $S$ -wave  $D\bar{D}^*$  bound state with  $I(J^{PC}) = 0(1^{++})$  can decay into the  $J/\psi\omega$  channel with very small width, which is due to the mass of the  $J/\psi\omega$  channel is extremely close to the threshold of the  $D\bar{D}^*$  channel. For the  $S$ -wave  $D\bar{D}$  bound state with  $I(J^{PC}) = 0(0^{++})$ , the  $\eta_c\eta$  channel is the only one two-body hidden-charm decay mode, and the corresponding partial decay width is around 1 MeV when the binding energies  $E$  is taken from -10 to -30 MeV. For the  $S$ -wave  $D\bar{D}^*$  bound state with  $I(J^{PC}) = 0(1^{+-})$ , there exist two allowed two-body hidden-charm decay channels, the  $\eta_c\omega$  and  $J/\psi\eta$  channels, and the decay width of the  $J/\psi\eta$  channel is larger than the  $\eta_c\omega$  channel.

## Acknowledgments

F. L. Wang would like to thank J. Z. Wang and M. X. Duan for very helpful discussions. This work is supported by the China National Funds for Distinguished Young Scientists

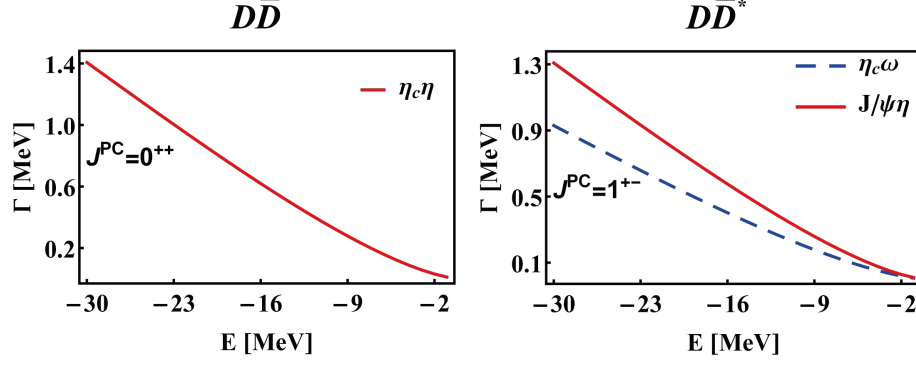


**Figure 16.** The binding energies  $E$  dependence of the decay widths for the  $S$ -wave isoscalar  $D\bar{D}$  with  $J^{PC} = 0^{++}$  and  $D\bar{D}^*$  with  $J^{PC} = 1^{+-}$  molecular candidates.

under Grant No. 11825503, National Key Research and Development Program of China under Contract No. 2020YFA0406400, the 111 Project under Grant No. B20063, and the National Natural Science Foundation of China under Grant No. 12047501. R. C. is supported by the National Postdoctoral Program for Innovative Talent.

## References

- [1] R. Aaij *et al.* [LHCb Collaboration], Observation of  $J/\psi p$  Resonances Consistent with Pentaquark States in  $\Lambda_b^0 \rightarrow J/\psi K^- p$  Decays, *Phys. Rev. Lett.* **115**, 072001 (2015).
- [2] R. Aaij *et al.* [LHCb Collaboration], Observation of a narrow pentaquark state,  $P_c(4312)^+$ , and of two-peak structure of the  $P_c(4450)^+$ , *Phys. Rev. Lett.* **122**, 222001 (2019).
- [3] X. Q. Li and X. Liu, A possible global group structure for exotic states, *Eur. Phys. J. C* **74**, 3198 (2014)
- [4] J. J. Wu, R. Molina, E. Oset and B. S. Zou, Prediction of narrow  $N^*$  and  $\Lambda^*$  resonances with hidden charm above 4 GeV, *Phys. Rev. Lett.* **105**, 232001 (2010)
- [5] M. Karliner and J. L. Rosner, New Exotic Meson and Baryon Resonances from Doubly-Heavy Hadronic Molecules, *Phys. Rev. Lett.* **115**, 122001 (2015)
- [6] W. L. Wang, F. Huang, Z. Y. Zhang and B. S. Zou,  $\Sigma_c \bar{D}$  and  $\Lambda_c \bar{D}$  states in a chiral quark model, *Phys. Rev. C* **84**, 015203 (2011)
- [7] Z. C. Yang, Z. F. Sun, J. He, X. Liu and S. L. Zhu, The possible hidden-charm molecular baryons composed of anti-charmed meson and charmed baryon, *Chin. Phys. C* **36**, 6 (2012)
- [8] J. J. Wu, T. S. H. Lee and B. S. Zou, Nucleon Resonances with Hidden Charm in Coupled-Channel Models, *Phys. Rev. C* **85**, 044002 (2012)
- [9] R. Chen, X. Liu, X. Q. Li and S. L. Zhu, Identifying exotic hidden-charm pentaquarks, *Phys. Rev. Lett.* **115**, 132002 (2015)
- [10] H. X. Chen, W. Chen, X. Liu, and S. L. Zhu, The hidden-charm pentaquark and tetraquark states, *Phys. Rep.* **639**, 1 (2016).
- [11] X. Liu, An overview of  $XYZ$  new particles, *Chin. Sci. Bull.* **59**, 3815 (2014).

- [12] A. Hosaka, T. Iijima, K. Miyabayashi, Y. Sakai, and S. Yasui, Exotic hadrons with heavy flavors:  $X$ ,  $Y$ ,  $Z$ , and related states, [Prog. Theor. Exp. Phys.](#) **2016**, 062C01 (2016).
- [13] Y. R. Liu, H. X. Chen, W. Chen, X. Liu, and S. L. Zhu, Pentaquark and tetraquark states, [Prog. Part. Nucl. Phys.](#) **107**, 237 (2019).
- [14] N. Brambilla, S. Eidelman, C. Hanhart, A. Nefediev, C. P. Shen, C. E. Thomas, A. Vairo and C. Z. Yuan, The  $XYZ$  states: Experimental and theoretical status and perspectives, [Phys. Rep.](#) **873**, 1 (2020).
- [15] S. L. Olsen, T. Skwarnicki, and D. Zieminska, Nonstandard heavy mesons and baryons: Experimental evidence, [Rev. Mod. Phys.](#) **90**, 015003 (2018).
- [16] F. K. Guo, C. Hanhart, U. G. Meiner, Q. Wang, Q. Zhao, and B. S. Zou, Hadronic molecules, [Rev. Mod. Phys.](#) **90**, 015004 (2018).
- [17] K. Abe *et al.* [Belle Collaboration], Observation of a near-threshold  $\omega J/\psi$  mass enhancement in exclusive  $B \rightarrow K\omega J/\psi$  decays, [Phys. Rev. Lett.](#) **94**, 182002 (2005).
- [18] T. Aaltonen *et al.* [CDF Collaboration], Evidence for a Narrow Near-Threshold Structure in the  $J/\psi\phi$  Mass Spectrum in  $B^+ \rightarrow J/\psi\phi K^+$  Decays, [Phys. Rev. Lett.](#) **102**, 242002 (2009).
- [19] X. Liu and S. L. Zhu,  $Y(4143)$  is probably a molecular partner of  $Y(3930)$ , [Phys. Rev. D](#) **80**, 017502 (2009).
- [20] R. Aaij *et al.* [LHCb Collaboration], Observation of  $J/\psi\phi$  structures consistent with exotic states from amplitude analysis of  $B^+ \rightarrow J/\psi\phi K^+$  decays, [Phys. Rev. Lett.](#) **118**, 022003 (2017).
- [21] R. Aaij *et al.* [LHCb Collaboration], Amplitude analysis of  $B^+ \rightarrow J/\psi\phi K^+$  decays, [Phys. Rev. D](#) **95**, 012002 (2017).
- [22] S. K. Choi *et al.* [Belle Collaboration], Observation of a ResonanceLike Structure in the  $\pi^\pm\psi'$  Mass Distribution in Exclusive  $B \rightarrow K\pi^\pm\psi'$  Decays, [Phys. Rev. Lett.](#) **100**, 142001 (2008).
- [23] X. Liu, Y. R. Liu, W. Z. Deng, and S. L. Zhu, Is  $Z^+(4430)$  a loosely bound molecular state?, [Phys. Rev. D](#) **77**, 034003 (2008).
- [24] X. Liu, Y. R. Liu, W. Z. Deng, and S. L. Zhu,  $Z^+(4430)$  as a  $D_1' D^*(D_1 D^*)$  molecular state, [Phys. Rev. D](#) **77**, 094015 (2008).
- [25] K. Chilikin *et al.* [Belle Collaboration], Experimental constraints on the spin and parity of the  $Z(4430)^+$ , [Phys. Rev. D](#) **88**, 074026 (2013).
- [26] R. Aaij *et al.* [LHCb Collaboration], Observation of the resonant character of the  $Z(4430)^-$  state, [Phys. Rev. Lett.](#) **112**, 222002 (2014).
- [27] E. Kou *et al.* [BelleII Collaboration], The Belle II Physics Book, [PTEP](#) **2019**, 123C01 (2019) [erratum: [PTEP](#) **2020**, 029201 (2020)].
- [28] R. Aaij *et al.* [LHCb Collaboration], Physics case for an LHCb Upgrade II - Opportunities in flavour physics, and beyond, in the HL-LHC era, [arXiv:1808.08865](#).
- [29] T. Barnes and E. S. Swanson, A Diagrammatic approach to meson meson scattering in the nonrelativistic quark potential model, [Phys. Rev. D](#) **46**, 131 (1992).
- [30] T. Barnes, N. Black, D. J. Dean and E. S. Swanson, B B intermeson potentials in the quark model, [Phys. Rev. C](#) **60**, 045202 (1999).



- [31] T. Barnes, N. Black and E. S. Swanson, Meson meson scattering in the quark model: Spin dependence and exotic channels, [Phys. Rev. C \*\*63\*\*, 025204 \(2001\)](#).
- [32] J. P. Hilbert, N. Black, T. Barnes and E. S. Swanson, Charmonium-Nucleon Dissociation Cross Sections in the Quark Model, [Phys. Rev. C \*\*75\*\*, 064907 \(2007\)](#).
- [33] M. B. Wise, Chiral perturbation theory for hadrons containing a heavy quark, [Phys. Rev. D \*\*45\*\*, R2188 \(1992\)](#).
- [34] P. A. Zyla *et al.* [Particle Data Group], Review of Particle Physics, [PTEP \*\*2020\*\*, 083C01 \(2020\)](#).
- [35] C. Hanhart, Y. S. Kalashnikova and A. V. Nefediev, Lineshapes for composite particles with unstable constituents, [Phys. Rev. D \*\*81\*\*, 094028 \(2010\)](#).
- [36] A. A. Filin, A. Romanov, V. Baru, C. Hanhart, Y. S. Kalashnikova, A. E. Kudryavtsev, U.-G. Meissner and A. V. Nefediev, Comment on ‘Possibility of Deeply Bound Hadronic Molecules from Single Pion Exchange’, [Phys. Rev. Lett. \*\*105\*\*, 019101 \(2010\)](#).
- [37] S. K. Choi *et al.* [Belle Collaboration], Observation of a Narrow Charmonium-Like State in Exclusive  $B^\pm \rightarrow K^\pm \pi^+ \pi^- J/\psi$  Decays, [Phys. Rev. Lett. \*\*91\*\*, 262001 \(2003\)](#).
- [38] C. Y. Wong, Molecular states of heavy quark mesons, [Phys. Rev. C \*\*69\*\*, 055202 \(2004\)](#).
- [39] E. S. Swanson, Short range structure in the  $X(3872)$ , [Phys. Lett. B \*\*588\*\*, 189 \(2004\)](#).
- [40] M. Suzuki, The  $X(3872)$  boson: Molecule or charmonium, [Phys. Rev. D \*\*72\*\*, 114013 \(2005\)](#).
- [41] Y. R. Liu, X. Liu, W. Z. Deng, and S. L. Zhu, Is  $X(3872)$  really a molecular state?, [Eur. Phys. J. C \*\*56\*\*, 63 \(2008\)](#).
- [42] C. E. Thomas and F. E. Close, Is  $X(3872)$  a molecule?, [Phys. Rev. D \*\*78\*\*, 034007 \(2008\)](#).
- [43] X. Liu, Z. G. Luo, Y. R. Liu, and S. L. Zhu,  $X(3872)$  and other possible heavy molecular states, [Eur. Phys. J. C \*\*61\*\*, 411 \(2009\)](#).
- [44] I. W. Lee, A. Faessler, T. Gutsche, and V. E. Lyubovitskij,  $X(3872)$  as a molecular  $DD^*$  state in a potential model, [Phys. Rev. D \*\*80\*\*, 094005 \(2009\)](#).
- [45] L. Zhao, L. Ma, and S. L. Zhu, Spin-orbit force, recoil corrections, and possible  $B\bar{B}^*$  and  $D\bar{D}^*$  molecular states, [Phys. Rev. D \*\*89\*\*, 094026 \(2014\)](#).
- [46] N. Li and S. L. Zhu, Isospin breaking, coupled-channel effects and diagnosis of  $X(3872)$ , [Phys. Rev. D \*\*86\*\*, 074022 \(2012\)](#).
- [47] M. B. Voloshin, Interference and binding effects in decays of possible molecular component of  $X(3872)$ , [Phys. Lett. B \*\*579\*\*, 316 \(2004\)](#).
- [48] F. E. Close and P. R. Page, The  $D^{*0}\bar{D}^0$  threshold resonance, [Phys. Lett. B \*\*578\*\*, 119 \(2004\)](#).
- [49] N. A. Tornqvist, Isospin breaking of the narrow charmonium state of Belle at 3872 MeV as a deuson, [Phys. Lett. B \*\*590\*\*, 209 \(2004\)](#).
- [50] J. He, Study of the  $B\bar{B}^*/D\bar{D}^*$  bound states in a Bethe-Salpeter approach, [Phys. Rev. D \*\*90\*\*, 076008 \(2014\)](#).
- [51] B. Aubert *et al.* [BaBar Collaboration], Observation of  $Y(3940) \rightarrow J/\psi \omega$  in  $B \rightarrow J/\psi \omega K$  at BABAR, [Phys. Rev. Lett. \*\*101\*\*, 082001 \(2008\)](#).
- [52] P. del Amo Sanchez *et al.* [BaBar Collaboration], Evidence for the decay  $X(3872) \rightarrow J/\psi \omega$ , [Phys. Rev. D \*\*82\*\*, 011101 \(2010\)](#).

- [53] B. Aubert *et al.* [BaBar Collaboration], Observation of the decay  $B \rightarrow J/\psi \eta K$  and search for  $X(3872) \rightarrow J/\psi \eta$ , [Phys. Rev. Lett. \*\*93\*\*, 041801 \(2004\)](#).
- [54] S. Chatrchyan *et al.* [CMS Collaboration], Observation of a Peaking Structure in the  $J/\psi \phi$  Mass Spectrum from  $B^\pm \rightarrow J/\psi \phi K^\pm$  Decays, [Phys. Lett. B \*\*734\*\*, 261 \(2014\)](#).
- [55] R. Aaij *et al.* [LHCb Collaboration], Search for the  $X(4140)$  state in  $B^+ \rightarrow J/\psi \phi K^+$  decays, [Phys. Rev. D \*\*85\*\*, 091103 \(2012\)](#).
- [56] V. M. Abazov *et al.* [D0 Collaboration], Search for the  $X(4140)$  state in  $B^+ \rightarrow J/\psi \phi K^+$  decays with the D0 Detector, [Phys. Rev. D \*\*89\*\*, 012004 \(2014\)](#).
- [57] J. P. Lees *et al.* [BaBar Collaboration], Study of  $B^{\pm,0} \rightarrow J/\psi K^+ K^- K^{\pm,0}$  and search for  $B^0 \rightarrow J/\psi \phi$  at BABAR, [Phys. Rev. D \*\*91\*\*, 012003 \(2015\)](#).
- [58] T. Aaltonen *et al.* [CDF Collaboration], Observation of the  $Y(4140)$  Structure in the  $J/\psi \phi$  Mass Spectrum in  $B^\pm \rightarrow J/\psi \phi K^\pm$  Decays, [Mod. Phys. Lett. A \*\*32\*\*, 1750139 \(2017\)](#).
- [59] R. Aaij *et al.* [LHCb Collaboration], Observation of new resonances decaying to  $J/\psi K^+$  and  $J/\psi \phi$ , [arXiv:2103.01803](#).
- [60] R. Aaij *et al.* [LHCb Collaboration], Evidence for an  $\eta_c(1S)\pi^-$  resonance in  $B^0 \rightarrow \eta_c(1S)K^+\pi^-$  decays, [Eur. Phys. J. C \*\*78\*\*, 1019 \(2018\)](#).
- [61] K. Chilikin *et al.* [Belle Collaboration], Observation of a new charged charmonium-like state in  $\bar{B}^0 \rightarrow J/\psi K^- \pi^+$  decays, [Phys. Rev. D \*\*90\*\*, 112009 \(2014\)](#).
- [62] V. M. Abazov *et al.* [D0 Collaboration], Evidence for  $Z_c^\pm(3900)$  in semi-inclusive decays of  $b$ -flavored hadrons, [Phys. Rev. D \*\*98\*\*, 052010 \(2018\)](#).
- [63] R. Aaij *et al.* [LHCb Collaboration], Model-Independent Observation of Exotic Contributions to  $B^0 \rightarrow J/\psi K^+ \pi^-$  Decays, [Phys. Rev. Lett. \*\*122\*\*, 152002 \(2019\)](#).
- [64] R. Mizuk *et al.* [Belle Collaboration], Dalitz analysis of  $B \rightarrow K \pi^+ \psi'$  decays and the  $Z(4430)^+$ , [Phys. Rev. D \*\*80\*\*, 031104 \(2009\)](#).
- [65] R. Mizuk *et al.* [Belle Collaboration], Observation of two resonance-like structures in the  $\pi^+ \chi_{c1}$  mass distribution in exclusive  $\bar{B}^0 \rightarrow K^- \pi^+ \chi_{c1}$  decays, [Phys. Rev. D \*\*78\*\*, 072004 \(2008\)](#).
- [66] J. P. Lees *et al.* [BaBar Collaboration], Search for the  $Z_1(4050)^+$  and  $Z_2(4250)^+$  states in  $\bar{B}^0 \rightarrow \chi_{c1} K^- \pi^+$  and  $B^+ \rightarrow \chi_{c1} K_S^0 \pi^+$ , [Phys. Rev. D \*\*85\*\*, 052003 \(2012\)](#).
- [67] V. Bhardwaj *et al.* [Belle Collaboration], Inclusive and exclusive measurements of  $B$  decays to  $\chi_{c1}$  and  $\chi_{c2}$  at Belle, [Phys. Rev. D \*\*93\*\*, 052016 \(2016\)](#).
- [68] V. Bhardwaj *et al.* [Belle Collaboration], Search for  $X(3872)$  and  $X(3915)$  decay into  $\chi_{c1} \pi^0$  in  $B$  decays at Belle, [Phys. Rev. D \*\*99\*\*, 111101 \(2019\)](#).
- [69] F. Close and C. Downum, On the possibility of Deeply Bound Hadronic Molecules from single Pion Exchange, [Phys. Rev. Lett. \*\*102\*\*, 242003 \(2009\)](#).
- [70] M. Ablikim *et al.* [BESIII Collaboration], Observation of a Charged Charmonium-like Structure in  $e^+e^- \rightarrow \pi^+ \pi^- J/\psi$  at  $\sqrt{s}=4.26$  GeV, [Phys. Rev. Lett. \*\*110\*\*, 252001 \(2013\)](#).
- [71] Z. Q. Liu *et al.* [Belle Collaboration], Study of  $e^+e^- \rightarrow \pi^+ \pi^- J/\psi$  and Observation of a Charged Charmonium-like State at Belle, [Phys. Rev. Lett. \*\*110\*\*, 252002 \(2013\)](#). Erratum: [\[Phys. Rev. Lett. \*\*111\*\*, 019901 \(2013\)\]](#).

- [72] H. Yukawa, On the Interaction of Elementary Particles I, [Proc. Phys. Math. Soc. Jap. \*\*17\*\*, 48 \(1935\)](#).
- [73] X. H. Liu, L. Ma, L. P. Sun, X. Liu and S. L. Zhu, Resolving the puzzling decay patterns of charged  $Z_c$  and  $Z_b$  states, [Phys. Rev. D \*\*90\*\*, 074020 \(2014\)](#).
- [74] L. Y. Xiao, G. J. Wang and S. L. Zhu, Hidden-charm strong decays of the  $Z_c$  states, [Phys. Rev. D \*\*101\*\*, 054001 \(2020\)](#).
- [75] Z. Y. Zhou, M. T. Yu and Z. Xiao, Decays of  $X(3872)$  to  $\chi_{cJ}\pi^0$  and  $J/\psi\pi^+\pi^-$ , [Phys. Rev. D \*\*100\*\*, 094025 \(2019\)](#).
- [76] G. J. Wang, L. Y. Xiao, R. Chen, X. H. Liu, X. Liu and S. L. Zhu, Probing hidden-charm decay properties of  $P_c$  states in a molecular scenario, [Phys. Rev. D \*\*102\*\*, 036012 \(2020\)](#).
- [77] G. J. Wang, L. Meng, L. Y. Xiao, M. Oka and S. L. Zhu, Mass spectrum and strong decays of tetraquark  $\bar{c}sqq$  states, [Eur. Phys. J. C \*\*81\*\*, 188 \(2021\)](#).
- [78] F. L. Wang, X. D. Yang, R. Chen and X. Liu, Hidden-charm pentaquarks with triple strangeness due to the  $\Omega_c^{(*)}\bar{D}_s^{(*)}$  interactions, [Phys. Rev. D \*\*103\*\*, 054025 \(2021\)](#).
- [79] X. D. Yang, F. L. Wang, Z. W. Liu and X. Liu, Newly observed  $X(4630)$ : a new charmonium-like molecule, [arXiv:2103.03127](#).
- [80] F. L. Wang, R. Chen, Z. W. Liu, and X. Liu, Probing new types of  $P_c$  states inspired by the interaction between  $S$ -wave charmed baryon and anti-charmed meson in a  $\bar{T}$  doublet, [Phys. Rev. C \*\*101\*\*, 025201 \(2020\)](#).
- [81] F. L. Wang, R. Chen, Z. W. Liu, and X. Liu, Possible triple-charm molecular pentaquarks from  $\Xi_{cc}D_1/\Xi_{cc}D_2^*$  interactions, [Phys. Rev. D \*\*99\*\*, 054021 \(2019\)](#).
- [82] F. L. Wang and X. Liu, Exotic double-charm molecular states with hidden or open strangeness and around  $4.5 \sim 4.7$  GeV, [Phys. Rev. D \*\*102\*\*, 094006 \(2020\)](#).
- [83] F. L. Wang, R. Chen, and X. Liu, Prediction of hidden-charm pentaquarks with double strangeness, [Phys. Rev. D \*\*103\*\*, 034014 \(2021\)](#).
- [84] R. Chen, F. L. Wang, A. Hosaka and X. Liu, Exotic triple-charm deuteronlike hexaquarks, [Phys. Rev. D \*\*97\*\*, 114011 \(2018\)](#).
- [85] G. Breit, The effect of retardation on the interaction of two electrons, [Phys. Rev. \*\*34\*\*, 553 \(1929\)](#).
- [86] G. Breit, The fine structure of HE as a test of the spin interactions of two electrons, [Phys. Rev. \*\*36\*\*, 383 \(1930\)](#).
- [87] N. A. Tornqvist, From the deuteron to deusons, an analysis of deuteronlike meson-meson bound states, [Z. Phys. C \*\*61\*\*, 525 \(1994\)](#).
- [88] N. A. Tornqvist, On deusons or deuteron-like meson-meson bound states, [Nuovo Cimento Soc. Ital. Fis. \*\*107A\*\*, 2471 \(1994\)](#).
- [89] G. J. Ding, Are  $Y(4260)$  and  $Z_2^+$  are  $D_1D$  or  $D_0D^*$  Hadronic Molecules?, [Phys. Rev. D \*\*79\*\*, 014001 \(2009\)](#).
- [90] R. Casalbuoni, A. Deandrea, N. Di Bartolomeo, R. Gatto, F. Feruglio, and G. Nardulli, Light vector resonances in the effective chiral Lagrangian for heavy mesons, [Phys. Lett. B \*\*292\*\*, 371 \(1992\)](#).

- [91] R. Casalbuoni, A. Deandrea, N. Di Bartolomeo, R. Gatto, F. Feruglio, and G. Nardulli, Phenomenology of heavy meson chiral Lagrangians, [Phys. Rep. \*\*281\*\*, 145 \(1997\)](#).
- [92] T. M. Yan, H. Y. Cheng, C. Y. Cheung, G. L. Lin, Y. C. Lin, and H. L. Yu, Heavy quark symmetry and chiral dynamics, [Phys. Rev. D \*\*46\*\*, 1148 \(1992\)](#); [[Phys. Rev. D \*\*55\*\*, 5851E \(1997\)](#)].
- [93] M. Bando, T. Kugo, and K. Yamawaki, Nonlinear realization and hidden local symmetries, [Phys. Rep. \*\*164\*\*, 217 \(1988\)](#).
- [94] M. Harada and K. Yamawaki, Hidden local symmetry at loop: A new perspective of composite gauge boson and chiral phase transition, [Phys. Rep. \*\*381\*\*, 1 \(2003\)](#).
- [95] B. Hu, X. L. Chen, Z. G. Luo, P. Z. Huang, S. L. Zhu, P. F. Yu and X. Liu, Possible heavy molecular states composed of a pair of excited charm-strange mesons, [Chin. Phys. C \*\*35\*\*, 113-125 \(2011\)](#).
- [96] L. L. Shen, X. L. Chen, Z. G. Luo, P. Z. Huang, S. L. Zhu, P. F. Yu and X. Liu, The Molecular systems composed of the charmed mesons in the  $H\bar{S} + h.c.$  doublet, [Eur. Phys. J. C \*\*70\*\*, 183-217 \(2010\)](#).
- [97] H. Y. Cheng and K. C. Yang, Charmless hadronic  $B$  decays into a tensor meson, [Phys. Rev. D \*\*83\*\*, 034001 \(2011\)](#).
- [98] Z. F. Sun, X. Liu, M. Nielsen, and S. L. Zhu, Hadronic molecules with both open charm and bottom, [Phys. Rev. D \*\*85\*\*, 094008 \(2012\)](#).
- [99] A. F. Falk and M. E. Luke, Strong decays of excited heavy mesons in chiral perturbation theory, [Phys. Lett. B \*\*292\*\*, 119 \(1992\)](#).
- [100] C. Isola, M. Ladisa, G. Nardulli, and P. Santorelli, Charming penguins in  $B \rightarrow K^*\pi, K(\rho, \omega, \phi)$  decays, [Phys. Rev. D \*\*68\*\*, 114001 \(2003\)](#).
- [101] M. Cleven and Q. Zhao, Cross section line shape of  $e^+e^- \rightarrow \chi_{c0}\omega$  around the  $Y(4260)$  mass region, [Phys. Lett. B \*\*768\*\*, 52 \(2017\)](#).
- [102] X. K. Dong, Y. H. Lin, and B. S. Zou, Prediction of an exotic state around 4240 MeV with  $J^{PC} = 1^{-+}$  as C-parity partner of  $Y(4260)$  in molecular picture, [Phys. Rev. D \*\*101\*\*, 076003 \(2020\)](#).
- [103] J. He, Y. Liu, J. T. Zhu, and D. Y. Chen,  $Y(4626)$  as a molecular state from interaction  $D_s^*\bar{D}_{s1}(2536) - D_s\bar{D}_{s1}(2536)$ , [Eur. Phys. J. C \*\*80\*\*, 246 \(2020\)](#).
- [104] Z. Y. Wang, J. J. Qi, J. Xu, and X. H. Guo, Studying the  $D_1D$  molecule in the Bethe-Salpeter equation approach, [Phys. Rev. D \*\*102\*\*, 036008 \(2020\)](#).
- [105] D. O. Riska and G. E. Brown, Nucleon resonance transition couplings to vector mesons, [Nucl. Phys. A \*\*679\*\*, 577 \(2001\)](#).
- [106] W. A. Bardeen, E. J. Eichten and C. T. Hill, Chiral multiplets of heavy - light mesons, [Phys. Rev. D \*\*68\*\*, 054024 \(2003\)](#).
- [107] H. Y. Cheng, C. K. Chua and A. Soni, Final state interactions in hadronic B decays, [Phys. Rev. D \*\*71\*\*, 014030 \(2005\)](#).
- [108] X. Liu, Z. G. Luo and S. L. Zhu, Novel charmonium-like structures in the  $J/\psi\phi$  and  $J/\psi\omega$  invariant mass spectra, [Phys. Lett. B \*\*699\*\*, 341-344 \(2011\)](#). [erratum: [Phys. Lett. B \*\*707\*\*, 577 \(2012\)](#)].

- [109] J. He and P. L. Lü, Understanding  $Y(4274)$  and  $X(4320)$  in the  $J/\psi\phi$  invariant mass spectrum, [Nucl. Phys. A \*\*919\*\*, 1-14 \(2013\)](#).
- [110] J. He, Understanding spin parity of  $P_c(4450)$  and  $Y(4274)$  in a hadronic molecular state picture, [Phys. Rev. D \*\*95\*\*, 074004 \(2017\)](#).
- [111] J. He, D. Y. Chen and X. Liu, New Structure Around 3250 MeV in the Baryonic B Decay and the  $D_0^*(2400)N$  Molecular Hadron, [Eur. Phys. J. C \*\*72\*\*, 2121 \(2012\)](#).
- [112] C. Y. Wong, E. S. Swanson and T. Barnes, Heavy quarkonium dissociation cross-sections in relativistic heavy ion collisions, [Phys. Rev. C \*\*65\*\*, 014903 \(2002\)](#), [Erratum: \[Phys. Rev. C \*\*66\*\*, 029901 \(2002\)\]](#).
- [113] S. Godfrey and N. Isgur, Mesons in a Relativized Quark Model with Chromodynamics, [Phys. Rev. D \*\*32\*\*, 189 \(1985\)](#).
- [114] H. G. Blundell, Meson properties in the quark model: A look at some outstanding problems, [\[arXiv:hep-ph/9608473 \[hep-ph\]\]](#).
- [115] C. Q. Pang, J. Z. Wang, X. Liu and T. Matsuki, A systematic study of mass spectra and strong decay of strange mesons, [Eur. Phys. J. C \*\*77\*\*, no. 12, 861 \(2017\)](#).
- [116] S. Weinberg, Elementary particle theory of composite particles, [Phys. Rev. \*\*130\*\*, 776 \(1963\)](#).
- [117] S. Weinberg, Quasiparticles and the Born Series, [Phys. Rev. \*\*131\*\*, 440 \(1963\)](#).
- [118] R. Chen, A. Hosaka, and X. Liu, Searching for possible  $\Omega_c$ -like molecular states from meson-baryon interaction, [Phys. Rev. D \*\*97\*\*, 036016 \(2018\)](#).
- [119] Z. F. Sun, J. He, X. Liu, Z. G. Luo and S. L. Zhu,  $Z_b(10610)^\pm$  and  $Z_b(10650)^\pm$  as the  $B^*\bar{B}$  and  $B^*\bar{B}^*$  molecular states, [Phys. Rev. D \*\*84\*\*, 054002 \(2011\)](#).
- [120] M. Z. Liu, D. J. Jia and D. Y. Chen, Possible hadronic molecular states composed of  $S$ -wave heavy-light mesons, [Chin. Phys. C \*\*41\*\*, 053105 \(2017\)](#).
- [121] L. Zhao, L. Ma and S. L. Zhu, The recoil correction and spin-orbit force for the possible  $B^*\bar{B}^*$  and  $D^*\bar{D}^*$  states, [Nucl. Phys. A \*\*942\*\*, 18 \(2015\)](#).
- [122] Z. F. Sun, Z. G. Luo, J. He, X. Liu and S. L. Zhu, A note on the  $B^*\bar{B}$ ,  $B^*\bar{B}^*$ ,  $D^*\bar{D}$ ,  $D^*\bar{D}^*$ , molecular states, [Chin. Phys. C \*\*36\*\*, 194-204 \(2012\)](#).
- [123] Y. R. Liu and Z. Y. Zhang, The Bound state problem of S-wave heavy quark meson-antimeson systems, [Phys. Rev. C \*\*80\*\*, 015208 \(2009\)](#).
- [124] X. K. Dong, F. K. Guo and B. S. Zou, A survey of heavy-antiheavy hadronic molecules, [Progr. Phys. \*\*41\*\*, 65 \(2021\)](#).
- [125] Y. Liu and I. Zahed, Heavy Exotic Molecules with Charm and Bottom, [Phys. Lett. B \*\*762\*\*, 362 \(2016\)](#).
- [126] L. R. Dai, G. Y. Wang, X. Chen, E. Wang, E. Oset and D. M. Li, The  $B^+ \rightarrow J/\psi\omega K^+$  reaction and  $D^*\bar{D}^*$  molecular states, [Eur. Phys. J. A \*\*55\*\*, 36 \(2019\)](#).
- [127] Z. M. Ding, H. Y. Jiang and J. He, Molecular states from  $D^{(*)}\bar{D}^{(*)}/B^{(*)}\bar{B}^{(*)}$  and  $D^{(*)}D^{(*)}/\bar{B}^{(*)}\bar{B}^{(*)}$  interactions, [Eur. Phys. J. C \*\*80\*\*, 1179 \(2020\)](#).
- [128] Y. C. Yang, Z. Y. Tan, J. Ping and H. S. Zong, Possible  $D^{(*)}\bar{D}^{(*)}$  and  $B^{(*)}\bar{B}^{(*)}$  molecular states in the extended constituent quark models, [Eur. Phys. J. C \*\*77\*\*, 575 \(2017\)](#).
- [129] Y. J. Zhang, H. C. Chiang, P. N. Shen and B. S. Zou, Possible S-wave bound-states of two pseudoscalar mesons, [Phys. Rev. D \*\*74\*\*, 014013 \(2006\)](#).

- [130] M. Ablikim *et al.* [BESIII Collaboration], Observation of  $e^+e^- \rightarrow \eta J/\psi$  at center-of-mass energy  $\sqrt{s} = 4.009$  GeV, [Phys. Rev. D \*\*86\*\*, 071101 \(2012\)](#).
- [131] T. Iwashita *et al.* [Belle], Measurement of branching fractions for  $B \rightarrow J/\psi \eta K$  decays and search for a narrow resonance in the  $J/\psi \eta$  final state, [PTEP \*\*2014\*\*, 043C01 \(2014\)](#).
- [132] F. Close, C. Downum and C. E. Thomas, Novel Charmonium and Bottomonium Spectroscopies due to Deeply Bound Hadronic Molecules from Single Pion Exchange, [Phys. Rev. D \*\*81\*\*, 074033 \(2010\)](#).
- [133] M. T. Li, W. L. Wang, Y. B. Dong and Z. Y. Zhang, A Study of One  $S$ - and One  $P$ -Wave Heavy Meson Interaction in a Chiral Quark Model, [Commun. Theor. Phys. \*\*63\*\*, 63 \(2015\)](#).
- [134] J. He and D. Y. Chen, Interpretation of  $Y(4390)$  as an isoscalar partner of  $Z(4430)$  from  $D^*(2010)\bar{D}_1(2420)$  interaction, [Eur. Phys. J. C \*\*77\*\*, 398 \(2017\)](#).
- [135] M. T. Li, W. L. Wang, Y. B. Dong and Z. Y. Zhang, A Study of P-wave Heavy Meson Interactions in A Chiral Quark Model, [arXiv:1303.4140](#).
- [136] W. Zhu, Y. R. Liu and T. Yao, Is  $J^{PC} = 3^{-+}$  molecule possible?, [Chin. Phys. C \*\*39\*\*, 023101 \(2015\)](#).
- [137] R. Chen, A. Hosaka and X. Liu, Heavy molecules and one- $\sigma/\omega$ -exchange model, [Phys. Rev. D \*\*96\*\*, 116012 \(2017\)](#).
- [138] M. Ablikim *et al.* [BESIII Collaboration], Precise measurement of the  $e^+e^- \rightarrow \pi^+\pi^- J/\psi$  cross section at center-of-mass energies from 3.77 to 4.60 GeV, [Phys. Rev. Lett. \*\*118\*\*, 092001 \(2017\)](#).
- [139] B. Aubert *et al.* (BaBar Collaboration), Observation of a Broad Structure in the  $\pi^+\pi^- J/\psi$  Mass Spectrum Around 4.26-GeV/ $c^2$ , [Phys. Rev. Lett. \*\*95\*\*, 142001 \(2005\)](#).
- [140] G. J. Ding, Possible Molecular States of  $D_s^*\bar{D}_s^*$  System and  $Y(4140)$ , [Eur. Phys. J. C \*\*64\*\*, 297-308 \(2009\)](#).
- [141] L. Meng, B. Wang and S. L. Zhu, Predicting the  $\bar{D}_s^{(*)}D_s^{(*)}$  bound states as the partners of  $X(3872)$ , [arXiv:2012.09813](#).
- [142] J. Z. Wang, D. Y. Chen, X. Liu and T. Matsuki, Constructing  $J/\psi$  family with updated data of charmonium-like  $Y$  states, [Phys. Rev. D \*\*99\*\*, 114003 \(2019\)](#).
- [143] J. Z. Wang, R. Q. Qian, X. Liu and T. Matsuki, Are the  $Y$  states around 4.6 GeV from  $e^+e^-$  annihilation higher charmonia?, [Phys. Rev. D \*\*101\*\*, 034001 \(2020\)](#).
- [144] R. Chen, X. Liu, Y. R. Liu and S. L. Zhu, Predictions of the hidden-charm molecular states with four-quark component, [Eur. Phys. J. C \*\*76\*\*, 319 \(2016\)](#).
- [145] Y. R. Liu and Z. Y. Zhang, A Chiral quark model study of  $Z^+(4430)$  in the molecular picture, [arXiv:0908.1734](#).
- [146] T. Uchino, W. H. Liang and E. Oset, Baryon states with hidden charm in the extended local hidden gauge approach, [Eur. Phys. J. A \*\*52\*\*, 43 \(2016\)](#).
- [147] L. Meng, B. Wang, G. J. Wang and S. L. Zhu, Implications of the  $Z_{cs}(3985)$  and  $Z_{cs}(4000)$  as two different states, [arXiv:2104.08469 \[hep-ph\]](#).
- [148] B. Wang, L. Meng and S. L. Zhu, Decoding the nature of  $Z_{cs}(3985)$  and establishing the spectrum of charged heavy quarkoniumlike states in chiral effective field theory, [Phys. Rev. D \*\*103\*\*, no.2, L021501 \(2021\)](#).



- [149] L. Meng, B. Wang and S. L. Zhu,  $Z_{cs}(3985)^-$  as the  $U$ -spin partner of  $Z_c(3900)^-$  and implication of other states in the  $SU(3)_F$  symmetry and heavy quark symmetry, [Phys. Rev. D \*\*102\*\*, no.11, 111502 \(2020\)](#).
- [150] B. Wang, L. Meng and S. L. Zhu, Deciphering the charged heavy quarkoniumlike states in chiral effective field theory, [Phys. Rev. D \*\*102\*\*, 114019 \(2020\)](#).
- [151] J. Z. Wang, D. Y. Chen, X. Liu and T. Matsuki, Mapping a new cluster of charmonium-like structures at  $e^+e^-$  collisions, [Phys. Lett. B \*\*817\*\*, 136345 \(2021\)](#).
- [152] J. Z. Wang, D. Y. Chen, X. Liu and T. Matsuki, Universal non-resonant explanation to charmonium-like structures  $Z_c(3885)$  and  $Z_c(4025)$ , [Eur. Phys. J. C \*\*80\*\*, 1040 \(2020\)](#).
- [153] J. Z. Wang, Q. S. Zhou, X. Liu and T. Matsuki, Toward charged  $Z_{cs}(3985)$  structure under a reflection mechanism, [Eur. Phys. J. C \*\*81\*\*, 51 \(2021\)](#).
- [154] D. Y. Chen, J. He and X. Liu, Nonresonant explanation for the  $Y(4260)$  structure observed in the  $e^+e^- \rightarrow J/\psi\pi^+\pi^-$  process, [Phys. Rev. D \*\*83\*\*, 054021 \(2011\)](#).
- [155] D. Y. Chen, J. He and X. Liu, A Novel explanation of charmonium-like structure in  $e^+e^- \rightarrow \psi(2S)\pi^+\pi^-$ , [Phys. Rev. D \*\*83\*\*, 074012 \(2011\)](#).
- [156] D. Y. Chen, X. Liu, X. Q. Li and H. W. Ke, Unified Fano-like interference picture for charmonium-like states  $Y(4008)$ ,  $Y(4260)$  and  $Y(4360)$ , [Phys. Rev. D \*\*93\*\*, 014011 \(2016\)](#).
- [157] D. Y. Chen, X. Liu and T. Matsuki, Interference effect as resonance killer of newly observed charmonium-like states  $Y(4320)$  and  $Y(4390)$ , [Eur. Phys. J. C \*\*78\*\*, 136 \(2018\)](#).
- [158] D. Y. Chen and X. Liu, Predicted charged charmonium-like structures in the hidden-charm dipion decay of higher charmonia, [Phys. Rev. D \*\*84\*\*, 034032 \(2011\)](#).
- [159] D. Y. Chen and X. Liu,  $Z_b(10610)$  and  $Z_b(10650)$  structures produced by the initial single pion emission in the  $\Upsilon(5S)$  decays, [Phys. Rev. D \*\*84\*\*, 094003 \(2011\)](#).
- [160] D. Y. Chen, X. Liu and T. Matsuki, Reproducing the  $Z_c(3900)$  structure through the initial-single-pion-emission mechanism, [Phys. Rev. D \*\*88\*\*, 036008 \(2013\)](#).
- [161] D. Y. Chen, X. Liu and T. Matsuki, Interpretation of  $Z_b(10610)$  and  $Z_b(10650)$  in the ISPE mechanism and the Charmonium Counterpart, [Chin. Phys. C \*\*38\*\*, 053102 \(2014\)](#).
- [162] X. Liu, D. Y. Chen and T. Matsuki, The Initial Single Chiral Particle Emission Mechanism and the Predictions of Charged Charmonium-like Structures, [Acta Phys. Polon. Supp. \*\*8\*\*, 153 \(2015\)](#).
- [163] D. Y. Chen, X. Liu and T. Matsuki, Charged charmonium-like structures and the initial single chiral particle emission mechanism, [AIP Conf. Proc. \*\*1701\*\*, 050010 \(2016\)](#).
- [164] Q. Huang, D. Y. Chen, X. Liu and T. Matsuki, Charged charmonium-like structures in the  $e^+e^- \rightarrow \psi(3686)\pi^+\pi^-$  process based on the ISPE mechanism, [Eur. Phys. J. C \*\*79\*\*, 613 \(2019\)](#).
- [165] F. K. Guo, X. H. Liu and S. Sakai, Threshold cusps and triangle singularities in hadronic reactions, [Prog. Part. Nucl. Phys. \*\*112\*\*, 103757 \(2020\)](#).
- [166] Z. Y. Wang, J. J. Qi, X. H. Guo and C. Wang,  $X(3872)$  as a molecular  $D\bar{D}^*$  state in the Bethe-Salpeter equation approach, [Phys. Rev. D \*\*97\*\*, 016015 \(2018\)](#).
- [167] B. X. Sun, D. M. Wan and S. Y. Zhao, The  $D\bar{D}^*$  interaction with isospin zero in an extended hidden gauge symmetry approach, [Chin. Phys. C \*\*42\*\*, 053105 \(2018\)](#).

- [168] G. J. Ding, J. F. Liu and M. L. Yan, Dynamics of Hadronic Molecule in One-Boson Exchange Approach and Possible Heavy Flavor Molecules, [Phys. Rev. D \*\*79\*\*, 054005 \(2009\)](#).